VOLUME XVII SECOND SERIES NUMBER 5

MAY - 1921
UNIV. OF MICH.

THE PHYSICAL REVIEW

A JOURNAL OF EXPERIMENTAL AND THEORETICAL PHYSICS

CONDUCTED BY

THE AMERICAN PHYSICAL SOCIETY

BOARD OF EDITORS

FREDERICK BEDELL, Managing Editor

HENRY CREW	E. L. NICHOLS	G. S. FULCHER
L. V. KING	C. M. SPARROW	F. A. SAUNDERS
H. S. UHLER	W. F. G. SWANN	O. M. STEWART

MAY, 1921

Graphical Determination of Hexagonal and Tetragonal Crystal Structure from X-Ray Data. ALBERT W. HULL and WHEELER P. DAVEY 549

X-Ray Crystal Analysis of Thirteen Common Metals. ALBERT W. HULL 571

The Balmer Series of Hydrogen and the Quantum Theory of Line Spectra. RAYMOND T. BIRGE 589

An Experimental Study of the Reflection of X-Rays from Calcite. BERGEN DAVIS and W. M. STEMPEL 608

Reflection of Radiation from an Infinite Series of Equally Spaced Planes. K. W. LAMBSON 624

The Current from the Photo-active Electrolytic Cell. C. C. MURDOCK 626

New Books 648

PUBLISHED BY
THE AMERICAN PHYSICAL SOCIETY
LANCASTER, PA., AND ITHACA, N. Y.

Entered at the post-office at Lancaster, Pa., as second class matter

AMERICAN PHYSICAL SOCIETY

OFFICERS OF THE SOCIETY

	THEODORE LYMAN	Harvard University, Cambridge, Mass.
President:	C. R. MENDENHALL	Univ. of Wisconsin, Madison, Wis.
	D. C. MILLER	Case School of Applied Science, Cleveland, Ohio
	G. B. PEGRAM	Columbia University, New York City
	F. BEDELL	Cornell University, Ithaca, N. Y.
Secretary for Pacific Coast:	E. P. LEWIS	University of California, Berkeley, Cal.

The Council of the Society consists of the president, vice-president, secretary, treasurer, managing editor, all living past presidents and eight elected members as follows:

Past Presidents: A. A. Michelson, A. G. Webster, Carl Barus, E. L. Nichols, Henry Crew W. F. Magie, Ernest Merritt, R. A. Millikan, J. S. Ames.

Elected Members: A. L. Day, G. F. Hull, G. K. Burgess, J. C. McLennan, F. B. Jewett, Max Mason, K. T. Compton, H. M. Randall.

A complete list of past officers is given on a back page of the REVIEW.

THE PHYSICAL REVIEW

Published Monthly — Two Volumes Annually

Subscription, throughout the Postal Union, $7.00, in advance; Single Copies, $.75.

General Index 1893–1920 (issued June, 1921) $4.00, postage extra. Back Volumes (either series) $4.50 per volume, carriage extra. Back Numbers (either series) $.75 a copy, postage extra. Discount to subscription agencies only, ten per cent.

Notice.—When remittance accompanies the order, the Index will be sent prepaid for $4.00 and single back numbers will be sent prepaid for $.75. Back numbers will only be sent when they can be furnished without breaking a volume, and back volumes when they can be furnished without breaking a continuous series. Orders that can not be completely filled will be filled so far as stock permits, unless otherwise specified in the order. Money will be refunded for any defective copies returned. No bound volumes can be supplied.

The REVIEW offers to purchase, at $1.50 a copy, a limited number of No. 1, Vol. I, *First Series*, and No. 2, Vol. IX, February 1917, *Second Series*.

Membership certificates will be furnished with bills, when so ordered, for twenty-five cents each; copies of bills, on forms furnished by customer, will be furnished for five cents each. Postage stamps will be accepted for these.

Members of the Physical Society may obtain back numbers at a discount of 10 per cent, provided statement of membership accompanies order. When a member's name has been removed from the mailing list of the REVIEW on account of non-payment of dues, it will be restored to the list when dues are paid; any numbers that he has failed to receive in the interim will be furnished without cost upon application to the REVIEW. *All complaints for failure to receive the Review should be addressed to the Review and not to any officer of the Society.*

First Series. From July 1, 1893, to January 1, 1913, the REVIEW was conducted by Edward L. Nichols, Ernest Merritt and Frederick Bedell, with the financial support of Cornell University. During this period thirty-five volumes were issued, constituting the First Series. The first four volumes were issued annually; subsequent volumes, semi-annually.

Second Series. On January first, 1913, the REVIEW was transferred to the American Physical Society. A second series was then begun, the January, 1913, number being designated Volume I., Number 1, Second Series. (An announcement of this transfer will be found on the first page of the new series.) Semi-annual volumes begin in January and July.

For advertising rates, address THE PHYSICAL REVIEW, *Ithaca, N. Y.* Change of copy in standing advertisements should be sent direct to the printers, THE NEW ERA PRINTING CO. *Lancaster, Pa. Old copy is used until new copy is received.*

Contributors to the REVIEW are referred to page two of the advertisements for further information. Permission is given to republish any article appearing in the REVIEW, provided proper credit is given.

Address Correspondence to

THE PHYSICAL REVIEW, ITHACA, N. Y.

Second Series *May, 1921* *Vol. XVII, No. 5*

THE

PHYSICAL REVIEW.

GRAPHICAL DETERMINATION OF HEXAGONAL AND TETRAGONAL CRYSTAL STRUCTURES FROM X-RAY DATA.

By Albert W. Hull and Wheeler P. Davey.

Synopsis.

Graphic Method for Interpreting X-Ray Patterns of Powders.—For each type of lattice the logarithms of the theoretical spacings of the different planes are plotted as functions of the axial ratio. Six such plots are reproduced, three for the hexagonal and three for the tetragonal system. By plotting the logarithms of the observed spacings on the edge of a strip of paper, this may be fitted by trial to the theoretical plot; the axial ratio and type of lattice being thus found in a few minutes.

Crystal Structure of Zn, Cd, In.—As examples three complete analyses are given. *Zinc* is shown to be a hexagonal close packed assemblage of prolate spheroids. The axial ratio is 1.860 and the side of the unit triangle 2.760 Å. *Cadmium* shows a structure like that of Zn, with axial ratio 1.89 and elementary triangle 2.980 Å. *Indium* shows a structure nearly like Al (cubic close-packed), viz., a tetragonal close packed arrangement of prolate spheroids, with axial ratio 1.06 and a unit square of 4.58 Å.

Introduction.

SUBSTANCES available for X-ray crystal analysis by the Bragg method fall into three classes:

A. Simple substances, *i.e.*, elements and simple compounds, regarding which no reliable crystallographic data exists;

B. Complex substances, *i.e.*, compounds containing three or more different kinds of atoms, with reliable crystallographic data;

C. Complex substances with no crystallographic data.

Substances of Class *B* are obtainable in large crystals, and hence are easy to investigate, and much useful information may be obtained. Their complete analysis, however, requires a better knowledge of the laws of X-ray scattering than we possess at present.

This knowledge may be most easily and reliably obtained from the study of Class *A* substances. There are a great many of these, and their

investigation in powder form is very easy, by the method previously described.[1]

In the X-ray powder photographs the patterns that represent cubic arrangements can be recognized at a glance, and their complete analysis requires only a few minutes. Anisometric crystals are almost as simple if correct crystallographic data are available. Without such data one must proceed either by systematic mathematical analysis,[2] or by a series of guesses. Either method is, in general, very laborious. The process of guessing becomes very easy, however, by the use of plots.

DESCRIPTION OF PLOTS.

The plots (Figs 6–11) show the spacings of all possible planes (within the range of the plot) as a function of axial ratio.[3]

The scale of abscissas is logarithmic, so that if the planer spacings are plotted on the same logarithmic scale (shown on the bottom of each plot) they may be compared directly with the observed values without regard to the absolute length of the unit axes.

Three plots are given for each system. The first represents a single lattice of right triangular prisms and tetragonal prisms respectively; the second, two intermeshed lattices; and the third, three intermeshed lattices for the hexagonal and four for the tetragonal system.

The single lattice is an aggregate of points whose cartesian coördinates are m, n, pc, where m, n, and p represent all possible integers, c is the axial ratio, and the unit of length is the side of the unit triangle or square respectively.

The two intermeshed lattices of triangular prisms have coördinates

$$m, n, pc,$$
$$m + 1/3; n + 2/3; (p + 1/2)c.$$

This is the arrangement which, when the axial ratio is 1.633, gives the closest possible packing of equal spheres. It is therefore designated as "hexagonal close packing," though it is obviously not the closest packed arrangement of spheres for all axial ratios.

The two intermeshed lattices of tegragonal prisms have coördinates

$$m, n, pc,$$
$$m + 1/2; n + 1/2; (p + 1/2)c$$

[1] A. W. Hull, PHYS. REV., 10, 661, 1917.

[2] C. Runge, Phys. Z., 18, 509, 1917.

Johnsen u. Toeplitz, Phys. Z., 19, 47, 1918.

[3] The term *axial ratio* is used in its strict sense, viz., the ratio of the fundamental translation distances of the point lattice along the vertical and lateral axes respectively.

For the hexagonal and tetragonal systems this is equal to the ratio of altitude to side of the unit triangular prism and tetragonal prism respectively.

and constitute a single lattice of body centered tetragonal prisms.

The three intermeshed triangular lattices have coördinates

$$m, n, pc,$$
$$m + 1/3; n + 2/3, (p + 1/3)c,$$
$$m + 2/3, n + 1/3, (p + 2/3)c.$$

This gives complete rhombohedral symmetry, and is equivalent to a single lattice of rhombohedra of which the edge is $\sqrt{1/3 + c^2/9}$ times the edge of the unit triangle, and the angles between edges *i.e.*, the face angles of the rhombhedra, are each equal to $2csc^{-1}2\sqrt{1/3 + c^2/9}$.

The four intermeshed tetragonal prisms have indices

$$m, n, pc,$$
$$m + 1/2, n + 1/2, pc,$$
$$m + 1/2, n, (p + 1/2)c,$$
$$m, n + 1/2, (p + 1/2)c,$$

and constitute a single lattice of face-centered tetragonal prisms.

USE OF PLOTS. EXAMPLES.

As illustrations of the use of the plots the complete analysis of zinc, cadmium and indium will be described.

Zinc.

Zinc has atomic weight 65.37, density 7.1, and crystallizes, according to Groth (measurements of Williams & Burton) holohedral hexagonal, with axial ratio 1.3564.

Powder photographs of pure zinc prepared in different ways gave identical patterns (using molybdenum monochromatic X-rays) with the spacings shown in Table I.

TABLE I.

Zinc

Intensity of Line (Estimated).	Planar Spacing in Ångstroms.	Intensity of Line.	Planar Spacing.
10	2.473	2	1.088
4	2.315	2	1.044
20	2.080	1	.947
4	1.684	2	.908
5	1.339	4	.857
5	1.333	2	.824
1	1.235	2	.770
4	1.173	1	.749
2	1.152	6	.734
4	1.121	3	.667
		2	.654

In order to compare these observed spacings with the theoretical ones of the plots, a strip of paper is placed beneath the scale of abscissas of the plot (position 1, Fig. 1) and the values of planar spacings from Table I. laid off along its edge. This strip with its pattern of lines is then moved over the plot, with its edge always parallel to the axis of abscissas, until a position is found where its pattern exactly coincides with that of the plot. "Position 2," Fig. 1, shows the best fit that can be obtained at the accepted axial ratio 1.356, and "position 3," Fig. 2, the correct position, at axial ratio 1.860. The agreement is exact. The plot shows that the second spacing, viz: 2.315 Å. belongs to the form $1\,0\,\bar{1}\,0$, hence the side of the unit triangle, which is $2/\sqrt{3}$ times the $1\,0\,\bar{1}\,0$ spacing, is 2.670 Å. The number of atoms per unit triangular prism is

$$n = \frac{\sqrt{3}}{4}\frac{a^3 c\rho}{M} = 1.00$$

a = side of elementary triangle in cm.
c = axial ratio,
ρ = density,
M = mass of 1 atom in grams.

which is correct for two intermeshed triangular prism lattices. *The zinc lattice is therefore similar to that of magnesium (hexagonal close-packed) except that it is elongated 14 per cent. in the direction of the principal hexagonal axis.* The arrangement is that of *closest packing of prolate spheroids*, indicating that the zinc atom is polar and elongated, as suggested by Langmuir.[1]

Cadmium.

Filings of pure cast cadmium were photographed with Mo. monochromatic X-rays and gave the spacings in Table II.

TABLE II.

Cadmium.

Intensity of Line (Estimated).	Planar Spacings in Ångstroms.	Intensity of Line.	Planar Spacing.
20	2.817	1	1.225
10	2.585	2	1.165
60	2.336	2	1.060
12	1.900	2	1.025
10	1.515	2	1.023
8	1.490	(wide, 4 not resolved)	.958
1	1.400	1	.918
10	1.313	3	.861
6	1.257	2	.820

[1] Langmuir, Arrangement of Electrons in Atoms and Molecules. J. Amer. Chem. Soc., 41, 879, 1919.

The scale of abscissas on the plots is not quite long enough to enable all the values of planar spacings in Table II. to be laid off directly. They may be brought within the range of the plot, however, by dividing them all by 2; or the first two spacings may be laid off with the strip in position 1, and the rest in position 2, Fig. 3. The strip is then moved about on the plots until the correct position is found. This is shown at position 3, Fig. 3, at axial ratio 1.89. The best fit that can be obtained at the commonly accepted axial ratio 1.335 is shown in position 4, Fig. 4, and position 5, Fig. 4, shows the next most plausible guess, at axial ratio 1.633, which is hexagonal close packing. This fit is very bad, but close enough to tempt one to look for the correct axial ratio in the immediate neighborhood of 1.633. This would be a false lead, however, since the order of many of the lines, notably the first two, reverses in passing from axial ratio 1.633 to 1.89.

From the value of the $1\,0\,\bar{1}\,0$ spacing, as identified by the plot (position 3, Fig. 3), the side of the elementary triangle may be calculated, viz.,

$$a = \frac{\sqrt{3}}{2} d_{10\bar{1}0} = 2.980\ \text{Å}.$$

The number of atoms per unit triangular prism is

$$\frac{\sqrt{3}}{4} \frac{a^3 c \rho}{M} = 1.005,$$

which is sufficiently close to the correct value, 1,000, for two intermeshed triangular prism lattices in close packed arrangement.

The cadmium lattice is therefore a close-packed arrangement of elongated atoms, like that of zinc, the elongation being 16 per cent., as compared with 14 per cent. for zinc.

Indium.

A photograph of finely powdered indium, of unknown purity, gave the following lines (Table III.).

TABLE III.

Indium.

Intensity of Line (Estimated).	Planar Spacings in Ångstroms.
40	2.70
1	2.42
10	2.29
4	1.675
1	1.617
2	1.450
4	1.392
4	1.348
1	1.150
2	1.080

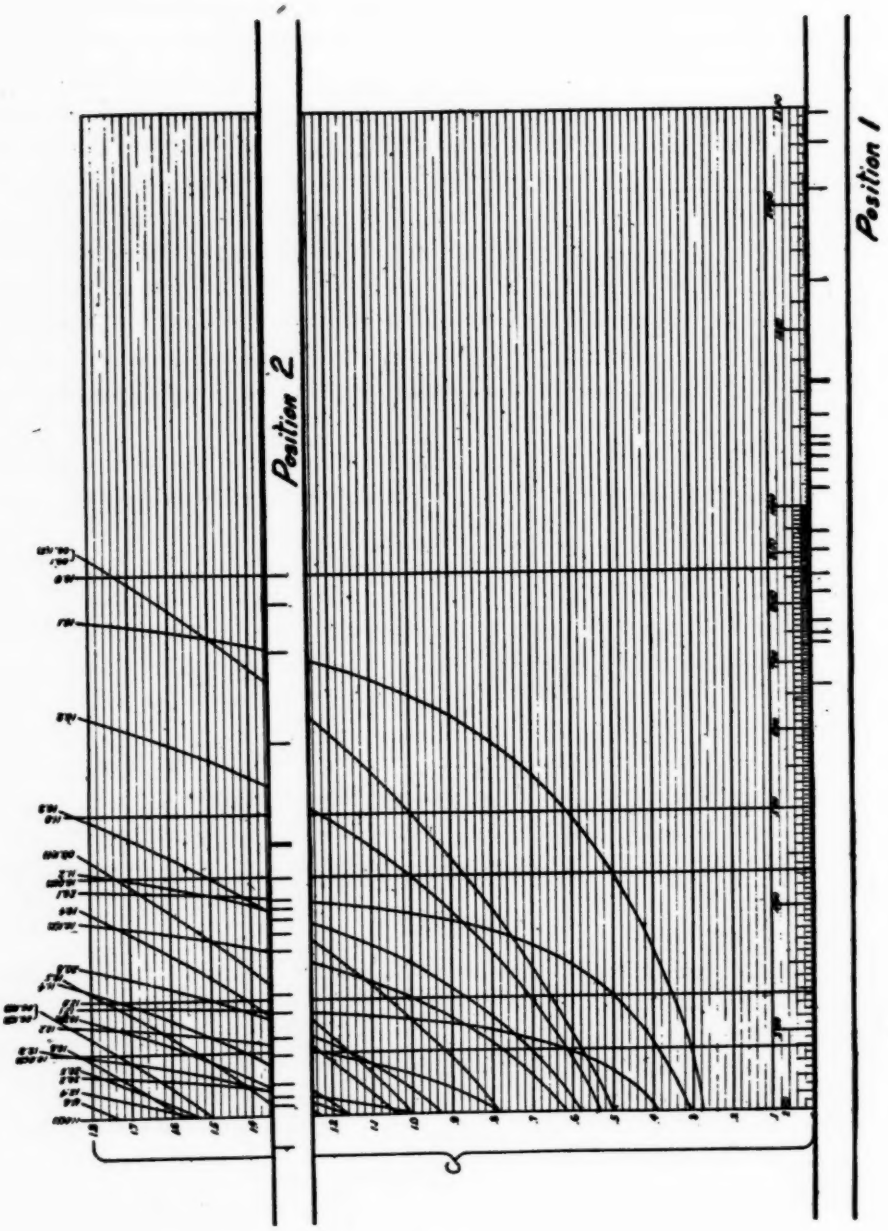

Fig. 1.

Zinc spacings compared with triangular close packing plot.

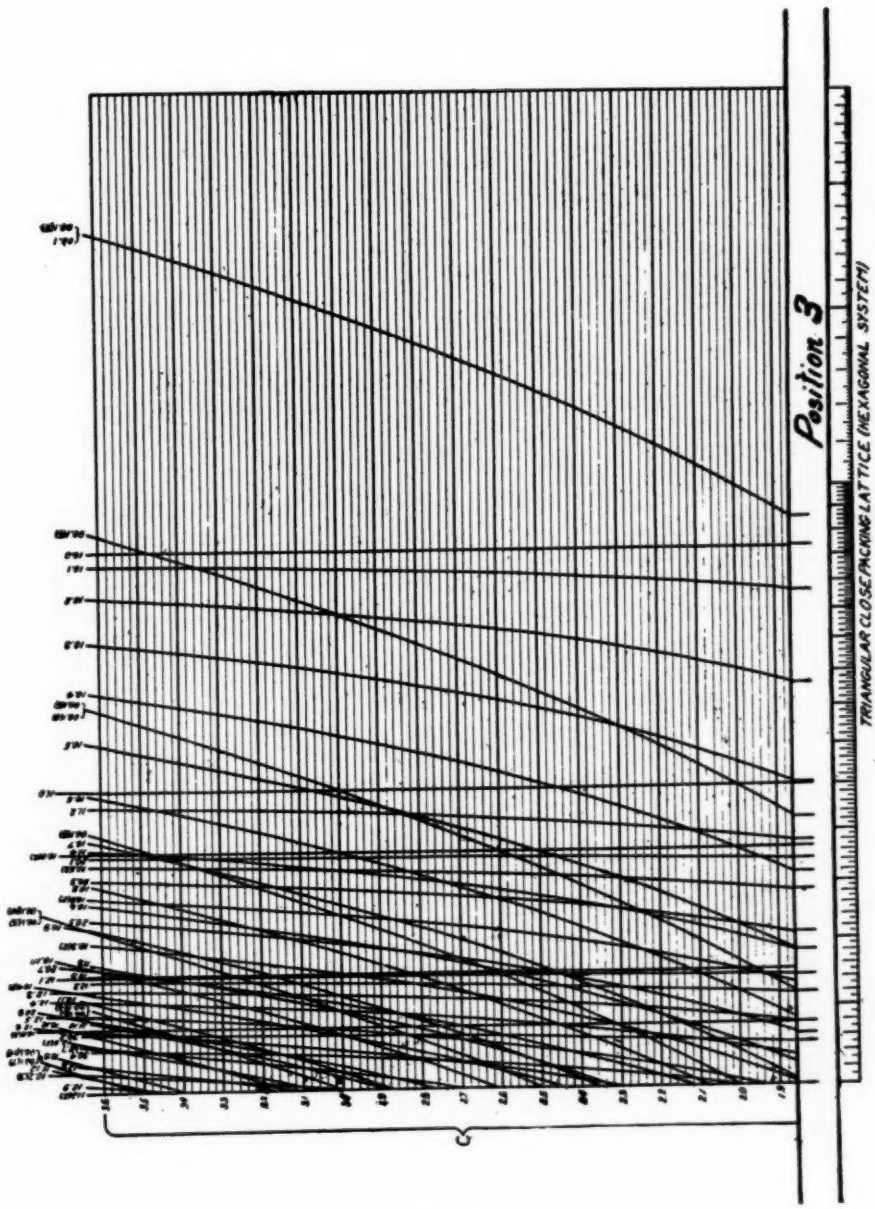

Fig. 2.

Zinc spacings compared with triangular close packing plot.

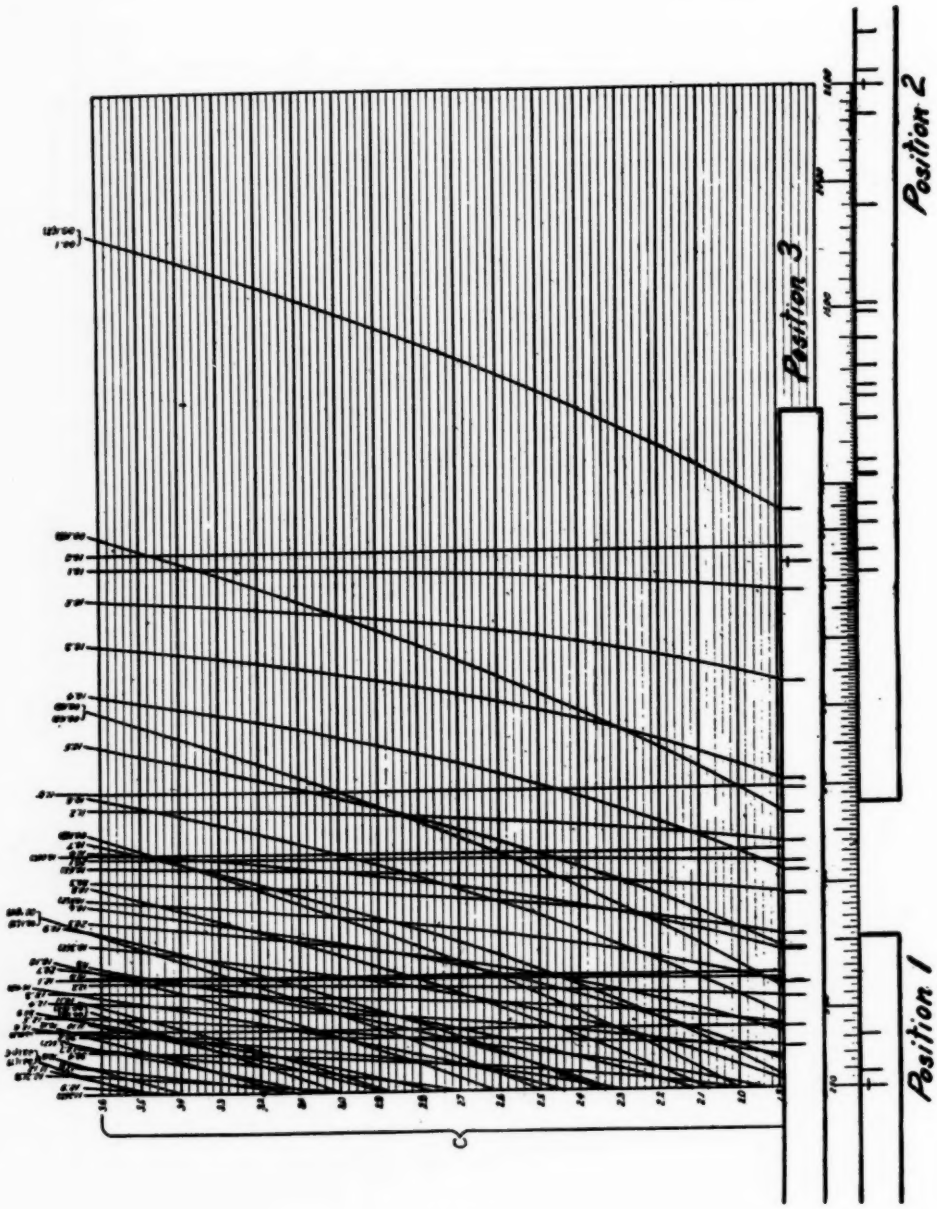

Fig. 3.

Cadmium spacings compared with triangnlar close packing plot.

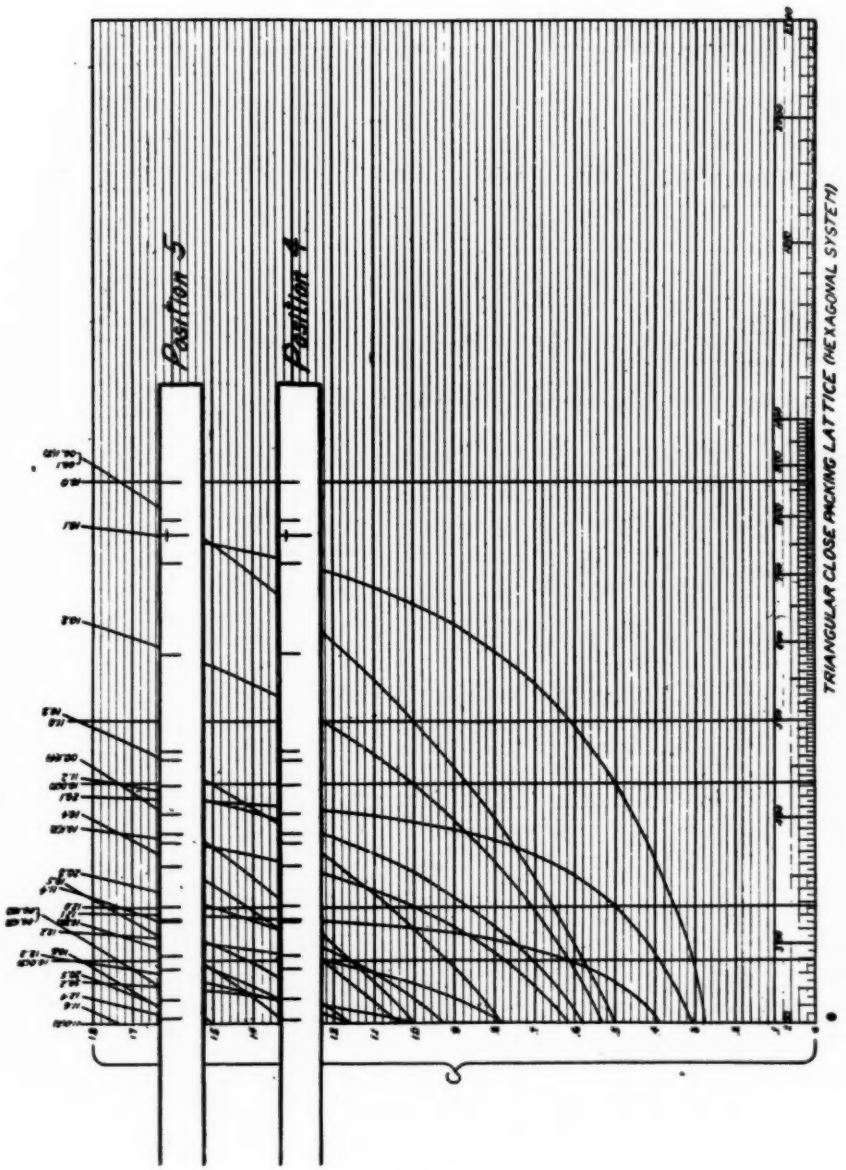

Fig. 4.

Cadmium spacings compared with triangular close packing plot.

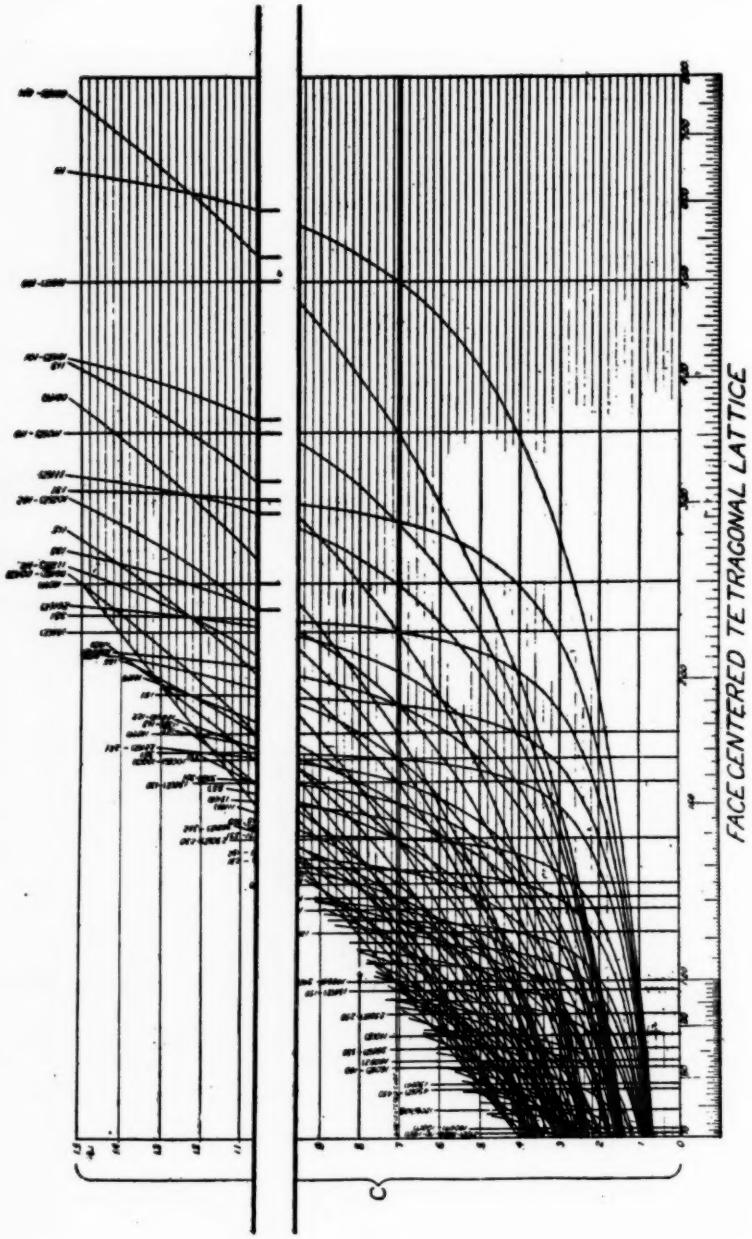

Fig. 5.

Indium spacings compared with face-centered tetragonal plot.

The spacings in Table III. are laid off on a strip of paper, and this strip moved about on the different plots until a position is found (Fig. 5) where the pattern exactly fits the plot.

The only data on indium given by Groth is an observation of Sachs that it crystallizes in regular octahedra. Inspection of the film showed at once that it was not cubic, and this was checked by trying the strip of paper on the tetragonal plots at axial ratio 1. It remained, therefore, to move the strip over the different plots until a position was found on one of them which matched the pattern of lines on the strip. In this case it took less than five minutes to find the correct position, as shown on Fig. 5, position 3.

The plot shows that the third spacing, 2.290Å., is half the fundamental spacing of the 100 planes (second order reflection from 100) of a simple tetragonal lattice. Hence the side of the unit square is $a = 4.58$Å., the height of the unit prism is $ca = 1.06 \times 4.58 = 4.86$Å., and the number of atoms per unit prism, taking the density of indium as 7.45 is

$$n = \frac{a^3 c \rho}{M} = 4.00,$$

which is correct for a face-centered tetragonal lattice.

The lattice of indium is therefore similar to that of aluminum (cubic close-packed) except that it is elongated 6 per cent. in the direction of the principal axis. This lattice, like that of zinc and cadmium, is a close packed arrangement for oblate spheroids, indicating that the indium atom also is slightly elongated.

General Remarks.

The plots reproduced in Figs. 6–11 are all drawn to the same scale, and photographed without distortion, so that experimental values laid off on a strip of paper according to the scale at the bottom of any one of the plots may be used on all the plots.

These plots cover all possible arrangements of atoms in the cubic, hexagonal (including trigonal) and tetragonal systems. Only three specific arrangements have been given for each system, viz., simple prism, centered, and face-centered arrangements in the cubic and tetragonal systems, and simple prism, close packed, and rhombohedral arrangements in the hexagonal system. It is obvious, however, that these and all other possible arrangements are obtained from the simple tetragonal and triangular prism lattices respectively by simply omitting part of the lines. This will be more obvious, perhaps, if stated in the form of two fundamental principles:

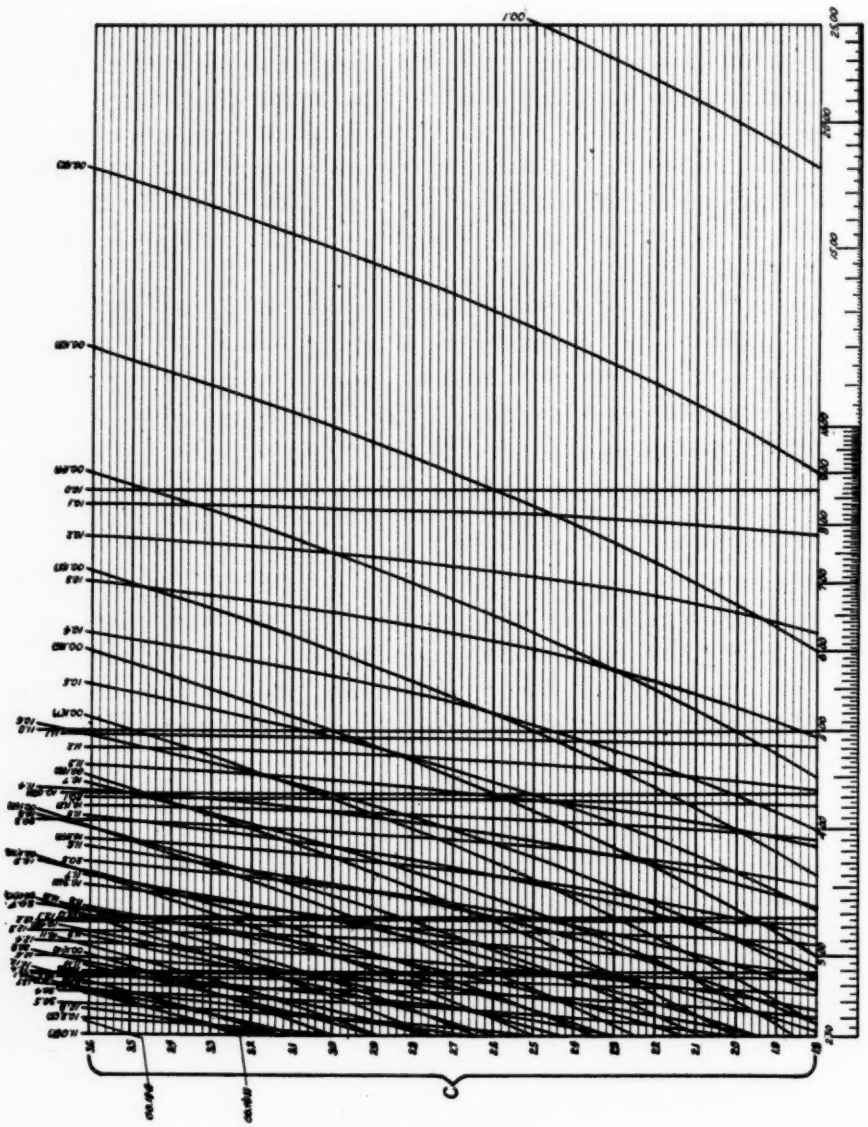

Fig. 6A.

Simple triangular lattice (hexagonal system).

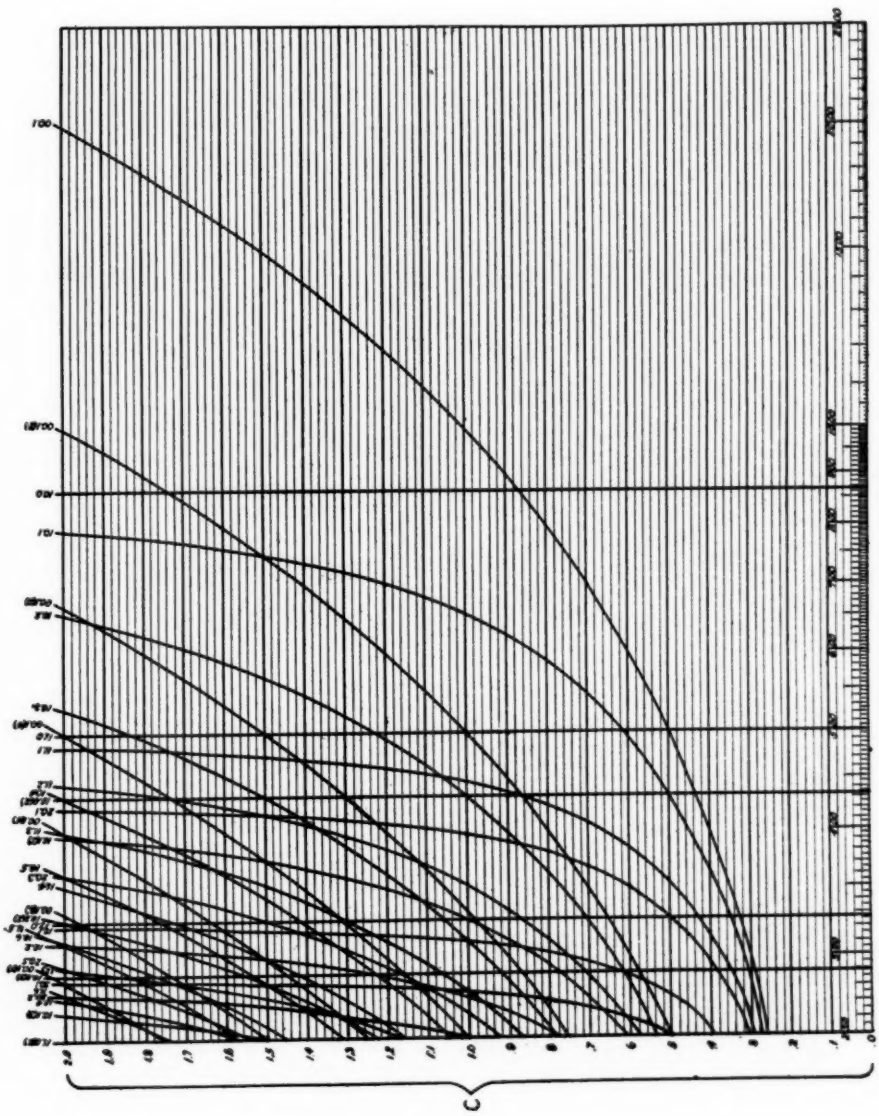

Fig. 6B.

Simple triangular lattice (hexagonal system).

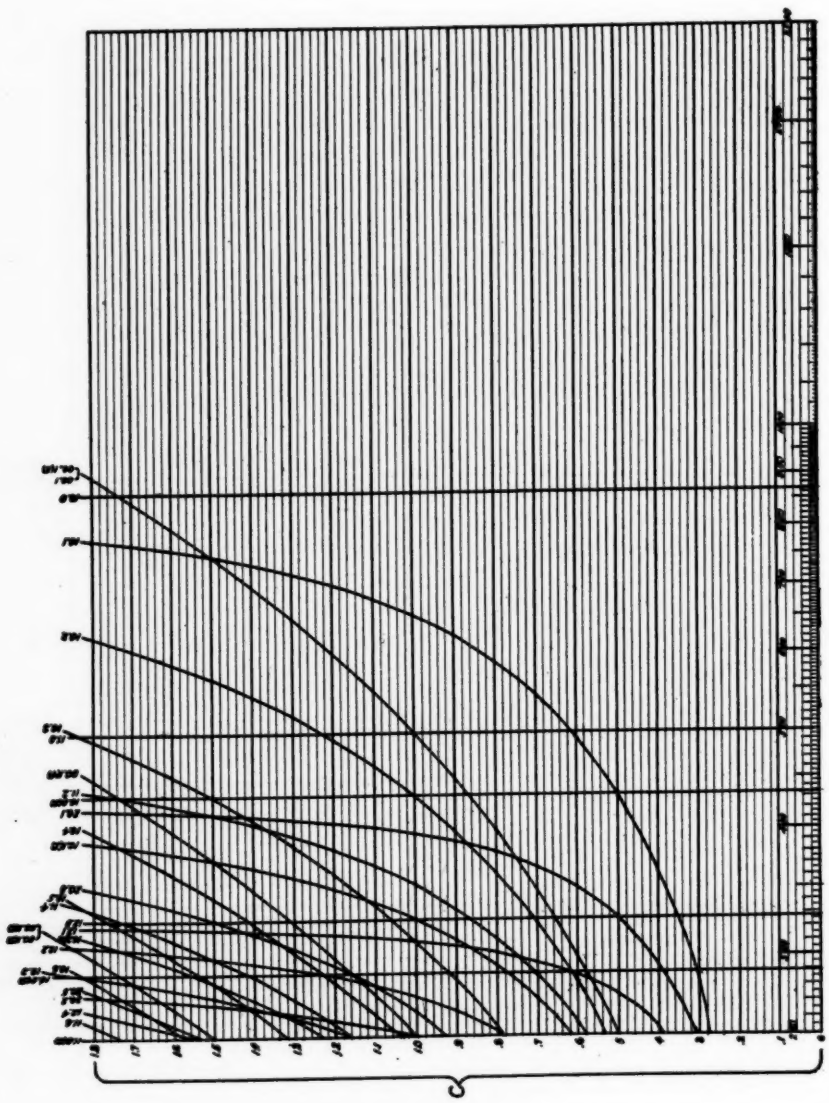

Fig. 7A.

Triangular close packing lattice (hexagonal system).

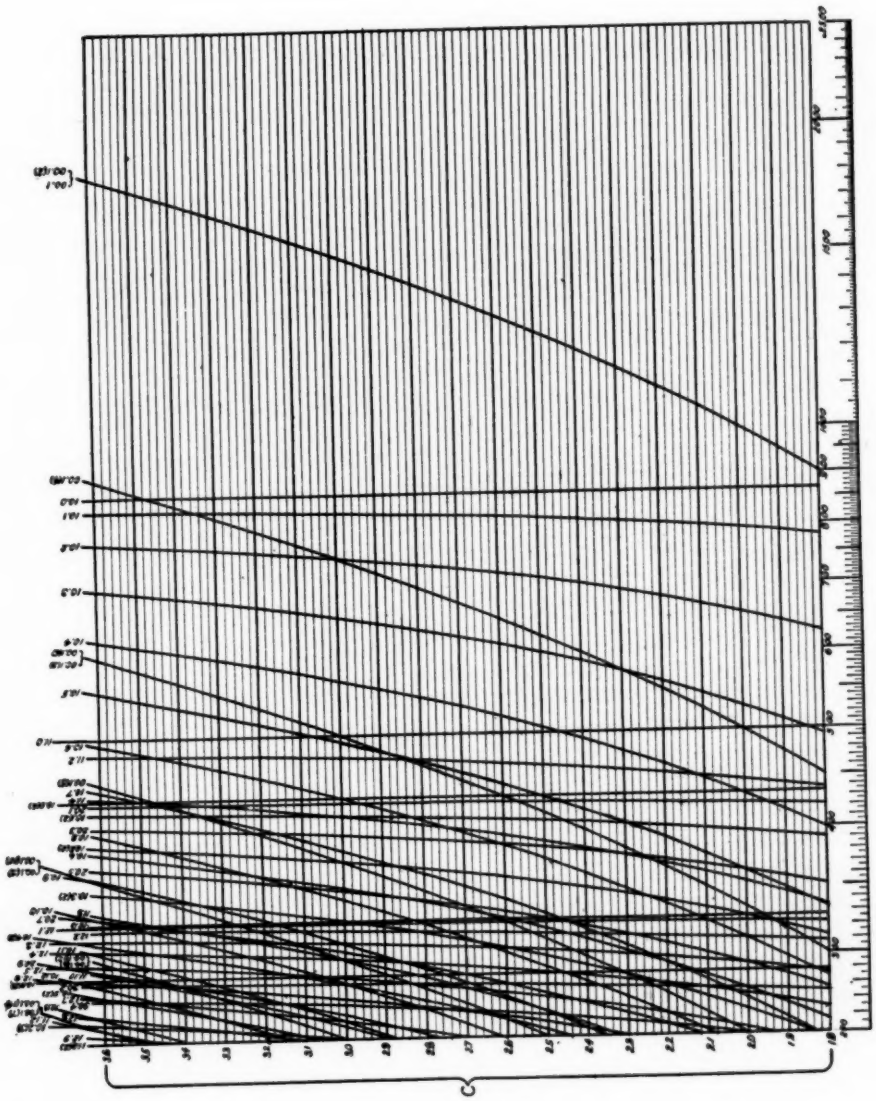

Fig. 7B.

Triangular close packing lattice (hexagonal system).

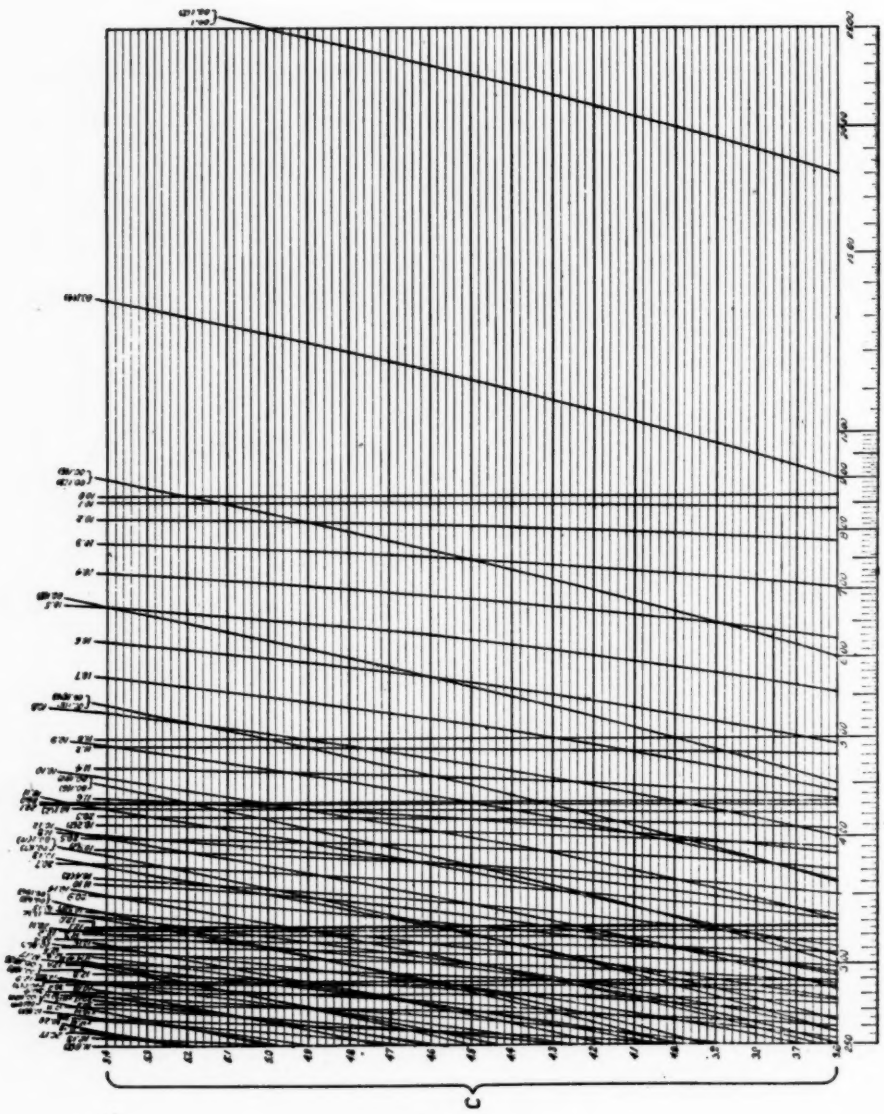

Fig. 7C.

Triangular close packing lattice (hexagonal system). [Scale 1 per cent. larger than the others.]

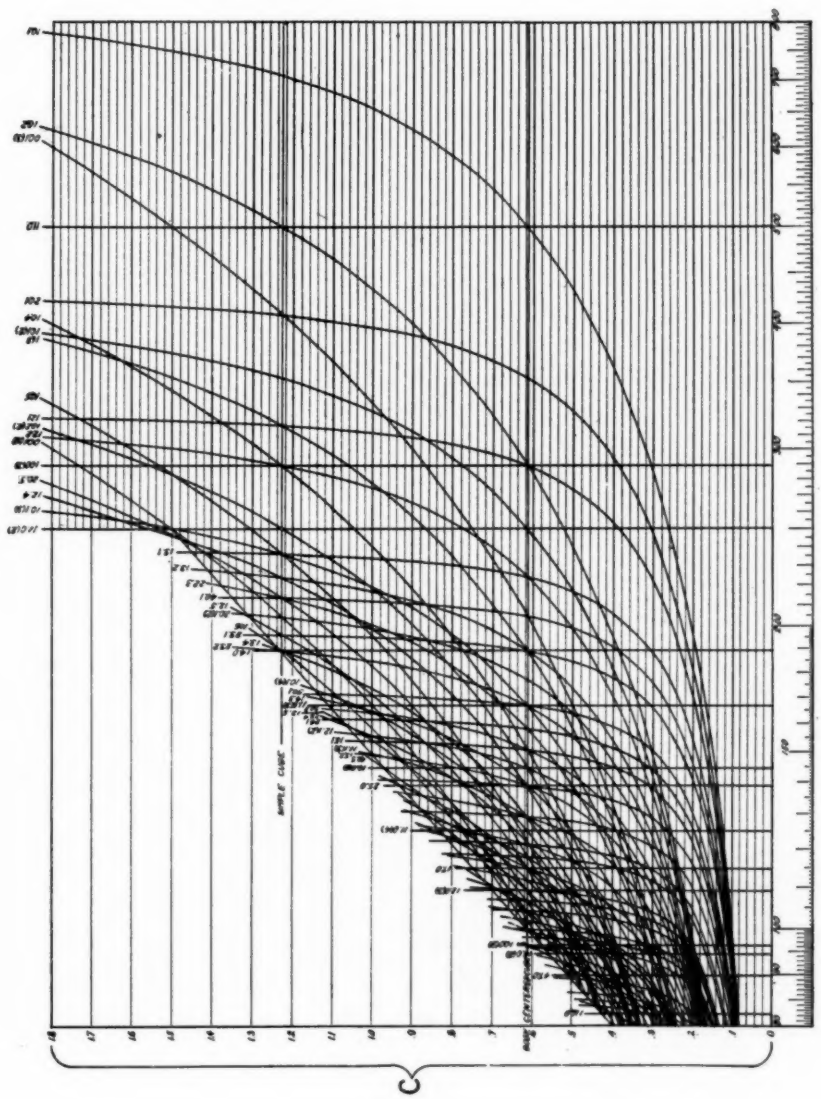

Fig. 8A.

Rhombohedral lattice (hexagonal system). [Scale 1 per cent. smaller than the others.]

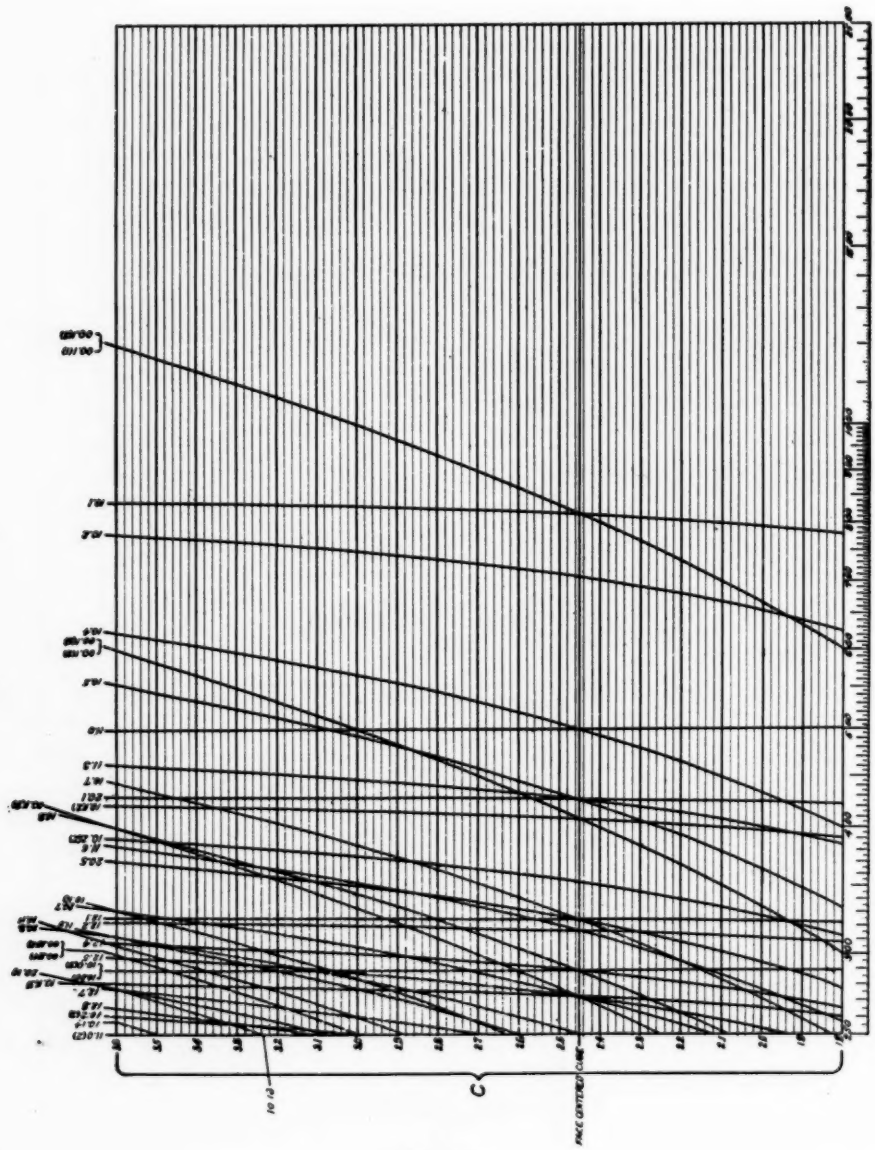

Fig. 8B.

Rhombohedral lattice (hexagonal system).

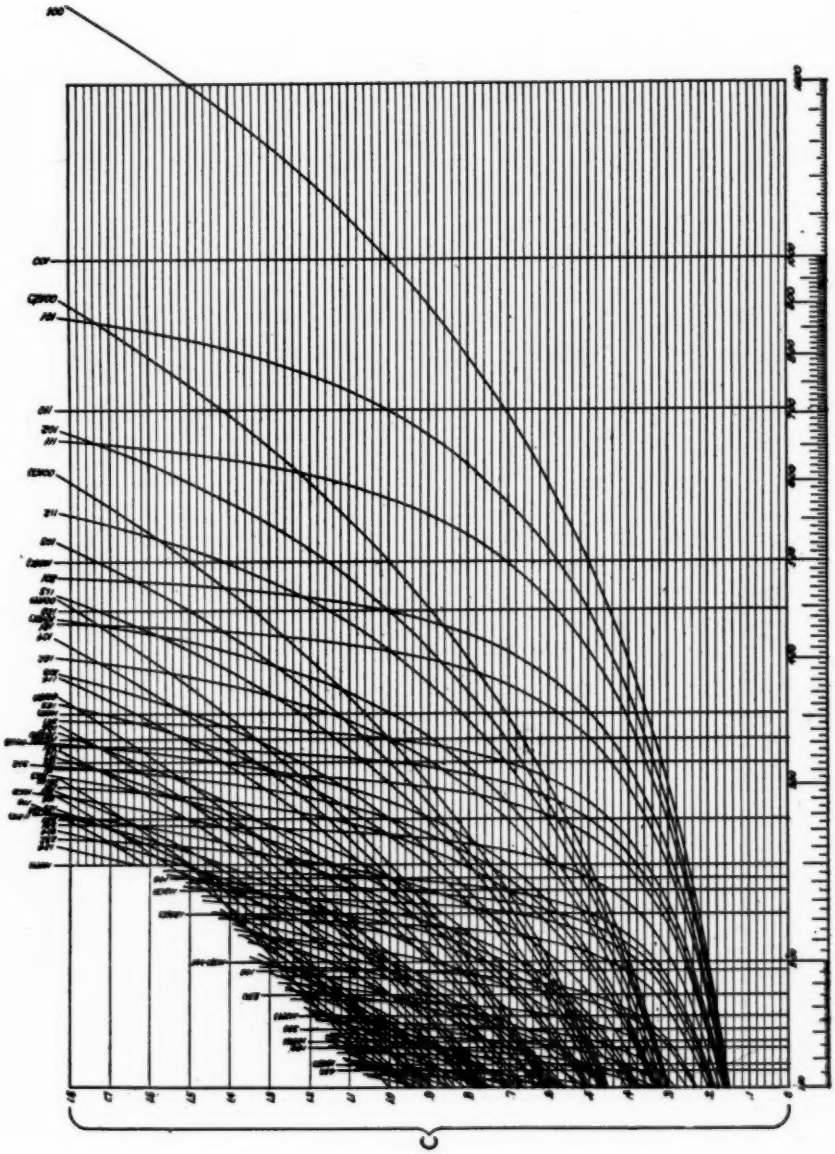

Fig. 9.

Simple tetragonal lattice. [Scale ½ per cent. smaller than the others.]

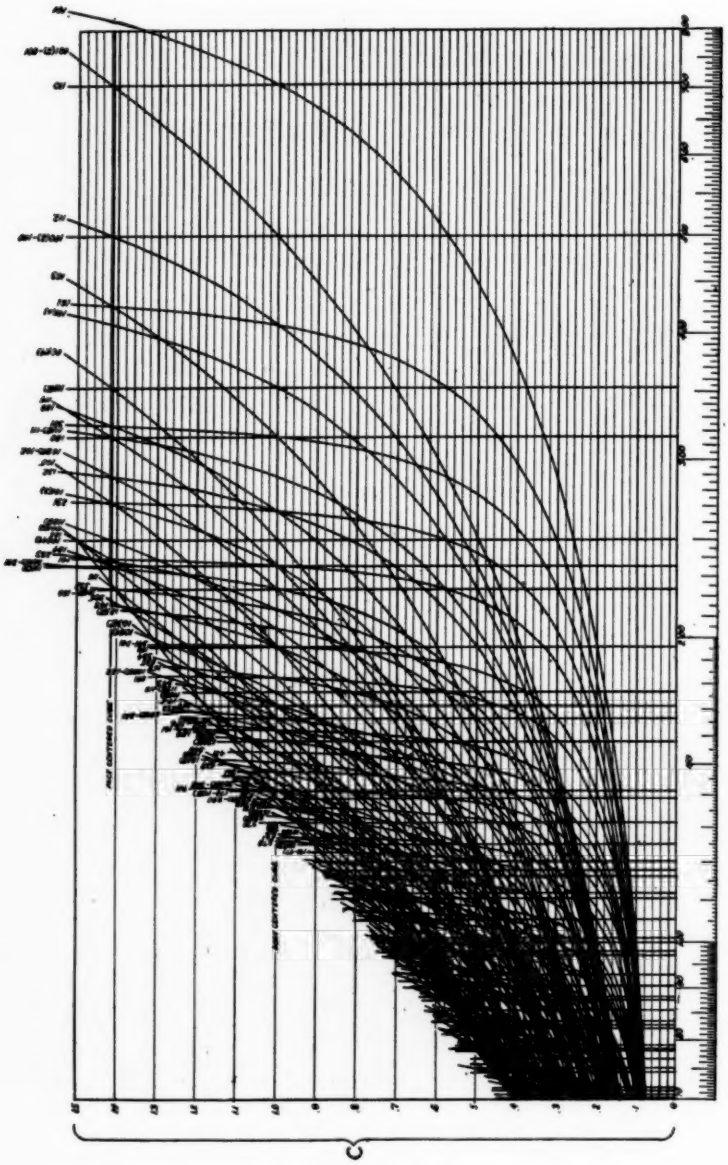

Fig. 10.

Body-centered tetragonal lattice.

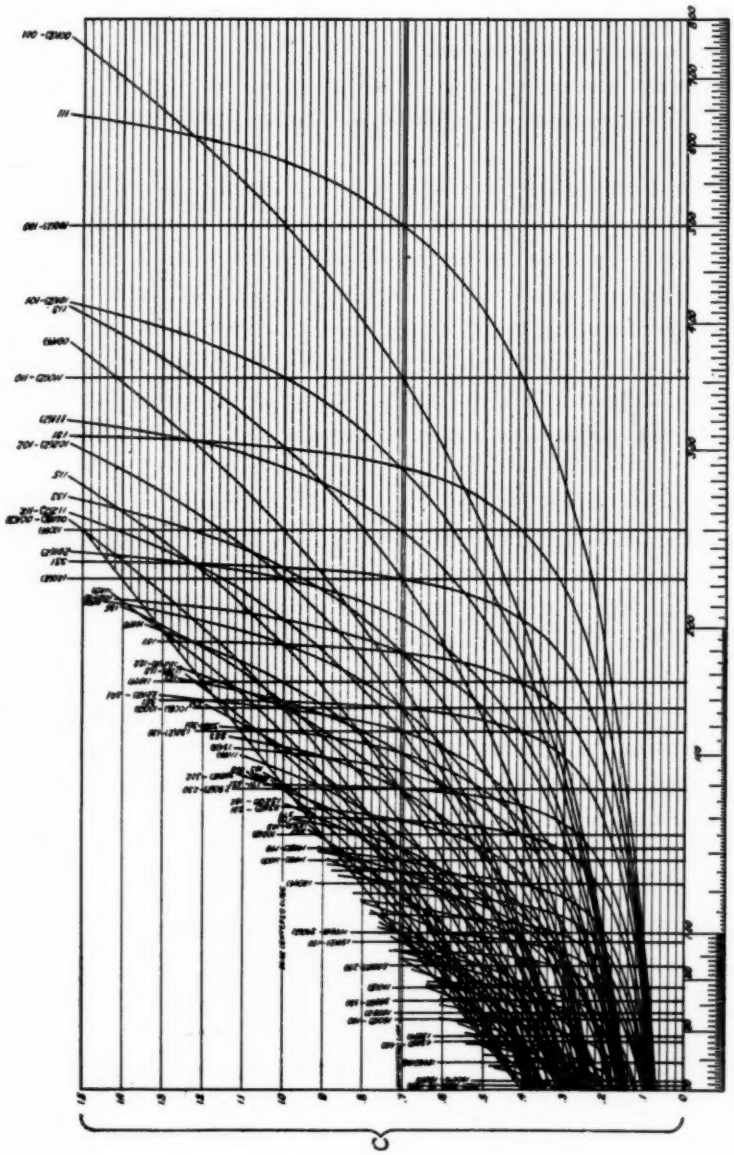

Fig. 11.

Face-centered tetragonal lattice.

1. All possible arrangements of atoms in the cubic, tetragonal, or hexagonal systems may be obtained by the combination of one or more identical simple space lattices of cubes, right tetragonal prisms, and right 60° triangular prisms respectively.

2. The intermeshing of two or more identical lattices weakens or causes to disappear some of the lines due to a single lattice, but can add no new lines.

The cubic forms may be found on either the tetragonal or hexagonal plots. For example, the simple cube is given by the simple tetragonal lattice with axial ratio 1.00, or the rhombohedral lattice with axial ratio 1.225; the centered cube by the centered tetragonal lattice with axial ratio 1.00, the face-centered tetragonal lattice with axial ratio .707, or rhombohedral lattice with axial ratio .612; the face-centered cube by the face-centered tetragonal lattice with axial ratio 1.00, the centered tetragonal lattice with axial ratio 1.414, or the rhombohedral lattice with axial ratio 2.45.

For the other three crystal systems, the orthorhombic, monoclinic, and tri-clinic, the graphical solution is less simple, since the relative crystal spacings must be expressed as a function of 2, 3, and 5 variables respectively. No simple method of representing these relations in a single plot is available, but in practice it may be found that many crystals belonging to these systems approximate sufficiently closely to one of the systems of higher symmetry, represented in Figs. 6–11, to enable the correct lattice to be guessed approximately from these plots, and found by a few trial calculations.

RESEARCH LABORATORY,
GENERAL ELECTRIC COMPANY,
Schenectady, N. Y.

X-RAY CRYSTAL ANALYSIS OF THIRTEEN COMMON METALS.[1]

By Albert W. Hull.

Synopsis.

Crystal Structure of Thirteen Metals Determined by X-ray Analysis.—The author's method of powder analysis was used. In the case of anisometric substances, the crystal system and axial ratio were found by means of plots by the method described in the preceding paper.[2] The lattices of *chromium*, *molybdenum* and *tantalum* were found to be body centered cubes with sides 2.895, 3.143 and 3.272 Å. respectively; *cobalt alpha*, *nickel*, *rhodium*, *palladium*, *iridium* and *platinum* have face centered cubic lattices with the sides of the cubes 3.554, 3.540, 3.820, 3.950, 3.805 and 3.930 Å. respectively; *cobalt beta*, *zinc*, *cadmium* and *ruthenium* have hexagonal lattices of the "close-packed" type with axial ratios 1.63, 1.86, 1.89 and 1.59 respectively and with the triangular sides 2.514, 2.670, 2.960 and 2.686 Å. respectively; and *indium* has a face-centered tetragonal lattice with axial ratio 1.06 and the side of elementary prism 4.58 Å. The structures found for cadmium, zinc and indium are close packed arrangements of solid prolate spheroids while that for ruthenium is a close packed arrangement of oblate spheroids.

Introduction.

THE extension of the Bragg method of crystal analysis to powdered materials has been described elsewhere[3] and need be only briefly summarized here. The photographs were taken with the same apparatus and in the same manner as those previously described, and the interpretations were made in the same manner, except that the process of guessing the correct lattice was greatly simplified by the use of logarithmic plots of crystal spacings against axial ratio. These plots are fully described in the preceding paper.[4]

For convenience of reference, the arrangement of apparatus is reproduced in Fig. 1. Intense characteristic X-rays of wave-length 0.712 Å. were produced by a water-cooled molybdenum Coolidge tube, running at 30,000 volts constant potential and 30 milliamperes. A filter, consisting of a thin sheet of cellulose binding material containing .05 gram

[1] The results of these analysis have been briefly announced elsewhere: Co, Ni, Cr, Mo, and Pt in Proc. A. I. E. E., 38, 1189, 1919; the rest in Science, 52, 227, Sept. 3, 1920.

[2] Graphical Determination of Hexagonal and Tetragonal Crystal Structures from X-Ray Data, by Albert W. Hull and Wheeler P. Davey. This number, pp. 549–570.

[3] Phys. Rev., 10, 661, 1917.

[4] Loc. cit.

of ZrO_2 per cm.^{2}, absorbed almost completely all wave-lengths except the K-alpha doublet, giving a monochromatic source. The smooth face of the X-ray target made an angle of 10° with the line joining it to the two defining slits. These were each 2 mm. wide and 1 cm. high, and 9 and 13 cm. respectively from the focal spot. This gave an intense beam of approximately 1° angular width, with a halo, due to rays pro-

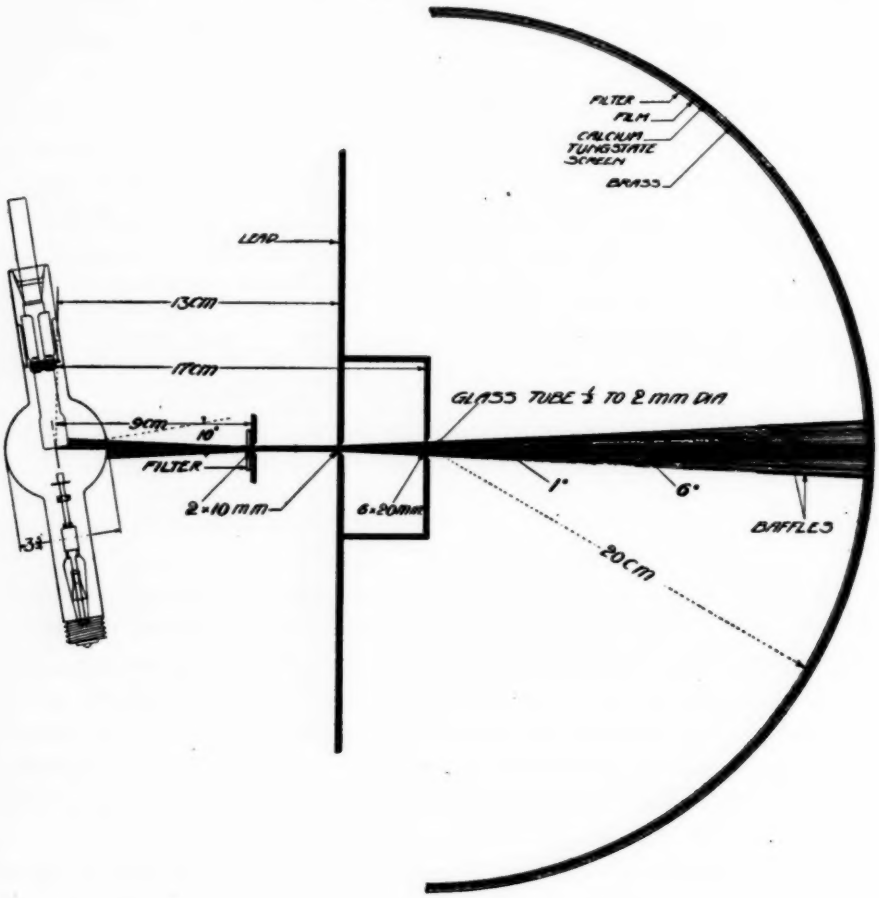

Fig. 1.

ceeding from the face and stem of the target, and secondary rays from other parts of the tube and lead box, of about 6°. A third slit, 6 mm. wide and 2 cm. high, was placed 4 cm. beyond the second defining slit; *i.e.*, 17 cm. from the focal spot. This slit was wide enough so that no primary rays which were able to get through the first two slits could strike it, and its function was to prevent secondary rays from the second slit from reaching the photographic film, except for an angular width of about 8° in the center.

Fig. 2.

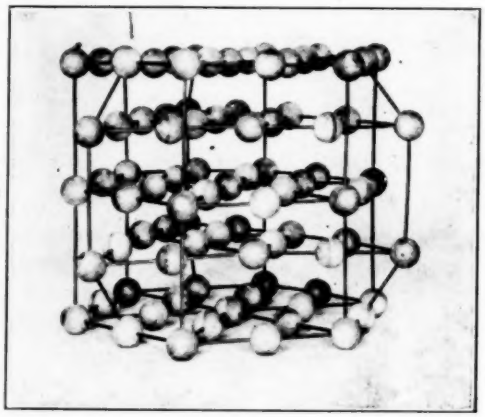

Fig. 3.

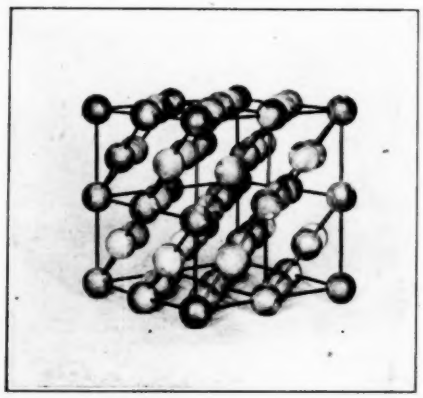

Fig. 4.

ALBERT W. HULL.

The powdered material to be examined was mounted in a thin-walled glass tube, of diameter ½ to 2 mm., according to density, directly in front of the third slit, and at the center of a semicircular brass frame of 20 cm. radius. Upon this frame was mounted a strip of standard Eastman portrait film 4 cm. wide and 60 cm. long, backed by a calcium tungstate intensifying screen. A second filter[1] sometimes of .0025 cm. iron, but generally and preferably a thin strip of cellulose containing .025 g. of ZrO_2 per cm.^{2}, was placed directly in front of the film to absorb fluorescent secondary rays from the powder. These rays, though they produce no lines, are often 100 times as intense as the scattered rays which produce the line patterns, and their fog completely obscures the lines. The exposure was usually over night, about 15 hours.

A typical film is shown in Fig. 2.

The films were measured on a standard Keuffel and Esser log log slide rule, with movable scale removed. The film was fastened with paper clips to the rule, with its center line at the zero of the scale of equal parts. The glass slider was then moved over the film, its index line placed successively over the centers of the lines on the film, viewed as a transparency, and the distances in metric inches read off on the scale of equal parts at the bottom. The lines on both sides of the center were read independently, so that any scratch or false line, as well as mistakes in measurement, could be detected by comparison, and the accuracy of reading could be estimated. The readings on the two sides always agreed within about ¼ of 1 per cent.

These distances of the lines from the center of the film were reduced to crystal degrees by dividing by 2 (radius of film $\times 2\pi/360$), or 0.2777, and then to planar spacings in Ångstroms by taking the quotient $\lambda/(2 \sin \theta)$ according to Bragg's law.

In the following tables only the planar spacings, with the estimated intensities of the lines from which they are calculated, will be given. The scale of intensities is chosen so that intensity 1 represents the weakest line that can be identified with certainty. Lines with intensity ½ or even ¼ are considered reliable if found in identical positions on both sides of the film.

For comparison with the observed spacings, the calculated spacings are given; *i.e.*, those of a theoretical lattice of the type assumed, as calculated by the equations published in an earlier paper.[2]

The calculation of the theoretical intensities of the lines requires a knowledge of the effect of temperature, absorption, size of crystals,

[1] The first filter was between the X-ray tube and first slit.

[2] PHYS. REV., 10, 671, 677, 1917.

shape of atoms, and variation of ideal reflecting power with angle, in addition to the number of coöperating planes. The effect of all these factors except the last, is to produce a nearly uniform decrease of intensity with increasing angle. The large fluctuations in intensity of consecutive lines are due to the variation in the number of different sets of planes which coöperate to produce the respective lines. Hence a comparison of the number of coöperating planes with the observed intensities is a valuable check on the correctness of the identification of the lines. These numbers are given in the second column.

As a final check the densities calculated from the X-ray data, by dividing the mass of the atoms in an elementary cell by the volume of the cell, are compared with the best values obtained by standard methods, as given in Van Nostrand's Chemical Annual for 1918.

TABLE I.

Chromium.

A sample of very fine chromium powder, from the Metal and Thermit Company, gave the following spacings:

Intensity of Line.	Number of Coöperating Planes.	Planar Spacings.		Indices of Form.
		Observed.	Calculated.	
100	6	2.048	2.047	100
20	3	1.448	1.448	100 (2)
50	12	1.183	1.183	211
10	6	1.025	1.024	110 (2)
30	12	.915	.915	310
5	4	.837	.836	111 (2)
30	24	.774	.774	321
½	3	.723	.724	100 (4)
20	18	.682	.683	411 110 (3)
5	12	.648	.647	210
2	12	.617	.617	332
1	12	.591	.591	211 (2)
15	36	.567	.567	431 510

Type of Lattice	Body-centered Cube.
Side of elementary cube	2.895 Å.
Distance between nearest atoms	2.508 Å.
Density from X-ray measurements	7.07
Density from standard methods	6.92

The calculated spacings are those of a *body centered cubic lattice*, the side of the cube being 2.895 Å., and the distance between nearest atoms 2.508 Å.

Since there are two atoms per elementary cube, the ideal density is

$$\frac{\text{mass}}{\text{volume}} = \frac{2M}{d_0^3} = \frac{2 \times 52.0 \times 1.650}{(2.895)^3} = 7.07;$$

M = mass of 1 atom in grams; d_0 = side of elementary cube in cm.

The density given by Van Nostrand is 6.92.

TABLE II.

Molybdenum.

Very fine powder, by reduction of oxide in H_2. Excellent photograph.

Intensity of Line.	Number of Coöperating Planes	Spacing of Planes.		Indices of Forms.
		Observed.	Calculated.	
100	6	2.215	2.221	110
50	3	1.569	1.571	100 (2)
100	12	1.283	1.284	211
35	6	1.109	1.111	110 (2)
60	12	.993	.993	310
10	4	.907	.907	111 (2)
70	24	.839	.839	321
5	3	.784	.785	100 (4)
30	18	.739	.740	110 (3), 411
20	12	.702	.702	210 (2)
20	12	.669	.670	332
20	12	.641	.641	211 (2)
35	36	.616	.616	431, 510
25	24	.574	.574	521
5	6	.554	.555	110 (4)
25	24	.538	.538	530, 433
20	15	.523	.525	100 (3), 221

Type of Lattice	Body-centered Cube.
Side of elementary cube	3.143 Å.
Distance between nearest atoms	2.720 Å.
Density from X-ray data	10.16
Density by standard methods	10.28

These spacings are identical, within experimental error, with those of tungsten. In order to detect the difference, if any, a special photograph was taken, giving tungsten and molybdenum on the same film, one above the other. This was accomplished by filling the lower half of a small glass tube with Mo and the upper half with W, and placing it symmetrically in the X-ray beam so that both halves received equal radiation. A brass septum prevented overlapping of the scattered radiation from the two samples.

This photograph showed the first 6 lines of W exactly above those of Mo. The seventh W line was noticeably displaced from that of Mo, and the fifteenth lines were displaced by the difference between the components of the clearly resolved α doublet (cf. Fig. 1), about 2 mm. The Mo lines were the farther from the center, on both sides, thus eliminating any error due to imperfect alignment of the samples.

This gives tungsten a spacing $\frac{1}{4}$ per cent. *greater* than that of Mo, viz., 3.150.

TABLE III.

Tantalum.

Filaments, taken from lamp, crushed. Very faint photograph.

Intensity of Line.	Number of Coöperating Planes.	Spacing of Planes.		Indices of Form.
		Observed.	Calculated.	
10	6	2.315	2.315	110
3	3	1.636	1.636	100 (2)
15	12	1.335	1.335	211
4	6	1.157	1.158	110 (2)
3	12	1.033	1.033	310
2	4	.946	.944	111 (2)
8	24	.872	.874	321
$\frac{1}{2}$	3	.818	.819	100 (4)
3	18	.773	.773	110 (3) 411
$\frac{1}{2}$	12	.732	.732	210 (2)
$\frac{1}{2}$	12	.697	.697	332
$\frac{1}{2}$	12	.667	.667	211 (2)
1	36	.643	.642	431 510

Type of Lattice	Body-centered Cube.
Side of elementary cube	3.272 Å.
Distance between nearest atoms	2.833 Å.
Density from X-ray data	17.09
Density by standard methods	14.49[1]

COBALT.

The powder photographs of cobalt show two crystalline forms, one face-centered cubic and the other hexagonal close packed, both stable at room temperature.

The relation of these two forms to each other, and especially to heat treatment and mechanical working, has not yet been studied.

Tests were made upon samples prepared in three different ways.

1. Two carefully analyzed samples of very pure cobalt were kindly

[1] This is the value given by Van Nostrand. The most recent determination cited by Landolt & Börnstein (v. Bolton, Zs. Electroch., 11, 45, '05) gives 16.64, in better agreement with the X-ray data.

furnished for this investigation by Dr. H. T. Kalmus. Filings from these samples gave identical patterns of lines, with the spacings given in Table IV. They show *a perfect hexagonal close-packed lattice* with no

TABLE IV.

Cobalt (1).[1]

Filings from cast cobalt (Kalmus), 99.7 per cent. pure.

Number of Coöperating Planes, N.	Phase Factor, F.	NF.	Intensity of Line (Estimated).	Spacing of Planes.		Indices of Form.
				Observed.	Calculated.	
3	$\frac{1}{4}$	.75	30	2.182	2.176	$10\bar{1}0$
1	1	1.	25	2.055	2.051	0001 (2)
6	$\frac{3}{4}$	4.5	50	1.920	1.920	$10\bar{1}1$
6	$\frac{1}{4}$	1.5	2	1.490	1.493	$10\bar{1}2$
3	1	3.	20	1.250	1.257	$11\bar{2}0$
6	$\frac{3}{4}$	4.5	5	1.145	1.158	$10\bar{1}3$
6	$\frac{1}{4}$	1.5	...	....	1.089	$10\bar{1}0$ (2)
6	1	6.	15	1.064	1.072	$11\bar{2}2$
6	$\frac{3}{4}$	4.5	5	1.045	1.051	$20\bar{2}1$
1	1	1.	$\frac{1}{2}$	1.013	1.026	0001 (4)
6	$\frac{1}{4}$	1.5	$\frac{1}{2}$	.953	.961	$10\bar{1}1$ (2)
6	$\frac{1}{4}$	1.5	...	...	.928	$10\bar{1}4$
6	$\frac{3}{4}$	4.5	2	.839	.853	$20\bar{2}3$
6	$\frac{1}{4}$	1.5	...	...	.823	$21\bar{3}0$
12	$\frac{3}{4}$	9.	2	.797	.807	$21\bar{3}1$
6	1	6.	2	.788	.794	$11\bar{2}4$
6	$\frac{3}{4}$	4.5	1	.752	.768	$10\bar{1}5$
12	$\frac{1}{4}$	3.	(wide)		.765	$21\bar{3}2$
6	$\frac{1}{4}$	1.5	$\frac{1}{4}$	.738	.747	$10\bar{1}2$ (2)
3	1	3.	$\frac{1}{4}$	.717	.727	$10\bar{1}0$ (3)

Type of Lattice	**Hexagonal Close-packed.**
Axial ratio	1.633
Side of elementary triangular prism	2.514 Å.
Distance between nearest atoms	2.514 Å.
Density { from X-ray data	8.66
Density { by standard methods	8.718

trace of a cubic form. The same filings, after annealing in H_2 at 600° for 6 hours, showed a mixture of cubic and hexagonal close packing in about equal proportions. It was not found possible by annealing at this temperature to cause the crystallization to go over entirely from hexagonal to cubic form.

[1] This film was taken in a casette of only 10 cm. radius, with the Co filings spread on a thin film nearly 3 mm. wide, and there is a systematic error in the readings, amounting to about 1 per cent. for the largest spacings. The accuracy is sufficient for the purpose, which is to show the perfect hexagonal character of the lattice. The correctness of the value chosen for the fundamental spacing was checked by other films.

2. A sample of fine powder, prepared by reduction of cobalt oxide in H_2 at about 600°, gave the spacings shown in Table V. These correspond to *a perfect cubic close-packed lattice.* A very faint trace of the hexagonal form is present, as shown by the first and third lines, 2.162 Å. and 1.922 Å. respectively.

TABLE V.

Cobalt (2).

Fine cobalt powder, from oxide reduced in H_2 at 600°. Lines broken and irregular, due to large crystals, making the estimation of intensities difficult, but not interfering with the measurement of the spacings.

Intensity of Line.	Number of Coöperating Planes.	Spacing of Planes.		Indices of Form.
		Observed.	Calculated.	
1	..	2.162	....	...
12	4	2.035	2.051	111
¼	..	1.922	....	...
1	3	1.775	1.777	100 (2)
10	6	1.257	1.257	110 (2)
12	12	1.071	1.072	311
1	4	1.024	1.025	111 (2)
¼	3	.888	.888	100 (4)
½	12	.814	.815	311
5	12	.795	.794	210 (2)
1	12	.726	.725	211 (2)
2	16	.686	.684	511 111 (3)
1	6	.630	.628	110 (4)
1	24	.603	.601	531
1	15	.595	.594	100 (6) 221 (2)

Type of Lattice	**Face-centered Cubic.**
Side of elementary cube	3.554
Distance between nearest atoms	2.514
Density from X-ray data	8.66
Density by standard methods	8.718

3. A third sample, prepared by dissolving a portion of sample 1, pure Kalmus cobalt, in H_2SO_4 and electrolyzing, showed *a mixture of about equal amounts of the two forms.* The spacings are tabulated in Table VI., together with the theoretical spacings of both the cubic and hexagonal lattices. It is seen that practically *all the spacings of both lattices are present.*

In Table IV. two extra columns have been added, to take account of the fact that in the hexagonal close-packed lattice the number of planes which coöperate to produce a line is not a correct index of the intensity to be expected, even for consecutive lines, since in some sets of planes the planes are not equally spaced, and hence their reflections are not all in

phase. The number, N, of coöperating sets of planes must be multiplied by the "phase factor," F, of each set of planes, which is the ratio of the square of the sum of the amplitudes of reflection from all the planes in the set *added as vectors*, to the square of their algebraic sum. The product NF will be seen to represent very well the fluctuations in intensity of consecutive lines, thus confirming their identification.

TABLE VI.

Cobalt (3).

Fine powder, obtained by rapid electrolysis of sulphate. Lines rather diffuse.

Intensity of Line.	Spacing of Planes.		
	Observed.	Theoretical Face-centered Cubic.	Theoretical Hexagonal Close-packed.
5	2.158	....	2.176
20	2.037	2.051	2.051
20	1.915	....	1.920
3	1.773	1.777	....
½	1.484	....	1.493
10	1.250	1.257	1.257
2	1.148	....	1.158
...	....	....	1.089
12	1.066	1.072	1.072
3	1.045	....	1.051
2	1.017	1.025	1.025
1	.952	...	.961
...	...	...	.928
...	...	.888	...
¼	.846	...	.853
...	...	...	.823
...	...	.815	...
½	.802	...	.807
1	.787	.794	.794
...	...	...	.768
...	...	...	.765
...	...	...	.747
¼	.723	.725	.727
¼	.701	...	.706
¼	.682	.684	.684

NICKEL.

In a previous paper[1] some preliminary measurements on nickel were reported, which seemed to indicate two crystal forms, one face-centered cubic, the other body-centered cubic. The photographs were very poor, and the results were given as questionable.

These experiments have been repeated with great care. Many photo-

[1] PHYS. REV., 10, 692, 1917.

graphs have been taken of nickel powder prepared in different ways, including electrolysis, reduction of oxide in hydrogen, filings from cast nickel, and the same annealed in hydrogen at different temperatures. *All gave identical patterns of lines, showing face centered cubic structure.* The samples used in the preliminary tests have been lost so that these tests cannot be checked; but sufficient data has been taken to show that the centered cubic form, if it exists, does not appear under ordinary conditions of preparation.

The following measurements, obtained with fine-nickel powder prepared by rapid electrolysis of nickel ammonium sulphate, are typical:

TABLE VII.

Nickel.

Fine powder, by electrolysis of nickel ammonium sulphate.

Intensity of Line.	Number of Coöperating Planes.	Spacing of Planes.		Indices of Form.
		Observed.	Calculated.	
50	4	2.038	2.042	111
25	3	1.766	1.770	100 (2)
20	6	1.252	1.253	110 (2)
30	12	1.067	1.065	311
5	4	1.022	1.022	111 (2)
1	3	.884	.885	100 (4)
10	12	.812	.812	331
8	12	.791	.791	210 (2)
5	12	.723	.722	211 (2)
5	16	.681	.681	111 (3) 511
½	6	.625	.625	110 (4)
4	24	.598	.598	531
2	15	.590	.591	100 (6) 221

Type of Lattice	**Face-centered Cubic.**
Side of elementary cube	3.540 Å.
Distance between nearest atoms	2.505 Å.
Density from X-ray data	8.72
Density by standard methods	8.6–8.93

ZINC.

The planar spacings obtained from measurements of the powder diffraction pattern do not fit an hexagonal lattice with the axial ratio 1.356 calculated from crystallographic measurements.[1] The determination of the true axial ratio, 1.860, by means of graphs representing planar spacings as a function of axial ratio, is described in the preceding

[1] See Groth, Chemische Krystallographie, Vol. 1.

TABLE VIII.

Rhodium.

Fine powder, from electrolysis of pure rhodium chloride.

Intensity of Line.	Number of Coöperating Planes.	Spacing of Planes.		Indices of Form.
		Observed.	Calculated.	
50	4	2.200	2.203	111
10	3	1.908	1.910	100 (2)
10	6	1.350	1.353	110 (2)
15	12	1.150	1.150	311
2	4	1.100	1.103	111 (2)
...	3	...	.955	100 (4)
2	12	.878	.875	331
1.5	12	.853	.853	210 (2)
1.0	12	.781	.779	211 (2)
½	16	.736	.731	111 (3) 511
...	6	...	.675	110 (4)
½	24	.647	.646	531

Type of Lattice ..... Face-centered Cubic.
Side of elementary cube ..... 3.820 Å.
Distance between nearest atoms 2.700
Density { from X-ray data 12.18
by standard method 12.1

TABLE IX.

Palladium.

Powder very fine, lines diffuse and faint.

Intensity of Line.	Number of Coöperating Planes.	Spacing of Planes.		Indices of Form.
		Observed.	Calculated.	
10	4	2.274	2.280	111
4	3	1.966	1.975	100 (2)
10	6	1.398	1.399	110 (2)
15	12	1.192	1.189	311
...	4	...	1.140	111 (2)
...	3	...	.987	100 (4)
3	12	.909	.906	331
1	12	.886	.882	210 (2)
1	12	.807	.806	211 (2)
⅔	16	.759	.760	111 (3) 511
...	6	...	.697	110 (2)
½	24	.668	.668	531
¼	15	.656	.660	100 (6) 221 (2)

Type of Lattice ..... Face-centered Cubic.
Side of elementary cube 3.950
Distance between nearest atoms ..... 2.795 Å.
Density { from X-ray data 11.40
by standard methods ..... 11.4 to 11.9

TABLE X.

Iridium.

Powder very fine, lines diffuse and faint.

Intensity of Line.	Number of Coöperating Plants.	Spacing of Planes.		Indices of Forms.
		Observed.	Calculated.	
4	4	2.185	2.193	111
2	3	1.898	1.902	100 (2)
4	6	1.346	1.347	110 (2)
4	12	1.150	1.145	311
1	4	1.092	1.096	111 (2)
..	3	...	.952	100 (4)
2	12	.872	.872	331
½	12	.847	.850	210 (2)
½	12	.776	.776	211 (2)
½	16	.732	.732	111 (3) 511
..	6	...	.672	100 (6)
2	24	.642	.643	531

Type of Lattice ..... Face-centered Cubic
Side of elementary cube ..... 3.805 Å.
Distance between nearest atoms ..... 2.690 Å.
Density { from X-ray data 23.15
by standard methods 22.42

TABLE XI.

Platinum.

Intensity of Line.	Number of Coöperating Planes.	Spacing of Planes.		Indices of Form.
		Observed.	Calculated.	
10	4	2.265	2.266	111
4	3	1.958	1.964	100 (2)
10	6	1.387	1.390	110 (2)
15	12	1.183	1.183	311
2	4	1.137	1.134	111 (2)
1	3	.983	.983	100 (4)
5	12	.902	.901	331
5	12	.878	.878	210 (2)
4	12	.800	.802	211 (2)
2	16	.758	.756	111 (3) 511
..	6	...	.694	110 (4)
2	24	.663	.664	531
1	15	.658	.657	100 (6) 221 (2)

Type of Lattice ..... Face-centered Cubic.
Side of elementary cube ..... 3.930 Å.
Distance between nearest atoms ..... 2.780 Å.
Density { from X-ray data 21.23
by standard methods 19.96

paper in this number, and only the summary of results need be given here.

The zinc lattice is found to be a combination of two simple right triangular prism lattices, each of axial ratio 1.860, and side of elementary prism 2.670 Å., with the atoms of one lattice at the centers of the prisms of the other lattice. The cartesian coördinates of the positions of the atoms are therefore

$$m,\ n,\ pc,$$

$$m + \tfrac{1}{3},\ n + \tfrac{2}{3},\ (p + \tfrac{1}{2})c,$$

TABLE XII.

Zinc.

Fine powder, from oxide reduced in H_2 at 600° C

Intensity of Line.	Number of Coöperating Planes × Phase Factor.	Spacing of Planes.		Indices of Form.
		Observed.	Calculated.	
3	1.0	2.472	2.466	0001 (2)
1	0.75	2.293	2.295	$10\bar{1}0$
10	4.5	2.077	2.080	$10\bar{1}1$
2	1.5	1.684	1.678	$10\bar{1}2$
10	4.5	1.339	1.337	$10\bar{1}3$
10	3.0	1.332	1.326	$11\bar{2}0$
½	1.0	1.235	1.232	0001 (4)
7	6.0	1.172	1.166	$11\bar{2}2$
½	0.75	1.152	1.148	$10\bar{1}0$ (2)
4	4.5	1.121	1.119	$20\bar{2}1$
½	1.5	1.088	1.087	$10\bar{1}4$
1	1.5	1.044	1.041	$10\bar{1}1$ (2)
2	4.5	.947	.948	$20\bar{2}3$
(doublet, not resolved) 2	4.5	.910	.913	$10\bar{1}5$
(doublet, not resolved) 2	6.0		.910	$11\bar{2}4$
...	1.5	...	.874	$21\bar{3}0$
3	9.0	.859	.861	$21\bar{3}1$
...	1.5	...	.845	$10\bar{1}2$ (2)
1	1.0	.827	.828	0001 (6)
1	3.0		.825	$21\bar{3}2$
...	1.5	...	.778	$10\bar{1}6$
2	9.0	.773	.773	$21\bar{3}3$
2	3.0		.771	$10\bar{1}0$ (3)
1	4.5	.756	.754	$20\bar{2}5$
2	6	.737	.736	$30\bar{3}2$
½	3	.717	.715	$21\bar{3}4$
½	6	.703	.703	$11\bar{2}6$

Type of Lattice	Hexagonal Close-packed
Axial ratio	1.860
Side of elementary triangular prism	2.670 Å.
Distance between nearest atoms: in basal plane	2.670 Å.
Distance between nearest atoms: in pyramid planes	2.920 Å.
Density: from X-ray data	7.04
Density: by standard methods	7.142

where m, n, and p have all possible integral values, c is the axial ratio 1.860, and the unit is the side of the elementary triangular prism, 2.670 Å.

The lattice is shown in Fig. 3. *It is one of the two closest packed arrangements of prolate spheroids whose axes are in the ratio* 1.140 : 1.

Each atom has six nearest neighbors in regular hexagonal arrangement about it (in the basal plane), at distances of 2.670 Å. (between centers), and six others almost as near, viz., 2.92 Å., three in the plane below, and three in exactly similar positions in the plane above.

The density is

$$\rho = \frac{\text{mass of 1 atom}}{\text{volume of triangular prism}}$$

$$= \frac{65.37 \times 1.650}{\frac{1}{4}\sqrt{3} \times (2.670)^3 \times 1.860} = 7.04.$$

CADMIUM.

The interpretation of the data obtained from powder photographs of cadmium, with the help of graphs of planar spacings against axial ratio, has been described in the preceding paper by A. W. Hull and W. P. Davey. The lattice is found to be hexagonal, of the close-packed type, with axial ratio 1.89, instead of the value 1.335 found in the literature.

A new and slightly better photograph gave the data in Table XIII.

The lattice is exactly like that of zinc, except for axial ratio, viz., *a close-packed arrangement of prolate spheroids whose axes are in the ratio* 1.158 : 1. The cartesian coördinates of the positions of the atoms are:

$$m,\ n,\ pc,$$

$$m + \tfrac{1}{3},\ n + \tfrac{2}{3},\ (p + \tfrac{1}{2})c,$$

where m, n, and p represent all possible integral numbers, c is the axial ratio, 1.890, and the unit is the side of the elementary triangular prism, 2.960. The lattice is therefore a combination of two simple lattices of right triangular prisms, each of side 2.960 Å. and height $1.89 \times 2.960 = 5.60$ Å., with the atoms of one lattice at the centers of the prisms of the other, and vice versa. Each atom is surrounded by six others, in the basal plane, in a regular hexagon about it, at distances of 2.960 Å., and by six others, almost as near, viz., 3.28 Å., three in the plane below and three in exactly similar arrangement in the plane above.

$$\text{The density} = \frac{\text{mass of one atom}}{\text{volume of triangular prism}} = 8.74.$$

Table XIII.

Cadmium.

Filings from pure cast cadmium. A good photograph.

Intensity of Line.	Number of Coöperating Planes × Phase Factor.	Spacing of Planes.		Indices of Form.
		Observed.	Calculated.	
10	1	2.790	2.798	0001 (2)
5	.75	2.565	2.564	$10\bar{1}0$
30	4.5	2.325	2.329	$10\bar{1}1$
6	1.5	1.893	1.892	$10\bar{1}2$
5	4.5	1.508	1.510	$10\bar{1}3$
4	3.0	1.476	1.480	$11\bar{2}0$
½	1.0	1.397	1.399	0001 (4)
5	6.0	1.306	1.311	$11\bar{2}2$
...	.75	1.287	1.283	$10\bar{1}0$ (2)
3	4.5	1.250	1.250	$20\bar{2}1$
½	1.5	1.224	1.230	$10\bar{1}4$
1	1.5	1.166	1.165	$10\bar{1}1$ (2)
1	4.5	1.055	1.057	$20\bar{2}3$
1	4.5	1.024	1.027	$10\bar{1}5$
1	6.0	1.014	1.017	$11\bar{2}4$
...	1.5	...	.969	$21\bar{3}0$
2	9.0	.953	.955	$21\bar{3}1$
...	1.5	...	.946	$10\bar{1}2$ (2)
...	1.0	...	.933	0001 (6)
½	3.0	.914	.915	$21\bar{3}2$
...	1.5	...	.878	$10\bar{1}6$
1.5	9.0	.860	.860	$21\bar{3}3$
...	3.0	...	.855	$10\bar{1}0$ (3)
½	4.5	.843	.844	$20\bar{2}5$
½	6.0	.817	.818	$30\bar{3}2$
...	3.0	...	.790	$21\bar{3}4$
...	6.0	...	.787	$11\bar{2}6$
½	4.5	.762	.765	$10\bar{1}7$
...	1.5	...	.756	$10\bar{1}3$ (2)
...	3.0	...	.740	$11\bar{2}0$ (2)
1	9.0	.732	.732	$21\bar{3}5$
½	6.0	.716	.715	$11\bar{2}1$ (2)
...	1.5	...	.710	$31\bar{4}0$
½	9.0	.706	.705	$31\bar{4}1$

Type of Lattice ..... **Hexagonal Close-packed.**

Axial ratio 1.89

Side of elementary triangular prism ..... 2.960 Å.

Distance between nearest atoms { in basal plane ..... 2.960 Å. / in pyramid plane ..... 3.280 Å.

Density { from X-ray data ..... 8.74 / by standard methods 8.642

RUTHENIUM.

There is no crystallographic data regarding ruthenium. The procedure was therefore as follows: A powder photograph was taken in the usual manner, the lines measured and the experimental crystal spacings calculated. These spacings were then laid off on a strip of paper, as described in the preceding article, and this strip moved over the different plots until a position was found on one of them where the experimental lines exactly matched the theoretical lines of the plot.

TABLE XIV.

Ruthenium.

Intensity of Line.	No. of Coöperating Planes × Phase Factor.	Spacing of Planes.		Indices of Form.
		Observed.	Calculated.	
3	0.75	2.315	2.325	$10\bar{1}0$
¼	1.0	2.160	2.134	0001 (2)
10	4.5	2.040	2.040	$10\bar{1}1$
2	1.5	1.572	1.575	$10\bar{1}2$
5	3.0	1.343	1.343	$11\bar{2}0$
5	4.5	1.212	1.214	$10\bar{1}3$
...	0.75	....	1.163	$10\bar{1}0$ (2)
5	6.0	1.139	1.136	$11\bar{2}2$
4	4.5	1.123	1.122	$20\bar{2}1$
...	1.0	....	1.067	0001 (4)
½	1.5	1.024	1.020	$10\bar{1}1$ (2)
1	1.5	.968	.971	$10\bar{1}4$
2	4.5	.902	.901	$20\bar{2}3$
...	1.5	...	.879	$21\bar{3}0$
3	9.0	.864	.861	$21\bar{3}1$
2	6.0	.838	.836	$11\bar{2}4$
¼	3.0	.816	.813	$21\bar{3}2$
½	4.5	.803	.802	$10\bar{1}5$
...	1.5	...	.788	$10\bar{1}2$ (2)
¼	3.0	.779	.776	$10\bar{1}0$ (3)
1	9.0	.750	.748	$21\bar{3}3$
1	6.0	.730	.728	$30\bar{3}2$

Type of Lattice	**Hexagonal Close-packed.**
Axial ratio	1.59
Side of elementary triangular prism	2.686 Å.
Distance between nearest atoms { in basal plane	2.686 Å.
Distance between nearest atoms { in pyramid planes	2.640 Å.
Density { from X-ray data	12.56
Density { by standard methods	12.26

The experimental values were found to agree exactly with an hexagonal close packed type of lattice, of axial ratio 1.59.—The indices of the crystal forms corresponding to each of the experimental spacings can be read off on the plot (cf. Fig. 3, p. 556, this number) and any one of them, *e.g.*, the $11\bar{2}0$

spacing, can be used to calculate the side of the elementary triangular prism. The density is then calculated as the ratio of the mass in the unit triangular prism, viz., one atom, to its volume. The side of the unit prism is thus found to be 2.686 Å., and the ideal density of ruthenium 12.56.

This lattice is a close packed arrangement of oblate spheroids whose axes are in the ratio 0.973 : 1. It is composed, like that of Zn and Cd, of two intermeshed lattices of right triangular prisms, each of side 2.686 Å. and height $1.59 \times 2.686 = 4.272$ Å., the atoms of the first lattice being in the centers of the prisms of the second and vice versa.

Each atom has as nearest neighbor the six atoms of the unit prism of which it is the center, at distances of 2.640 Å., and six others almost as near, in a regular hexagon about it (in the basal plane) at distances of 2.686 Å.

INDIUM.

The interpretation of the X-ray diffraction pattern of indium powder, with the help of graphs of axial ratio against crystal spacings, has been described in the foregoing article, and need only be summarized here.

Indium was found to consist of *a face-centered tetragonal lattice of atoms, with axial ratio* 1.06.

TABLE XV.

Indium.

Intensity of Line.	Number of Coöperating Planes.	Spacing of Planes.		Indices of Form.
		Observed.	Calculated.	
20	4	2.70	2.693	111
½	1	2.42	2.428	001 (2)
5	2	2.29	2.292	100 (2)
2	4	1.675	1.665	101 (2)
½	2	1.617	1.620	110 (2)
1	4	1.450	1.449	113
2	8	1.392	1.390	311
2	4	1.348	1.347	111 (2)
...	1	....	1.215	001 (4)
¼	2	1.150	1.146	100 (4)
1	8	1.080	1.082	133

Type of Lattice	**Face-Centered Tetragonal.**
Axial ratio	1.06
Side of elementary tetragonal prism	4.58 Å.
Height of elementary tetragonal prism	4.86 Å.
Distance between nearest atoms { in basal plane	3.24 Å.
Distance between nearest atoms { in pyramid planes	3.33 Å.
Density { from X-ray data	7.42
Density { by standard methods	7.12

The coördinates of the atoms are

$$m,\ n,\ pc,$$
$$m + \tfrac{1}{2},\ n + \tfrac{1}{2},\ pc,$$
$$m + \tfrac{1}{2},\ n,\ (p + \tfrac{1}{2})c,$$
$$m,\ n + \tfrac{1}{2},\ (p + \tfrac{1}{2})c,$$

where m, n, and p have all possible integral values, c is the axial ratio, 1.06, and the unit of length is the side of the elementary face-centered square which is the base of the unit prism. The lattice obviously consists of four intermeshed lattices of right tetragonal prisms, each of side 4.58 Å. and height 4.86 Å. It is shown in Fig. 4.

Each atom has four nearest neighbors, viz., the four corner atoms of the 001 face at whose center it is, at distances of 3.24 Å., and eight others almost as near, four in the centers of the lateral faces of the cube above and four similarly below, at distances of 3.33 Å.

This lattice is a close packed arrangement for prolate spheroids with axes in the ratio 1.06 : 1. It is an alternative arrangement to the hexagonal type exemplified by Zn and Cd, corresponding to the cubic and hexagonal arrangements, respectively, of close-packed spheres.

RESEARCH LABORATORY,
GENERAL ELECTRIC CO.,
Schenectady, N. Y.

THE BALMER SERIES OF HYDROGEN, AND THE QUANTUM THEORY OF LINE SPECTRA.

BY RAYMOND T. BIRGE.

SYNOPSIS.

Balmer Series of Hydrogen.—(1) *A rigid comparison of experimental with theoretical results* is the main purpose of the paper. It is concluded that Merton's measurements of the separation, half-width and relative intensity of the H_α and H_β doublets check with values derived from the recent Bohr-Kramers developments of the quantum theory, if a general field of 100 volts per cm. is assumed. After the fine structure has been analyzed and the "circle" line computed, determining the position of the components from the Sommerfeld theory and the relative intensities from the Bohr-Kramers theory, the frequencies of all lines are fitted into the Bohr relativity formula. (2) *The Rydberg constant* for H is then calculated to be 109,677.7 ± 0.2. (3) *A discussion of observations in mixtures of hydrogen and helium* made by Merton and Nicholson at relatively high pressures concludes the paper.

Rydberg spectral series constant for a nucleus of infinite mass is computed to be 109,736,9 ± 0.2.

INTRODUCTION.

THE purpose of this paper is to make as accurate a comparison as possible between the best experimental results for the Balmer series of hydrogen, and the theoretical results to be expected according to the latest developments of the quantum theory of line spectra. The experimental data are as follows:

1. Grating measurements by Paschen[1] of H_α, H_β, H_γ, and H_δ, (all unresolved) giving 6562.797, 4861.326, 4340.465, and 4101.735 I.A. respectively. The experimental error is estimated at ±0.004 Å. in each case.

2. Grating measurements by Paschen[1] of H_α (resolved) giving 6562.853 and 6562.732 I.A. for the components.

3. Interferometer measurements by Meissner[1] of H_α, giving a doublet, 6562.849 and 6562.725 I.A., of intensity 7 and 5 respectively, and of H_β (unresolved) giving 4861.329 I.A.

4. Grating measurements by Curtis[2] of the first six lines of the series (all unresolved) giving 6562.793, 4861.326, 4340.467, 4101.738, 3970.075, and 3889.051 I.A. respectively. The probable errors range from 0.0017 Å. to 0.0006 Å. (see Table II., column 3). The correct reduction to vacuum

[1] Ann. d. Phys. (4), 50, 901, 1916.

[2] Proc. Roy. Soc., A, 90, 605, 1914.

and a discussion of various possible series formulae was given by Curtis[1] in 1919.

5. A study by Merton[2] of the fine structure of H_α and H_β, under various experimental conditions. These results supplement and in part correct previous results by Merton and Nicholson.[3] The later results are to the effect that the most distinct doubling of both H_α and H_β is observed at liquid air temperature, in a mixture of helium and hydrogen at a few millimeters pressure. Under these conditions H_α is a doublet of 0.1446 Å. separation, the components having a half-width of 0.028 Å. and an intensity ratio of 2.18 to 1 (the red component being the stronger). H_β is a doublet of 0.093 Å. separation, and 0.045 Å. half-width of components. The intensity ratio was not measured. Further details of this work are given later in the present paper.

6. Data by Merton and Nicholson[4] and by Wood[5] as to the appearance of higher members of the Balmer series in mixtures of hydrogen and helium, at relatively high pressures, and in long vacuum tubes respectively.

There are also data on the Stark effect for the Balmer series, but this subject will not be discussed, since the agreement between theory and experiment, in the case of strong electric fields, has already been shown by Kramers[6] to be perfect. The results for weak fields will however be treated, in connection with the fine structure of the lines.

The quantum theory of line spectra, as applied to the Balmer series, may be summarized as follows:

In 1914–1915 Bohr[7] applied Rutherford's nuclear theory of the atom and general quantum theory to the case particularly of a single electron of charge e and mass m revolving about a nucleus of charge Ne and mass M. On the hypothesis of circular orbits, and the atomicity of angular momentum, the Balmer formula

$$\nu = \nu_1 = N_0 N^2 \left(\frac{1}{n''^2} - \frac{1}{n'^2} \right) \qquad (1)$$

was theoretically deduced. In this expression the angular momentum in the initial state of the electron is given by $n'h/2\pi$, in the final state by $n''h/2\pi$. For the Balmer series $n'' = 2$, $n' = 3, 4, 5$ etc. $N = 1$ for all Hydrogen series and $N = 2$ for Helium enhanced series. N_0 is the

[1] Proc. Roy. Soc., A, 96, 147, 1919.
[2] Proc. Roy. Soc., A, 97, 307, 1920.
[3] Phil. Trans., A, 217, 237, 1917.
[4] Proc. Roy. Soc., A, 96, 112, 1919.
[5] Proc. Roy. Soc., A, 97, 455, 1920.
[6] D. Kgl. Danske Vid. Selsk. Skr. natur og math. Afd., 8, R. III., 3, 1919.
[7] Phil. Mag., 26, 1, 476, and 857, 1913; 27, 507, 1914; 29, 332, 1915; 30, 394, 1915.

so-called Rydberg constant, and is *not* a constant, depending for its value on the mass of the nucleus. For Hydrogen it is designated N_∞ and is given theoretically by $N_\infty \times M_H/(M_H + m)$, where N_∞ is the constant for a nucleus of infinite mass and given by $2\pi^2 e^4 m/ch^3$, in terms of frequency number. The spectroscopically observed value of N_∞ and the theoretical value deduced from this expression check within the limits of experimental error.[1] Because however of the relatively large errors in "h" and "e," and the small error in N_∞ (regardless of the particular formula used for the Balmer series), N_∞ must be considered as an undetermined constant, in testing various series formulæ.

In 1915 Bohr[2] applied relativity mechanics to his atomic model, and thus obtained, in place of (1), the more complex expression

$$\nu = \nu_1 + \nu_2 = \nu_1 + 1/4 N_0 \alpha^2 N^4 \left(\frac{1}{n''^4} - \frac{1}{n'^4} \right), \tag{2}$$

where $\alpha = 2\pi e^2/hc$. Equation (2) is frequently written

$$\nu = N_0 N^2 \left(\frac{1}{n''^2} - \frac{1}{n'^2} \right) \left[1 + \frac{\alpha^2 N^2}{4} \left(\frac{1}{n''^2} + \frac{1}{n'^2} \right) \right]. \tag{2'}$$

Equation (2) or (2′) indicates a shift of all wave-lengths to the violet as compared with the values given by equation (1). For the Balmer series this shift varies from 0.039 Å. for H_α to 0.010 Å. for the head of the series. Since the frequencies given by (2) correspond to an electron falling from one circle to another circle, the corresponding spectral lines will be called "circle lines."

In 1915–1916 Sommerfeld[3] extended the Bohr theory to the case of elliptic orbits. For a "hydrogen-like" atom, *i.e.*, a single electron revolving about a nucleus, there is both angular and radial momentum. The angular momentum is constant and is given by $n_2 h/2\pi$. The radial momentum has an average value of $n_1 h/2\pi$. The total momentum is given by $nh/2\pi$ where $n = n_1 + n_2$, and as before n' will be used to designate the initial state and n'' the final. The emitted frequency is then given by

$$\nu = \nu_1 + \nu_2 + \nu_3, \tag{3}$$

where

$$\nu_3 = N_0 \alpha^2 N^4 \left[\frac{1}{n''^4} \left(\frac{n_1''}{n_2''} \right) - \frac{1}{n'^4} \left(\frac{n_1'}{n_2'} \right) \right]. \tag{4}$$

Equation (3) indicates the so-called "fine-structure" of spectral lines. Each line given by the Bohr theory (*i.e.*, each circle line) is split up into

[1] Birge, Phys. Rev., 14, 363, 1919.

[2] Phil. Mag., 29, 332, 1915.

[3] Main article, Ann. d. Phys., 51, 1–125, 1916.

a number of components, obtained by combining the various possible states $n_1'' + n_2'' = n'' =$ constant, with the possible states $n_1' + n_2' = n$ = another constant. This is now known as the "combination-principle." Formulæ (2) and (3) are both approximate, terms in $(\alpha N)^4$ and higher powers having been neglected in comparison with $(\alpha N)^2$. It is only in the case of X-ray spectra that these higher powers need be considered. (See Sommerfeld, loc. cit., p. 55.)

In discussing the relative intensity which the various fine structure components of a line might be expected to possess, Sommerfeld made certain arbitrary assumptions, as his theory gave no theoretical basis for the matter. Paschen (loc. cit.) tested these assumptions, using the "4686" helium enhanced series, in which the "fine structure" is sixteen times as broad as in the corresponding hydrogen series, due to the N^4 term in (4). Paschen concluded that the fine structure components agreed in position with Sommerfeld's theory, but agreed only partially in intensity, especially in the case of the spark discharge. Paschen found a striking difference in appearance between the spark and the constant current discharge, a difference not predicted by the theory.

A notable advance in the quantum theory of line spectra was made in 1918 by Bohr,[1] who worked out a logical basis for the intensity and state of polarization of the various fine structure lines. This theory he applied also to the Stark and to the Zeeman effect. Kramers (loc. cit.), working under Bohr, made a detailed application of Bohr's ideas to the Stark effect, in hydrogen and in helium, and to the fine structure of the lines, in these two gases. The agreement between theory and experiment, in the case of the Stark effect, is very remarkable. The position of the Stark effect components had already been predicted by Epstein[2] and Schwarzschild.[3] The advance made by Bohr and Kramers consisted in the correct prediction of the intensity and state of polarization of each component.

Kramers' work on the fine structure of the lines indicated that the intensity of the various components varied enormously with the strength of the electric field, especially in the case of the hydrogen series. Electric fields such as are found in the ordinary vacuum tube are evidently primarily responsible for the appearance of the lines, and especially for the change of appearance with varying physical conditions, as observed by Merton. The chief purpose of the present paper is to apply Kramers' theoretical results to the Balmer series, since Kramers himself made no detailed comparison except in one case to be mentioned presently.

[1] D. Kgl. Danske Vid. Selsk. Skr. natur og math. Afd., 8, R. IV., 1 and 2, 1918.

[2] Ann. d. Phys., 50, 489, 1916; 51, 168, 1916.

[3] Ber. Akad. Berlin, p. 548, 1916.

The articles by Sommerfeld, (1916) Bohr (1918), and Kramers (1919), are all very long and involved, especially the Kramers article. Consequently it is not possible to give a logical summary of the assumptions and conclusions, without making the present paper unduly long. Such material as is needed will be used without explanation, except by reference to the page number of the original article.

THE FINE STRUCTURE OF THE BALMER SERIES, ACCORDING TO SOMMERFELD.

As shown by equation (4), each spectral line consists of a number of components. In this equation $\alpha^2 = 5.308 \times 10^{-5}$ (using 6.555×10^{-27} for "h"). Sommerfeld (p. 68) used 5.30×10^{-5} for α^2. The equation, as applied to the Balmer series, may therefore be written (in terms of frequency-number)

$$\nu_3 = 5.822\left[\frac{1}{n''^4}\left(\frac{n_1''}{n_2''}\right) - \frac{1}{n'^4}\left(\frac{n_1'}{n_2'}\right)\right], \qquad (5)$$

where $n_1'' + n_2'' = n'' = 2$, and $n_1' + n_2' = n' = 3, 4, 5$, etc., and ν_3 gives the distance of the various components from the circle line. Any spectral line may be indicated by $(n_1'n_2', n_1''n_2'')$. The H_α circle line is therefore (03, 02), the H_β circle line (04, 02). The separation $(n_1'n_2',$ 11) $-$ $(n_1'n_2',$ 02) is known as the fundamental hydrogen separation. It is given by $5.822/2^4 = 0.3639$, or 0.3640 approximately. For this very important constant Paschen (p. 910) derived the experimental value of 0.3645 ± 0.0045, and used this value in all his calculations. The author has, however, used the theoretical value 0.3640. The H_α line thus consists of two sets of identical triplets (see Table I., and Fig. 1 *a*), separated by 0.3640ν ($= 0.1568$ Å.). The H_β line consists of two identical quadruplets, separated by 0.3640ν ($=0.0858$ Å.), etc. The Balmer series therefore consists of a doublet of constant $\Delta\nu$, the components of each member being themselves complex, but (as shown by equation 4) the total width of each component growing rapidly narrower, as n' increases.

A convenient method (used by Paschen) for labeling the various fine structure components is indicated in Table I., where the components of H_α, beginning at the red, are given in order, with the successive separations, in terms of Ångstroms. (See also Fig. 1 *a*.)

States in which $n_2 = 0$ are excluded, for this indicates no angular momentum, and the electron would therefore collide with the nucleus. The number of possible states is therefore only $n' \times n''$. Sommerfeld's first assumption as to intensity is that it is proportional to $(n_2'/n')(n_2''/n'')$, thus giving the maximum intensity (unity) to the circle line I_α. The

TABLE I.

1	2				3	4	5
Name.	n_1'	n_2'	n_1''	n_2''	Separation in Å.	Intensity Paschen 1.	Intensity Paschen 2.
I_c.....	2	1	0	2		2/6	small
I_b.....	1	2	0	2	0.0464	4/6	4/6
I_a.....	0	3	0	2	0.0155	6/6	6/6
II_c.....	2	1	1	1	0.0949	1/6	1/6
II_b.....	1	2	1	1	0.0464	2/6	2/6
II_a.....	0	3	1	1	0.0155	3/6	zero

intensities for the H_α components are given in the 4th column of Table I. Sommerfeld then makes the second assumption that, in an electron transition, the radial momentum never increases. This excludes the II_a line of each member of the Balmer series. He also makes the third

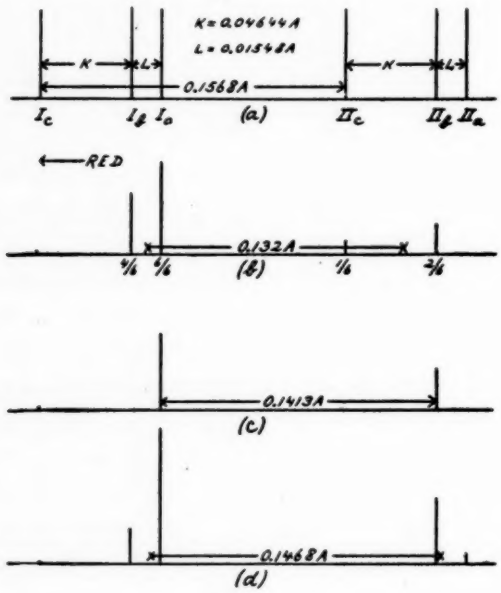

Fig. 1.

(*a*) H_α fine structure,—location only.
(*b*) Intensity relations according to Sommerfeld's theory.
(*c*) Intensity relations, with no electric field, according to Bohr-Kramers' theory.
(*d*) Intensity relations, with a field of 100 volts/cm., according to Bohr-Kramers' theory.
The crosses represent the centers of gravity of the two components of H_α.

assumption that an increase of angular momentum rarely if ever occurs. This indicates a very small intensity for the least refrangible member of each Balmer series line. The results, applied to H_α, are given numerically in Table I., column 5, and graphically in Fig. 1 *b*. They indicate a

doublet (each component of which is itself double), having a separation of 0.132 Å., and an intensity ratio of 3.3 to 1. Paschen, however, found that in the "4686" line the component III_a, corresponding to an increase of two units of radial momentum, appeared in the spark discharge with relatively great intensity. II_a, corresponding to an increase of one unit, was also very strong. Neither appeared in the constant current discharge. On the other hand, lines corresponding to an increase of angular momentum appeared faintly in both types of discharge. In fact, Sommerfeld made his third intensity assumption to agree with this observed fact.

Spectral Formulæ for the Balmer Series.

In measuring the wave-lengths of the Balmer series, as has been done by Curtis and others, what is actually observed is the apparent center of gravity of the complex line.[1] In order to interpret the results it is necessary to make assumptions in regard to the intensity, as well as the position, of the fine structure components. With such assumptions made, it is possible to compute, from the observed center of gravity of the line, the true wave-length of the circle component I_a. It is to this component alone that formula (2) or (2′) applies. This is the procedure followed by Paschen (loc. cit.). Curtis however, in his 1919 article, applied (2′) directly to the original measurements. He also took α^2 as an undetermined constant, obtaining by a Least Squares solution a value of 15.48×10^{-5}, as compared to the theoretical value 5.308×10^{-5}. The author has found that an almost equally good agreement between the observed and computed wave-lengths can be obtained by using the theoretical value of α^2. There is however a definite divergence between theory and experiment which appears more clearly by handling the data in a different way, as indicated below.

Curtis uses other two constant and even three constant formulæ. Since the deviations from equation (1) are very small, it is to be expected that the addition of one or two additional constants, in almost any functional form, will result in a fairly good agreement, such as Curtis found. But formula (2), as applied to the Sommerfeld theory, has only one undetermined constant (N_0). Even this would be a determined constant, if we had accurate enough values of "h" and "e." α^2 is also a function of these quantities, but considerable changes in the assumed value of α^2 make but slight alterations in the computed frequency. Equation (2) is then practically a one constant formula.

The deviations of the observed lines from equation (1) are best exhibited

[1] Curtis says that he intended to set on the actual center of the line. The matter is discussed in a later section of this paper.

by computing a value of N_0 ($= N_\infty$) from each observed wave-length. The results,[1] taken directly from Curtis' 1919 paper appear in Table II.,

TABLE II.

1, n'.	2, λ (Air).	3, Error.	4, N_∞ (1).	5, ΔN (1).	6, $\Delta\lambda$ (1).	7, ΔN (2).	8, $\Delta\lambda$ (2).
3.....	6562.793	0.0017	109,679.155	+0.402	−0.0251	+0.278	−0.0166
4.....	4861.326	0.0010	78.896	+0.143	−0.0063	+0.057	−0.0025
5.....	4340.467	0.0006	78.776	+0.023	−0.0009	+0.003	−0.0001
6.....	4101.738	0.0013	78.748	−0.005	+0.0002	−0.009	+0.0003
7.....	3970.075	0.0016	78.738	−0.015	+0.0005	−0.007	+0.0003
8.....	3889.051	0.0011	78.750	−0.003	+0.0001	+0.013	−0.0005

column 4. As this column shows, the values of N_∞ become sensibly constant, beginning with $n' = 5$ (H_γ). Accordingly the average value of N_∞, using the last four values only, has been computed, and then the deviations from this average value (which is 109, 678.753). The results, in terms of frequency, are given in column 5, and in terms of Ångstroms, in column 6.

In a similar manner, formula (2′) has been applied to the Curtis data, using the theoretical value of α^2. (This is the author's own work.) Again it appears that N_∞ is sensibly constant after the first two wave-lengths. Its average value, from the last four, is 109,678.351. In column 7 are given the deviations from this average, in frequency units, and in column 8, the deviations in Ångstroms. A comparison of columns 8 and 6 indicates a reduction of error to 66 per cent. for H_α, 40 per cent. for H_β, 10 per cent. for H_γ, and no sensible change for the others. The discrepancy for H_α is still however ten times the experimental error. It is thus quite clear that the application of relativity mechanics to the Balmer formula results in a definite reduction of the discrepancy between observed and computed values, but does not in any way obliterate the discrepancy. The explanation must therefore be sought in the fine structure of the lines.

To make a rigid test between theory and experiment, it is necessary to make definite assumptions as to the position and intensity of every fine structure component. It is then possible to treat each Balmer series line as a doublet, each member of which is complex. Knowing the structure of the red component of the doublet, it is possible to compute the frequency of the circle line I_α (always the most refrangible member of

[1] In the reduction to vacuum, Curtis uses the new figures of the Bureau of Standards. These will be used exclusively in the present article. Paschen uses older data, which are not so accurate, and therefore his vacuum values are not quite correct.

Table II., column 3, gives Curtis' estimate of the probable error of each line, in Ångstroms.

the red component) if the position of the center of gravity of the red component is known. This center of gravity, in turn, can be computed from the observed center of gravity of the entire line, knowing the separation of the centers of gravity of the two components of the doublet, and their intensity ratio. But these latter data depend on the exact assumptions made as to the intensity of the fine structure lines.

Paschen applied this general process to the analysis of his own measurements, using ostensibly the Sommerfeld theory as to the position and intensity of the fine structure components. He however made a number of simplifying assumptions, as well as one inadvertent error. The strict application of the Sommerfeld theory (using all three assumptions as to intensity) gives for the intensity ratio of the doublets, 3.3 to 1 (H_α), 3 to 1 (H_β), 2.8 to 1 (H_γ), 2.67 to 1 (H_δ), 2.57 to 1 (H_ϵ), etc., the limiting value being 2 to 1. The corresponding doublet separations are, 0.3130ν (= 0.1320 Å), 0.3489ν (= 0.0822 Å), 0.3587ν (= 0.0676 Å.), 0.3639ν (= 0.0613 Å.), 0.3640ν (= 0.0574 Å.), respectively. Paschen however used a constant intensity ratio of 2 to 1 for all lines, and a constant doublet separation of 0.3645ν. The distance of the circle line from the center of gravity of the red component is also variable, and has been used as such by the author. Paschen assumed the distance always equal to $1/4(I_a - I_b)$. This is incorrect even for the H_α line, and is due to Paschen's accidental assumption of an intensity ratio of 3 to 1 for I_a/I_b, instead of the correct 3 to 2 ratio. The error thus introduced is 0.0023 Å. for H_α. For the other lines it is practically negligible. The correct H_α structure, on the Sommerfeld theory, is shown in Fig. 1 *b*.

As has already been noted, Sommerfeld's assumptions as to intensity do not agree with experimental results, in the case of the helium lines. The discrepancies have now been explained by Kramers, who shows that the relative intensity of all fine structure components depends upon the exact strength of the electric field in the vacuum tube. This matter will presently be treated in detail. Another serious conflict between the Sommerfeld theory and observed facts is in the matter of the half-breadth of the red and violet components. Merton observed 0.028 Å. for H_α, and 0.045 Å. for H_β. A careful computation of the Doppler effect gave 0.023 Å. and 0.017 Å. for these widths. But on the Sommerfeld theory, the red component of H_α should be about 0.015 Å. wide, and the violet component 0.046 Å. wide, regardless of *any* Doppler effect. Conversely, for H_β, the Sommerfeld theory gives a width of only 0.005 to 0.014 Å., much less than the observed, with the full Doppler effect counted in.

Using all available data and the new figures for reduction to vacuum, the author has computed the position of the circle line, from the observed

center of gravity of the entire line. This has been done according to the strict Sommerfeld theory, and also on the assumption of a constant 2 to 1 intensity ratio for the doublet. In view however of the discrepancy of this theory with observations, in the case of H_α and H_β, it does not seem advisable to present the results in detail. The values of N_∞ obtained from the various lines are as consistent as those of Paschen.[1] Using a 2 to 1 intensity ratio, but the theoretical value of the doublet separation, an average value for N_∞ of 109,677.826 is obtained. Using the theoretical intensity ratios given previously, the value is 109,677.944. The Curtis and Paschen wave-lengths, treated separately, yield the same average by the first method, but slightly different averages by the second. Neither of these averages includes H_α, since this line requires individual treatment. It will be noted that the values of N_∞ are somewhat higher than that of Paschen.[2]

The Bohr-Kramers Theory of Intensity.

Bohr's new "Selective" principle (Auswahlprinzip) for obtaining at least a rough estimate of the intensity of the fine structure components is based on the idea that the actual orbit of the electron, in the initial and in the final state, can be considered as the sum of a number of harmonic vibrations. The intensity of an emitted line of any given frequency is then connected with the amplitudes of the harmonic vibrations of corresponding frequency in the initial and in the final state of the electron. The type of harmonic vibration (linear, circular, or elliptic) indicates the polarization (linear, circular, or elliptic) of the emitted line.

As applied by Kramers to the case of a strong electric field, the principle yields results in remarkable agreement with experiment. The intensity, as well as the state of polarization, of every component of the Stark effect, in the hydrogen and helium (enhanced) series is theoretically accounted for. The same principle, applied to the fine structure of

[1] P. 935, loc. cit. Paschen obtained a weighted mean of 109,677.691, and gives the probable error as ± 0.06, although the probable error, by the ordinary Least Squares formula is only ± 0.0145. The author, in all computations in this paper, has used only an unweighted average.

[2] All the computations of the present article had been completed, and the article partly written, when there appeared a brief paper by Herbert Bell (Phil. Mag., 40, 489, 1920) on the "Helium-Hydrogen Series Constants." The only point at which this paper overlaps the present work is in regard to the results just given. Bell uses both Paschen and Curtis wave-lengths, and the new reduction to vacuum. He however follows exactly the method of Paschen, assuming a 2 to 1 intensity ratio, and a constant doublet separation of 0.3650. Like Paschen, he uses the erroneous intensity ratio 3 to 1, for I_a/I_b. Bell also makes a computation with an assumed 3 to 1 intensity ratio for the doublet components. His results naturally differ slightly from those just presented due to the different method of making the fine structure corrections.

these series, with no electric field, indicates (Kramers, p. 355) that only those transitions are possible for which the angular momentum *increases* or *decreases* by $h/2\pi$, *i.e.*, $n_2' - n_2'' = \pm 1$. In the case of the Balmer series this indicates the presence of only *three* fine structure components for each member, contrasted to $n'(n'' - n' + 1)$ components on the Sommerfeld theory. They are I_a, I_c and II_b for H_α, I_b, I_d and II_c for H_β, I_c, I_e and II_d for H_γ, etc.

The intensity of each component is given by an expression (Kramers p. 356) involving Bessel functions. The results for H_α, on an arbitrary scale, are 5.00 for I_a, 1.36 for II_b, 0.04 for I_c. The true intensity of I_a is then taken as about one half of 5.00, because I_a is a circle line, and in the case of the Stark effect it was found that the theory gave too high values for the intensity, in the case of circle lines (due presumably to the various approximations introduced in the application). This conclusion was deduced by checking the results with the known fact that in the Stark effect, the polarized components into which an unpolarized spectral line is split will, when taken together, show no characteristic polarization in any direction. The results thus show that there may be errors up to possibly 100 per cent. in Kramers' computed intensities, but these are relatively small compared to the discrepancies in Sommerfeld's work, which were sometimes in excess of 1000 per cent.

The Kramers results for H_α are given in Fig. 1 *c*. They indicate a doublet separation of 0.1413 Å., and an intensity ratio of about 2 to 1. For H_β the results give a doublet separation ($I_b - II_c$) of 0.0822 Å., and an intensity ratio of about 1.25 to 1. The half-width of the H_β components, observed by Merton, is still less accounted for than on the Sommerfeld theory, although the H_α separation and intensity ratio checks very closely with Merton's experimental results.

Kramers (p. 359–378) then considers the effect of a weak electric field on the fine structure lines. His previous formulæ for the Stark effect hold only for strong fields. A rigid theory holding in all cases would be extremely complex, and has not yet been worked out. The results for a weak field indicate (as expected) that each fine structure component is broken up into a number of Stark effect components. Since the electric field is assumed very weak, the separation of these electric components may be neglected, and the intensity of any fine structure component may be judged by the sum of the intensities of all the Stark effect components composing it.

The calculations then show the extremely important result that various fine structure components previously missing may now appear, some of them with considerable intensity. In fact (Kramers, p. 364), while

previously there appeared only those transitions for which the angular momentum changed by one unit, we may now have the additional transitions for which the angular momentum remains unchanged, or changes by two units. If the intensities of the new components are small, compared to the original components, the intensity of the old components will be practically uninfluenced by the perturbing electric field. These new components, in the case of the helium lines, explain with one questionable exception the experimental observations of Paschen (see Kramers, pp. 372–376).

The equations for obtaining the intensity of the new components are given on page 367 of Kramers. They are very complex, and contain, it may be noted, several typographical errors. These errors may however be readily identified by comparing the expressions with those on pages 318–320, from which they were derived. Kramers computes numerical results for H_α and for Helium 4686 and 3203 only. The author has checked most of Kramers' calculations. The only serious error found is in the case of the II_α component of both H_α and Helium 4686, for which Kramers computes practically zero intensity, while the correct results are 1.588 and 0.115 respectively.[1] These intensities are for an electric field of 300 volts per cm. The intensity of the line varies as the square of the field intensity, and inversely as the fifth power of N. It also depends, in a more complex manner, on n' and n'', increasing very rapidly with increase in either or both.

The author believes that the last two sentences furnish the clue to the interpretation of all of Merton's results, in mixtures of hydrogen and helium.[2] Merton himself remarks (p. 310) "the only cause of broadening to be suspected would be . . . due to the influence of the electric field of neighboring charged particles on radiating atoms, operating in accordance with the Stark effect. It is true that this effect is greater for hydrogen than for other elements, but the effect in the case of helium is comparable in magnitude and the excellent agreement between the experimentally measured widths of helium lines and the widths calculated on the basis

[1] For H_α, R'^2 is 1.141 and 0.447 for the two components of II_α, *i.e.*, (03,11). For He 4686 the R'^2 of the five components of II_α, *i.e.*, (04,12), is 0.025, 0.039, 0.0149, 0.0189, and 0.0173, respectively. The Kramers results for R''^2 are correct. The author's corrected intensity for II_α of 4686 accounts better for Paschen's observed line, in the spark discharge, at 4685.687.

[2] The Balmer series, with the fine structure predicted by theory, seems to appear only in mixtures of hydrogen and helium. No attempt is made in this paper to explain the various effects noted by Merton in pure hydrogen, and in hydrogen containing a trace of impurity. The cause of these effects is undoubtedly to be looked for in the *irregular, local* fields of force of the surrounding atoms, as contrasted to the *general* electric field discussed here. It is only the helium atom which has practically no electron "affinity," and so no appreciable local field.

of the Doppler effect in the experiments of Buisson and Fabry would seem to leave little room for broadening of this type."

Using Kramers' results, this conclusion is not justified. The author has found that by assuming a uniform field of 100 volts per cm., such as has experimentally been found to exist in the hydrogen positive column, under a few mm. pressure, the effect for helium and for hydrogen is very different, and is quite capable of explaining the experimental results. It is not possible to give with authority the exact quantitative figures. In the case of H_β such a field produces a Stark effect splitting which is comparable in magnitude with the fine structure separation. For this line one therefore is effectively dealing with a "strong" electric field, to which the simpler Epstein-Schwarzschild formula applies. Moreover, the computed intensity of some of the new fine structure components is many times as great as the intensity of the strongest of the original components, whereas the formulæ used are intended only for the case where these new components are comparatively weak. When they are strong the original components themselves will have changed in magnitude by an amount comparable with the intensity of the new components, but Kramers has derived no formula for this increase. The actual relations are therefore only very approximate.

The results are as follows. For a field of 100 volts per cm., the total Stark effect width for He 4686 is 0.0085 Å. But the strong components are all near the center (Kramers, Plate III.) so that the observed broadening might appear much less. For He 3203, the breadth is 0.0092 Å. This should be observed, since the strong components are on the outside. The regular fine structure components of 4686 are all at intervals of 0.05 Å. or more (Paschen, p. 916), and the observed breadths 0.03 Å. or more. The electric fields in Paschen's work may therefore be much stronger than 100 volts per cm.

For H_α, a field of 100 volts per cm. gives a total possible Stark effect width of 0.0224 Å., but the outer components are much weaker than the central (Kramers, Plate I.) so that the effective half-width is probably less than half as great. Merton computes 0.023 Å. for the Doppler effect and observes 0.028 for the half-width. This is in reasonable agreement with theory, especially as the broadening due to the electric field and that due to the Doppler effect may not be simply additive. The only fine structure components that are really effective are still I_a and II_b so there is no effective broadening due to the fine structure. The exact results are shown in Fig. 1 *d*, where, according to Kramers' suggestion, the intensity of the new components is added to the neighboring old components. The figures then become (with corrections to

Kramers' computations previously noted) $I_a = 2.237$, $I_b = 0.577$, $II_a = 0.196$, $II_b = 1.096$. The intensity ratio for the doublet is $(2.237 + 0.577)/(0.196 + 1.096) = 2.18$ to 1, or exactly equal to Merton's observed value. The center of gravity of the red component is 0.0032 Å. to the red of I_a, while that of the violet component is 0.0023 Å. to the violet of II_b. The separation of the doublet is 0.1468 Å., compared to Merton's observed value of 0.1446 Å.

For H_β with a field of 100 volts per cm., the total Stark effect width is 0.0304 Å., and the strongest components are on the outside (Kramers, Plate I.) so that this value should represent the observed broadening. The Doppler effect is 0.017 Å., and if this is simply additive, the total width is 0.0474 Å., as compared to Merton's observed value of 0.045 Å. It is probable that 0.002 to 0.004 Å. should be added for the fine structure, making a total expected half-width of as much as 0.051 Å. Again however this assumes the Stark effect broadening and the Doppler effect broadening as simply additive.

The fine structure broadening of 0.002 to 0.004 Å. is the result of the author's computations, Kramers having done no work on this line. The original components, with their relative intensities are I_b (0.104), II_c (0.085), and I_d (0.002). The *new* components, due to an electric field of 100 volts per cm., with their intensities, are I_a (11.85), II_b (8.29), and I_c (1.72). We have thus, as previously noted, new components much stronger than the old, with no means of accurately computing the intensity change in the old. Assuming it to be the same as in the new components, we have the red member of the doublet composed of two almost equally strong lines I_a and I_b, with a separation of 0.0018 Å., together with the comparatively weak I_c line, while the violet member is composed of two strong lines II_b and II_c, separated 0.0036 Å. The intensity ratio is roughly $11.85/8.29 = 1.43$ to 1, while the separation[1] is about 0.0840, compared to Merton's 0.093 Å. (Merton himself thinks that this value may be too large.) Merton did not measure the intensity ratio for H_β but a mere visual inspection of the published photographs (p. 316) indicates that the ratio is much less for H_β than for H_α.

For H_γ the Stark effect broadening is 0.0435 Å., with again the strong components on the outside. As the total doublet separation is only about 0.068 Å., it is not to be expected that this line can be resolved, under any of the experimental conditions realized by Merton. Many of the changes of appearance observed by Merton, with varying chemical and electrical conditions, can thus doubtless be explained by changing

[1] This assumes the center of gravity of the violet component halfway between II_b and II_c, and of the red component at I_b (due to the influence of I_c.)

electric fields, interatomic if not general. That the electric field is competent to explain all observed half-widths, for resolved helium and hydrogen lines, seems evident in the light of the above figures.

The Value of the Rydberg Constant N_∞.

We are now ready to return to the original problem of testing equation (3). The test consists of computing a theoretical value for the circle line and substituting this in equation (2). The values for N_∞ ($= N_0$ of equation 2) should be constant, and may be compared to the values given in Table II.

As previously mentioned, the Sommerfeld theory of intensities yields a constant N_∞, provided H_α is excluded. The Bohr-Kramers theory is equally satisfactory. The results are given in Table III.

Table III.

1.	2, N_∞.	3, $r(\nu)$.	4, $r(\lambda)$.	5, N_∞.	6, $r(\nu)$
H_β Paschen.....	7.815	−0.006	+0.0003	7.665	+0.048
" Meissner.....	7.747	−0.074	+0.0033	7.597	−0.020
" Curtis.....	7.815	−0.006	+0.0003	7.665	+0.048
H_γ Paschen.....	7.851	+0.030	−0.0012	7.660	+0.043
" Curtis.....	7.800	−0.021	+0.0008	7.609	−0.008
H_δ Paschen.....	7.887	+0.066	−0.0025	7.642	+0.025
" Curtis.....	7.807	−0.014	+0.0005	7.561	−0.056
H_ϵ Curtis.....	7.821	±0.	±0.	7.571	−0.046
H_ζ Curtis.....	7.848	+0.027	−0.0010	7.587	−0.030
Average.....	7.821	0.027	0.0011	7.617	0.036

Column 2 gives the value of N_∞ (the integral part 109,677 being omitted) using a constant intensity ratio of 2 to 1 for the doublet, but the theoretical separation.[1] In order to obtain the circle line, the center of gravity of the red component, in the case of H_β, is assumed at I_b, as explained in the previous note, *i.e.*, 0.0018 Å to the red of the circle line I_a. For H_γ the corresponding correction is about 0.0007 Å. For the other lines it is negligible.

On these assumptions, the average value of N_∞ is 109,677.821, and the average residual, in frequency, is 0.027, as shown in column 3, or 0.0011 Å, as shown in column 4.

The same process has been repeated, using the true intensity ratio given by the Bohr-Kramers theory, *i.e.*, 2.18 to 1 for H_α and 1.43 to

[1] This separation is 0.0840 Å. for H_β, and 0.0674 for H_γ, with the electric field used. For the other lines the constant separation of $0.3640\,\nu$ is used, as the error thus introduced is negligible.

1 for H_β. The results for the other lines have not been determined as the computations are very laborious; but it is evident that the ratio is rapidly declining, and will reach unity in the limit. I have accordingly assumed ratios as follows, 1.2 to 1 for H_γ, 1.1 to 1 for H_δ, 1.05 to 1 for H_ϵ, and 1 to 1 for H_ζ. The results are given in column 5 of Table III. (where again the integral part 109,677 is omitted), and the frequency residuals in column 6.[1]

The final problem is to determine how the experimental results for H_α check with these values of N_ω. To do this it seems simpler to use the average N_ω already obtained to compute a theoretical value for the wave-length (in air) of the circle line of H_α. Using 109,677.821 for N_ω, we obtain 6562.8413 Å. Using 109,677.617, we obtain 6562.8535 Å. As previously deduced, using the Bohr-Kramers theory and 100 volts per cm., the center of gravity of the red component should be 0.0032 Å. to the red of the circle line. This gives for its theoretical position 6562.-8445 Å. or 6562.8567 Å. The average is 6562.8506. For the center of gravity of the red component Paschen observed 6562.853, while Meissner observed 6562.849. The average is 6562.851 which agrees exactly with the theoretical average. In other words, various theories as to the intensity of the electric field and the resulting intensity of the components of the lines lead to somewhat different expected results for the position of the red component of H_α, but the observed results also vary, and the various experimental and theoretical results all lie in the same region, and have the same average.

The second method of checking H_α is from the observed position of the center of gravity of the entire line. This position is 6562.797, according to Paschen, and 6562.793, according to Curtis. If 6562.8445 is the true position of the center of gravity of the red component, and if Merton's experimental value of 0.1446 Å. is assumed for the doublet separation (the theoretical value being about 0.1468 Å.), then Paschen's

[1] Curtis mentions that, in measuring the position of a line, he attempted to set on the actual center of the line, and not on its center of gravity. Paschen however says he attempted to set on the center of gravity. Bell calls attention to a slight systematic drift of Paschen's wave-lengths, as compared to Curtis'. There *is* such a drift, but it is doubtless due to the different reference standards used, and not to the method of setting. Thus if Curtis *really* set on the center of the line, his readings should be corrected (to a first approximation) by assuming a 1 to 1 intensity ratio of doublet components, instead of that actually used. This change in method would shift the $H\beta$ circle line by 0.0092 Å, from its predicted position on a 1.43 to 1 intensity ratio, or by 0.0158 Å., on a 2 to 1 ratio. Yet the Curtis and Paschen measurements agree for this line, (to 0.001 Å.), and differ by 0.004 Å. or less for all the others. It thus does not seem possible that Curtis and Paschen used essentially different methods of setting. If it *is* assumed that Curtis set on the actual center of the line, then, using only his values of wave-length, the average N_w is 109,677.524 and its constancy is about the same as before.

observation requires an intensity ratio of 2.04 to 1, while Curtis' requires 1.81 to 1. If 6562.8567 is the true value of the center of gravity, then Paschen's observation requires an intensity ratio of 1.42 to 1, while Curtis' requires 1.27 to 1. Meissner observed 1.4 to 1 ratio, while Merton observed 2.2 to 1.[1] With such discordant experimental results, it is hard to decide what ratio should be used, and it is evident that the value of the ratio depends greatly upon experimental conditions. A measurement of the center of gravity of the entire line is thus valueless, unless the intensity ratio, for the *same* conditions, is known. Moreover, the slightest change in the ratio makes a perceptible difference in the final comparison of theory and experiment. The only valid method at present available seems then that of using the directly observed center of gravity of the red component, and this, as shown, leads to a fairly satisfactory agreement of theory and experiment.

The various values for N_∞ are summarized as follows,

Sommerfeld theory, 2 to 1 ratio	109,677.826
Sommerfeld theory, theoretical ratio	109,677.944
Bohr-Kramers theory, 2 to 1 ratio	109,677.821
Bohr-Kramers theory, theoretical ratio	109,677.617

These may be compared to previous results,

Paschen (Sommerfeld theory)	109,677.691
Curtis (empirical formulæ)	109,677.58 to 109,678.76

The author recommends for N_∞ the value **109,677.7**, which is probably correct to 0.2.

The best value of e/m is 1.773×10^7,[2] and this, combined with 4.774×10^{-10} for e, and 96,470 for the Faraday,[1] gives 1.6636×10^{-24} grams for the mass of the hydrogen atom, and 1853 to 1, as the ratio of its mass to that of the electron. We have therefore

$$N_\infty = \frac{2\pi^2 me^4}{ch^3} = 109{,}677.7\left(1 + \frac{1}{1853}\right) = \mathbf{109{,}736.9 \pm 0.2.}$$

This may be compared to Paschen's determination (p. 936, loc. cit.) of 109, 737.18, using 1843.7 for the above ratio of M_H to m.

It has thus been shown that the quantum theory of line spectra, using the "Selective principle" of Bohr, leads, in the case of the Balmer series, to consistent values of N_∞, as well as to a satisfactory explanation of the

[1] On the assumption that Curtis set on the center of each line, thus giving 109,677.525 for N_∞, we obtain 6562.8622 Å. for the center of gravity of the red component. For this Curtis' H_α value demands an intensity ratio of 1.09 to 1, as compared to a theoretical 1 to 1 ratio on this assumption. We again have consistent results, but a slightly lower value of N_∞.

[2] Birge, PHYS. REV., 14, 361, 1919.

observed doublet separation, the observed intensity ratio of the components, and the observed half-width of the components.

THE BALMER SERIES IN MIXTURES OF H AND He AT HIGH PRESSURES.

An entirely different type of phenomena is that illustrated by the appearance of the Balmer series, down to $n' = 14$, in mixtures of H and He at 41 mm. pressure. Merton and Nicholson consider this important evidence against the entire Bohr theory of the hydrogen atom, but in view of the many exact quantitative agreements of this theory, little doubt can remain as to its general validity. It is therefore necessary to "explain" these observations. Assuming a *constant* temperature of 15° C., and a *constant* separation of the atoms, it appears, as stated by Merton and Nicholson, that the diameter of the ring (2.08×10^{-6} cm.) for $n' = 14$, is twice the distance apart of the atoms (1.0×10^{-6} cm.)

Qualitatively, all phenomena agree with the Bohr atom. Wood (loc. cit.) finds that, aside from the disturbing effects due to the secondary spectrum, the successive lines of the Balmer series appear as the pressure is lowered. Merton and Nicholson find that the higher members have relatively less intensity at high pressures. Wood finds that H_{20} has only 1/600,000 the intensity of H_α, in a long vacuum tube at 0.4 mm. pressure, while in the nebulæ the intensity decrement is much smaller. The Merton and Nicholson figures for the intensity decrement lead to 1/4,000,000 for this ratio.

It thus follows that, considering *only* those atoms which, at any instant, are radiating monochromatic energy, it is merely necessary that an extremely small fraction of this number need to be several times as far from all neighboring atoms as the average distance. With a Maxwellian distribution of velocities and distances, this seems easily possible. The question as to what fraction of the total number of atoms is at any instant emitting monochromatic radiation does not enter here. Except in the case of the "first resonance" line, this fraction also is believed to be very small. Furthermore, it is well known that the helium atom has practically no effect, either attractive or repulsive, on near-by electrons. This explains simultaneously why the predicted fine structure of the Balmer series appears *only* in mixtures of H and He, why the 12th member of the series can appear at all in such mixtures at high pressure, and why the higher members are extraordinarily sharp in such mixtures. Merton and Nicholson themselves remark the absence of broadening of the higher members, indicating an absence of any interatomic electric field, in spite of the proximity of the helium atoms.

There still remains the question of the temperature of the radiating

source. Because of the work of Buisson and Fabry[1] on the width of the helium lines, this temperature is now usually considered roughly that of the walls of the tube, and Merton uses this assumption, in his calculation of the Doppler effect for H_α and H_β. In view of the narrowing of these lines, at liquid-air temperature, it would appear that the assumption is certainly approximately correct for hydrogen, as well as for helium.

It seems to the author, therefore, that the well-known neutral effect of helium on neighboring electrons, together with the Maxwellian distribution of velocities, separations, etc., is quite sufficient to account for the experimental results thus far obtained. The fact that a small trace of impurity such as oxygen (see Wood, loc. cit.) seems necessary to the best production of the Balmer series would indicate that a strong field of force (due to the oxygen atom) is present under these conditions in the immediate neighborhood of the emitting atom. Yet this produces only a slight blurring of the emitted line (*i.e.*, frequency shifts of possibly one part in 50,000). All the more then can helium atoms be very close to the emitting center, without appreciably disturbing the emission.

University of California,
December, 1920.

[1] Jour. de Phys., 2, Ser. 5, pp. 442–464, 1912.

AN EXPERIMENTAL STUDY OF THE REFLECTION OF X-RAYS FROM CALCITE.

BY BERGEN DAVIS AND W. M. STEMPEL.

SYNOPSIS.

Per cent., of monochromatic X-rays reflected from calcite, for wave length ranging from .3Å. to .8Å. was studied by means of a *double X-ray spectrometer.* A narrow beam of general radiation fell at an angle upon a crystal designated as *A* and the reflected beam was allowed to fall upon a second crystal designated *B*. The intensity of the beam from *B* was then compared, by means of the ionization produced in an ionization chamber with the direct beam from *A*. *Per cent., reflection was found surpisingly large* when the surfaces of the two crystals were strictly parallel. The per cent., reflection will depend upon the character of the beam reflected and therefore upon crystal A.

Significant energy distribution curves were found when the crystal B was rocked through a small angle on either side of parallelism. *A very sensitive micrometer motion* was provided for rotating crystal *B* about both a horizontal and also about a vertical axis, necessitated by the extremely narrow energy distribution curves obtained.

Three pairs of crystals were investigated. Pair (A_1–B_1) where *A* was a rather imperfect specimen of *Montana calcite* and B_1 was a clear specimen of Iceland spar. The surface of both crystals were polished. Pair ($A_2 - B_2$). Here a clear specimen of *Iceland spar* was split. The two split surfaces were polished and the crystals mounted so that reflection was from the surfaces that had been contiguous before splitting. Pair ($A_3 - B_3$) was another pair obtained by splitting a clear specimen of Iceland spar, but leaving surfaces unpolished. Mounted same as ($A_2 - B_2$).

The rocking curves vary greatly in width, depending upon the nature of the reflecting surface; 16″ of arc for width of half maximum when crystal is a good sample and the surface is the natural split surface (not polished). When crystals are not perfect samples and surface polished as much as 57″ of arc was obtained. For any one pair of crystals the width of the half maximum of these rocking curves is a *linear function of the wave length* with a *definite finite intercept* depending upon the condition of the surface. The more perfect the crystal the less does this width depend upon wavelength.

Per cent., reflection is a function of wave length, but is less so the more perfect the crystal. For the pair ($A_3 - B_3$), it was nearly independent of wave length. It would seem that the *reflection from a really perfect crystal would be independent of wavelength and would probably be greater than fifty per cent.*

A KNOWLEDGE of the proportion of the incident X-rays of any frequency that are reflected from the cleavage surface of a crystal is of great importance in determining the distribution of energy in the continuous X-ray spectrum and also the partition of energy among the many lines of the characteristic spectra. It is also of prime importance in the development of an adequate explanation of crystal reflection itself.

Measurements of the relative reflection of X-rays in the several orders have been made by Professor W. H. Bragg and W. L. Bragg, as well as the relative reflectivity of various crystals for the same radiation. The percentage reflection or the coefficient has also been measured by Professor Bragg, using a single crystal. Such determinations must contain an error due to the presence of the general radiation in addition to the line radiation in the original beam before reflection. A. H. Compton[1] has made a direct determination of the coefficient of reflection of rock salt and calcite for one particular wave-length. Compton allowed the radiation reflected from a crystal placed on one spectrometer to fall on a second crystal placed on another spectrometer suitably placed near the first. The apparatus was arranged so as to give an integral area of the curves as the crystals were rocked through a small angle. The small value of the reflection obtained by Compton would

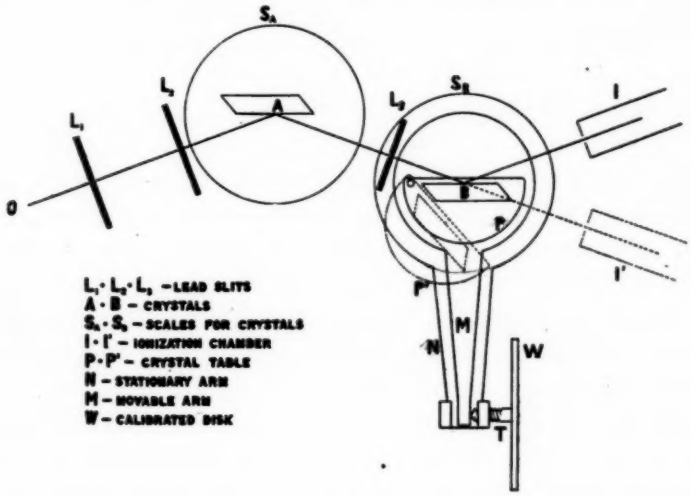

Fig. 1.

indicate that the two crystals were not placed with the crystal faces parallel, as we have done, but were placed nearly $(180°-2\theta)$ to this position so that only a small portion of the ray from first crystal could be reflected from the second crystal in any one position. (This point is not mentioned in his description of the experiment.)

For the purpose of this study of crystal reflection a special double X-ray spectrometer was constructed. A plan of this instrument is shown in Fig. 1. The arrangement of the parts is sufficiently shown in the figure as not to need a detailed description. The heterogeneous beam passing through the slits L_1L_2 falls on Crystal A. The position of this

[1] Proc. Am. Phys. Soc., PHYS. REV., July, 1917.

crystal is read on the vernier scale S_A in the usual manner. The pencil of rays reflected from A is nearly homogeneous, the range of wavelengths ($\Delta\lambda$) included depending on the degree of divergence of the original beam. The beam reflected from A falls on crystal B and suffers a second reflection. The intensity of this reflected beam is measured by the ionization current in the ionization chamber I as shown. The crystal B is mounted on a movable plate P which can be thrown back as indicated by the dotted lines in the figure. The beam from crystal A can then pass directly into the ionization chamber placed in the position I'. The intensities of the two beams before and after reflection are thus compared by the ionization produced in the chamber in the two positions I and I'. A stop is provided so that the crystal B will return exactly to the same position each time after displacement.

The source of X-rays was a standard Coolidge tube with a tungsten target. This tube was energized by a high tension transformer supplied by a 500-cycle generator. The alternating potential was rectified by a kenetron set and the electricity stored in a large plate-glass condenser immersed in oil. The capacity of this condenser was such that the voltage applied to the tube was practically constant, the momentary fluctuations being of the order of one half of one per cent. of the total voltage (50,000) when a current of 2 milliamperes was flowing through the tube. The speed of the 500-cycle generator was also controlled to a constancy of one half of one per cent. The voltage applied to the tube and the current flowing could be controlled and measured to this degree of accuracy. The voltage was measured by a specially designed repulsion electrometer that had a range from 5,000 to 100,000 volts.

The scale S_B, the mounting for the crystal and the ionization chamber I were all mounted on an arm (not shown in the figure) and could be rotated about center of scale S_A as axis and the angle read by a vernier on scale S_A in the usual manner. The angle of crystal B was read by a vernier on scale S_B. The position of the ionization chamber was read by another vernier on this scale. The arm M was attached to the table carrying crystal B. This arm extended out from the axis as shown and could be moved through a small angle when so desired by the finely threaded screw T. The disc W attached to the screw was graduated on its edge. The parts were so proportioned that one scale division on the periphery of disc W represented a rotation of crystal B through 2 seconds of arc. In this way it was possible to give crystal B an angular displacement as small as one fifth second of arc and read the same with considerable accuracy.

The slightly divergent beam passing through the slits L_1, L_2 after

reflection from crystal A falls on the reflecting face of crystal B. A third slit L_3 was introduced in the path of this beam as shown in the figure. This narrow slit was necessary to keep the beam sufficiently narrow that it would not spread over an area broader than the face of crystal B at small glancing angles.

Maximum reflection was obtained at a certain setting of crystal B, presumably this is the position in which the reflecting planes of B are parallel to those of A. The position of parallelism referred to in this paper is the position at which maximum reflection is obtained. When the reflecting planes of the two crystals are parallel, the ray ee' from crystal A for instance will strike crystal B in such manner that angle b will equal angle a. Another ray striking crystal A at f will meet B at f' and the angle c will equal angle d. The same is true for every ray re-

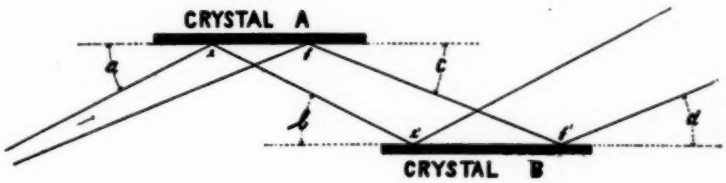

Fig. 2.

flected from A between the points e and f. *Every ray reflected from A will meet B at the proper angle for maximum reflection for the same setting of B.* The above statement is only strictly true if the planes of A and B are perfect and the reflection follows strictly the law $\lambda = 2d \sin \theta$. An imperfection of any kind in crystal A would make the reflected ray slightly non-homogeneous, that is along any path as ee' for instance the radiation would not only consist of a beam of wave-length given by $\lambda = 2d \sin \theta$, but would contain other radiation of slightly different wave-length.

Since every pencil of rays reflected from A to B falls on B at the proper angle for best reflection (when the planes are parallel) we shall consider the coefficient of reflection as determined in this investigation to be the ratio of the intensity of the beam after reflection from B to its intensity before such reflection. These two intensities are measured by means of the ionization chamber in the two positions I and I'.

It is at once evident from Fig. 2 that a ray ee' of given wave-length reflected from A and a ray ff' of another wave-length so reflected cannot both meet the crystal B at proper angle for reflection if the two crystals differ at all in structure or in crystal spacing. If the crystals A and B do differ in structure or spacing a small rotation of crystal B will bring

the crystal to the proper position for reflection of the rays falling on different portions of its surface.

In addition to the lever arm M and slow screw device T for rotating B through small angles about a vertical axis, a similar device (not shown in the figure) was constructed for rotating crystal B about a horizontal axis. In this way the reflecting planes of B could be brought accurately parallel to those of crystal A.

The first pair of crystals investigated was A_1 a Montana calcite, and B_1 a very old and clear specimen of Iceland spar. The reflection was from the (100) planes of each crystal. The surfaces were polished on a plane parallel plate in the usual manner of obtaining an optical polish. The crystals being carefully mounted and crystal A_1 set for

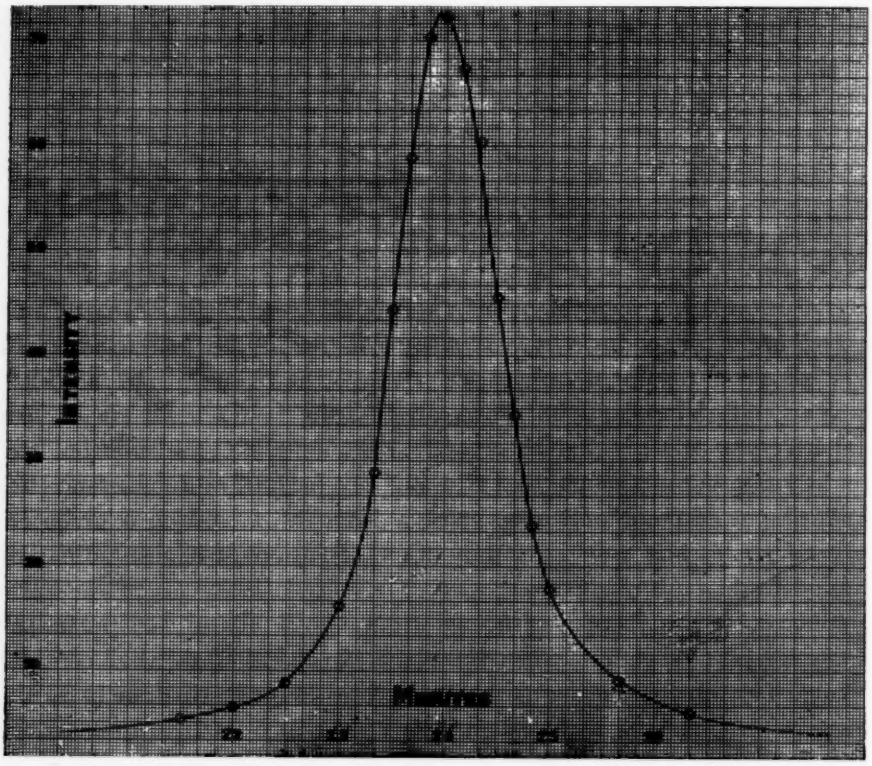

Fig. 3.

reflection of a portion ($\Delta\lambda$) of the general radiation of a desired wavelength, it was found on rotating crystal B_1 through small angles each side the maximum, that a very regular curve of intensity was obtained. A typical curve for these two crystals is shown in Fig. 3 and is given to indicate how accurately such curves can be obtained. The observed

points lie on a very smooth regular curve. It should be pointed out that the principal irregularities in X-ray spectrometer observations do not arise from irregularities in the radiation but are due to the fact that close settings and readings of small angular changes can not be made with verniers. The smoothness of the curves here presented is due to the accuracy of measuring small angular changes by the slow screw device.

The curve (Fig. 3) is seen to have considerable width. The width of curve referred to throughout this paper is the width at half-maximum indicated by the length of the lines a *aa'*, *bb'*, *cc'* in Figs. 4, 5, 6 and 7.

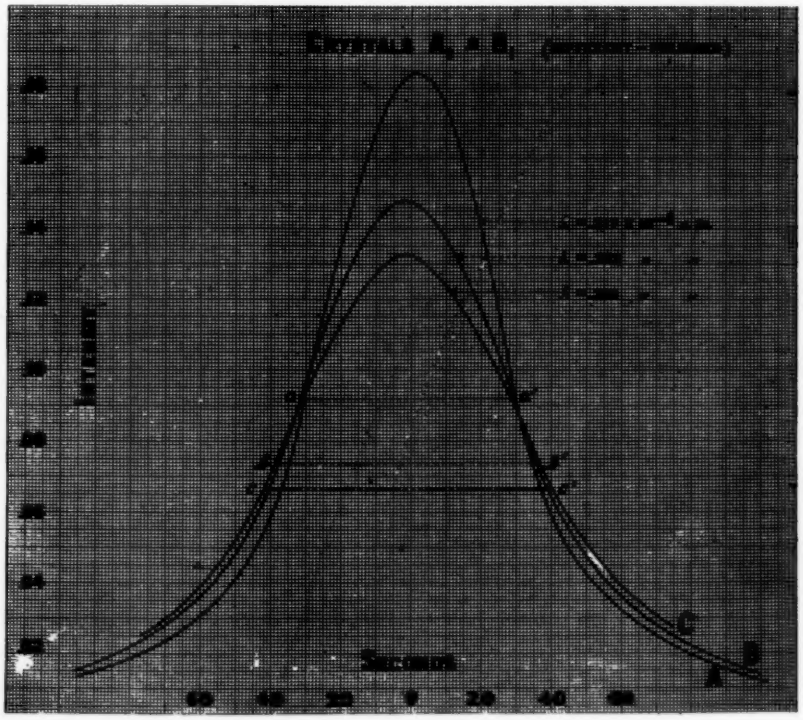

Fig. 4.

After observation of this effect due to *rocking the crystal* through small angles a systematic investigation was undertaken to ascertain its cause.

The width of curve at half-maximum was found to be independent of:

(*a*) Width of the slits L_1L_2.

(*b*) Voltage applied to X-ray tube.

(*c*) Current through X-ray tube.

It was found to depend on:

(*a*) Angle of reflection (wave-length).

(*b*) The nature of the crystals.

(*c*) The state of polish of the surfaces and the similarity of crystals.

Three combinations of crystals were investigated designated as follows:

Crystals $A_1 - B_1$. Crystal A_1 was a Montana calcite. Slight flows were visible in the interior. Surface polished. Crystal B_1. An old clear specimen of Iceland spar. Surface polished.

Crystals $A_2 - B_2$. A clear specimen of Iceland spar was split in two portions. The surfaces polished. The two reflecting surfaces as mounted (Fig. 2) were the surface planes that had been in contact before splitting.

Crystals $A_3 - B_3$. A clear specimen of Iceland spar was split into portions. The freshly split surfaces were *not polished*. The two reflecting surfaces as mounted were the contiguous planes before splitting.

These combinations of crystals showed marked differences in reflectivity and in width of *rocking curves*.

TABLE I.

Crystals A_1 and B_1.

Grazing Angle.	Wave-length.	% Reflection.		Width of Half Maximum.		Width of Half Max. × % Reflec.	Width of Half Maximum Minus Intercept = Q.	Sin θ.	Sin θ. / Q
3° 00′	.317×10⁻⁸		25.8		58.0	1,495	11.7	.0523	
							(58.0−46.3)		.0045
3 30	.369×10⁻⁸		24.6		67.8	1,670	21.5	.0610	.0028
4 00	.422×10⁻⁸	23.3							
		22.2							
		24.8							
			23.4						
5 00	.527×10⁻⁸	21.7							
		21.3							
			21.5						
5 30	.580×10⁻⁸		20.8	72.0		1,510	26.4	.0958	.0037
				73.5					
				72.5					
					72.7				
6 00	.632×10⁻⁸	19.5							
		19.1							
		20.7							
			19.8						
7 00	.737×10⁻⁸	18.3							
		19.0							
			18.7						
7 30	.790×10⁻⁸		18	78.2					
				79.6					
					78.8	1,475	32.5	.1305	.0040
8 00	.842×10⁻⁸		17.3		83.4	1,445	37.1	.1392	.0038

The curves obtained by slightly rocking crystal B_1 through small angles each side of the maximum are shown in Fig. 4. Observations were made at three different wave-lengths. The coefficients of reflection obtained at a number of glancing angles are given in Tables I and IV.

The fourth column of Table I. gives the widths at half-maxima (aa', bb' and cc') expressed in seconds of arc. The fifth column gives the product of width at half-maximum and the per cent. reflection (proportional to maximum ordinate). This product is probably proportional to the areas of the curves. The table shows these areas to be nearly constant. The widths at half-maxima are plotted in Fig. 8. The

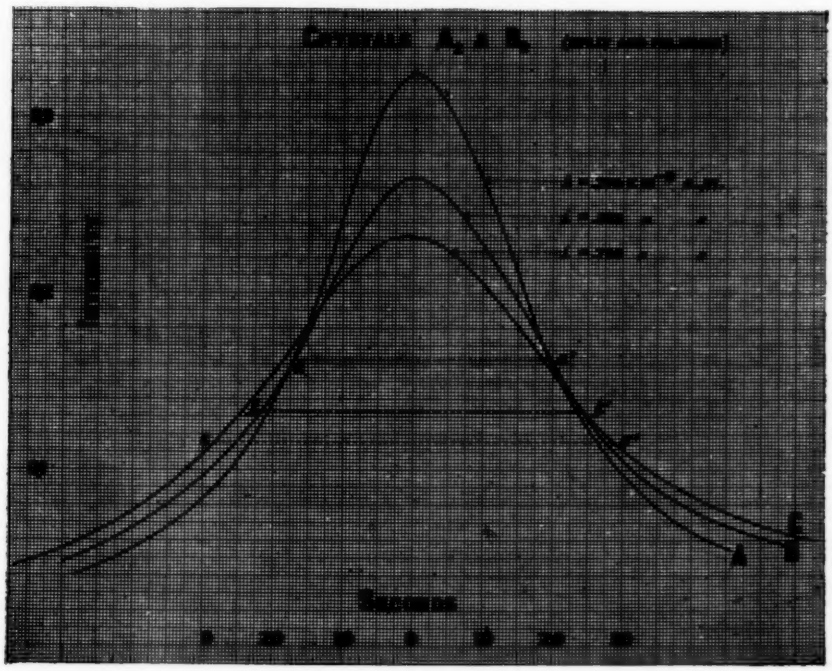

Fig. 5.

straight line drawn through the points intercepts the ordinate axis at points designated by g_1. The width at half-maxima minus the intercept g_1 is given in the sixth column of the table (Q).

The fact that the points in Fig. 8 lie approximately on a straight line suggests that the curve width is made up of two parts, one part a constant g_1 and another part proportional to the sine of the glancing angle. This is indicated by the constancy of the ratio $\sin\theta/Q$ shown in the last column of the Table, where Q represents the widths at half-maxima minus the intercept g_1.

Crystals A_2 and B_2. A clear specimen of Iceland spar was split into two parts along a cleavage plane. The two split surfaces were polished on a plate using fine rouge and water as the abrasive. The crystals were mounted on the spectrometer in such position that the reflection took place at the two surfaces that had been continguous before cleavage. The coefficient of reflection was considerably larger than that obtained with the two dissimilar crystals $A_1 - B_1$. The width of rocking curves

TABLE II.

Crystals A_2 and B_2.

Grazing Angle.	Wave-length.	% Reflection.	Width of Half Maximum.		Width of Half Max. × % Reflec.	Width of Half Maximum Minus Intercept = Q.	Sin θ.	$\frac{\text{Sin } \theta}{Q}$.
3° 00′	$.317\times10^{-8}$	37.3						
3 30	$.369\times10^{-8}$	(curve) 35.4	34.3		1,245	18.7	.0610	.00326
			36.3			(35.2–16.5)		
			35.0					
				35.2				
4 00	$.422\times10^{-8}$	34.3						
		32.9						
		33.6						
4 30	$.474\times10^{-8}$	(curve) 32.9	41.5		1,371	25.2	.0785	.00312
			41.9					
				41.7				
5 00	$.527\times10^{-8}$	30.5						
5 30	$.580\times10^{-8}$	(curve) 29.2	45.6		1,343	29.5	.0958	.00325
			46.5					
				46.0				
6 00	$.632\times10^{-8}$	27.9						
6 30	$.684\times10^{-8}$	(curve) 26.9	54.6		1,417	36.2	.1132	.00313
			50.9					
				52.7				
7 00	$.737\times10^{-8}$	26.0						
7 30	$.790\times10^{-8}$	(curve) 25.3	57.0		1,452	40.9	.1305	.00319
			57.8					
				57.4				
8 00	$.842\times10^{-8}$	24.6						

on the other hand was much less. The widths at half-maxima, the products of widths at half-maxima and per cent. reflection are given in Table II. The product of width at half-maxima and per cent. reflection is not quite constant but progressively increases with glancing angle as

shown in the fifth column of the table. The widths at half-maxima plotted against glancing angle lie sensibly on a straight line (Fig. 8). The widths at half-maxima minus the intercept g_2 is given in the sixth column of the table (Q). The ratio sin θ/Q is a constant. The width of rocking curve is composed of two parts. One part is a constant g_2, and the other part varies as the sine of the glancing angle.

Crystals $A_3 - B_3$. A clear crystal of Iceland spar was split into two parts along a cleavage plane. The crystals were so mounted that the molecular planes that were contiguous before splitting became the two reflecting surfaces of the crystals. The surfaces were not polished, and

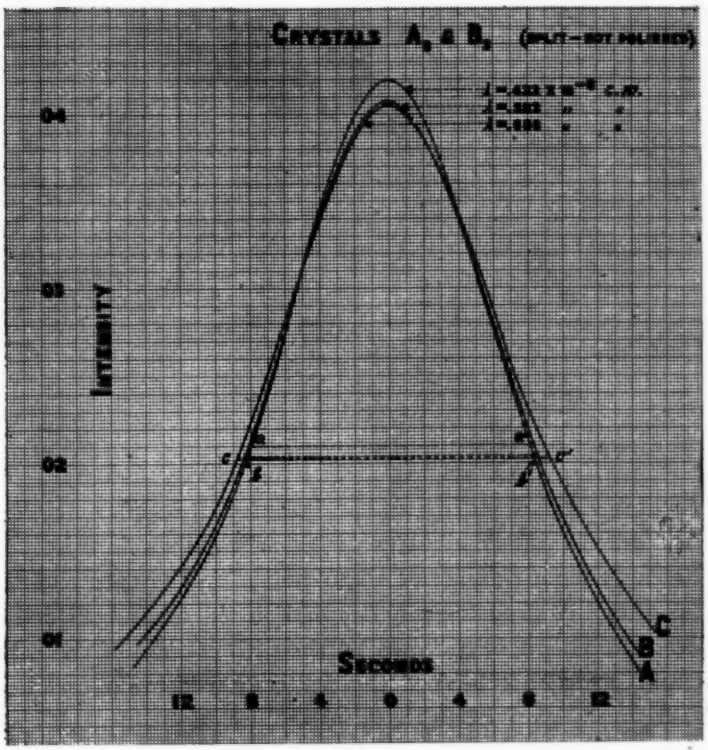

Fig. 6.

care was taken not to touch them in any way so that the surface molecular layers should remain in as perfect a state as possible.

The reflection was very much greater than that obtained with the other crystals described. The results are shown in Table III., where the several columns have the significance previously described. The curves obtained by *rocking* crystal B_3 are shown in Fig. 6. The product of widths at half-maxima and per cent. reflection is nearly constant, in-

creasing slightly with increasing wave-length. The intercept on the width at half-maxima ordinate at zero angle is shown at g_3 in Fig. 8. The ratio sin θ/Q is a constant. The curve width may be regarded as comcomposed of two parts, one part is a constant g_3, the other part varies as the sine of the glancing angle.

TABLE III.

Crystals A_3 and B_3.

Grazing Angle.	Wave-length.	% Reflection.		Width of Half Maximum.		Width of Half Max. ×% Reflec.	Width of Half Maximum Minus Intercept = Q.	Sin θ.	$\frac{\text{Sin } \theta}{Q}$.
4 00′	.422×10⁻⁸	44.4		16.1		717	3.6		
		44.4		16.2			(16.2–12.6)	.0698	.0199
			44.4		16.2				
5 30	.580×10⁻⁸	42.9		17.3		752	4.9	.0958	.0195
		43.3		17.6					
			43.1		17.5				
6 30	.686×10⁻⁸	42.4		18.1		787	5.8	.1132	.0195
		43.2		18.6					
			42.8		18.4				
7 30	.790×10⁻⁸	42.4							
		43.3							
			42.8						

The effect of similarity of crystal and treatment of surface on the width of rocking curves and their areas is clearly shown in Fig. 7. These curves are for glancing angles of 3°–30′ and 4°. They are given to scale. The areas of curves progressively decrease as the crystal surfaces become more perfect. This is also shown by the fifth column of the tables.

For convenience of reference the per cent. reflection for the several crystals at various wave-lengths is assembled in Table IV. and shown graphically in Fig. 9.

The last two columns of the table give the calculated variation of reflection with wave-length by an equation derived by C. G. Darwin[1] for imperfect crystals. All of the constants in this equation including the Debye heat term are collected into a single constant A, and the equation written in the form

$$R = A \frac{\lambda^3(1 + \cos^2 2\theta)}{\mu \sin \theta \cos \theta}.$$

[1] Phil. Mag., Feb. and April, 1914.

For purposes of comparison the constant A is taken to be such as to give the observed reflection at a particular angle (6°). The reflection at other angles is then calculated for the absorption $\mu \sim \lambda^{2\cdot4}$. For this

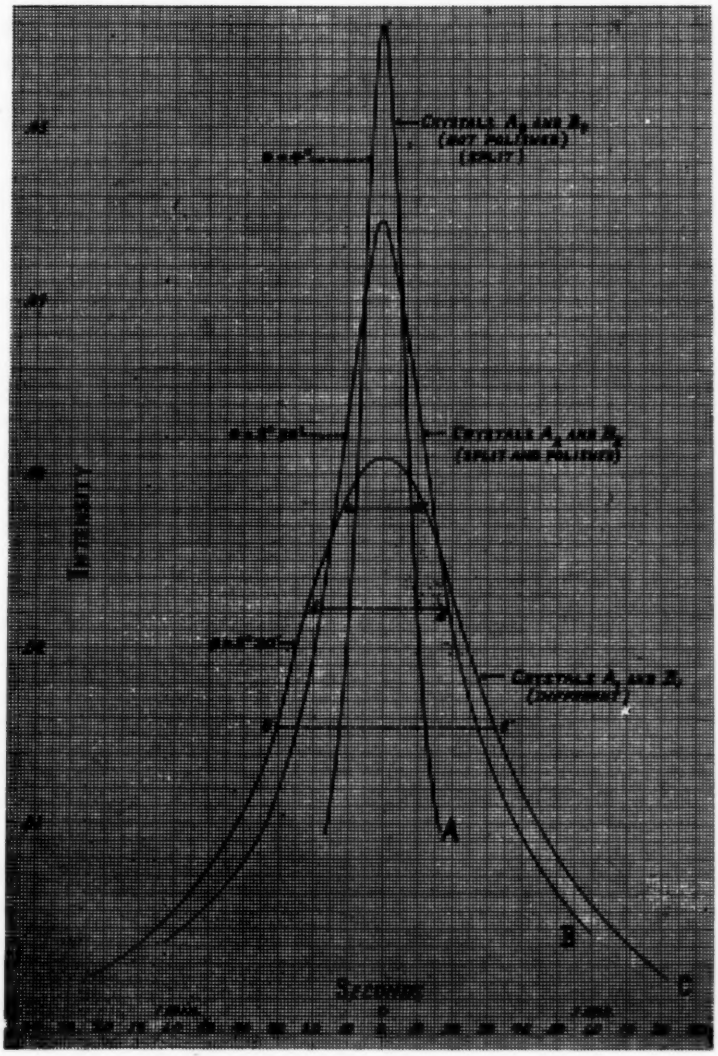

Fig. 7.

value of μ the equation agrees very closely with the observed results for the two pairs of polished crystals. This is particularly true for crystals $A_2 - B_2$.

It should be pointed out that the per cent. reflection or coefficient of reflection here determined is considered to be that of crystal B in every

TABLE IV.

Angle.	λ.	Per Cent. Reflection.				
		Observed.			Computed (Darwin).	
		A_1-B_1.	A_2-B_2.	A_3-B_3.	A_1-B_1.	A_2-B_3.
3	.317	25.8	37.3		26.5	37.2
3-30	.369	24.6				
4	.422	23.4	33.6	44.4	23.5	33.1
5	.527	21.5	30.5		21.6	30.1
5-30	.580	20.8		43.1		
6	.632	19.8	27.9		19.8	27.9
6-30	.686			42.8		
7	.737	18.7	26		18.6	25.9
7-30	.790			42.8		
8	.842	17.3	24.6		17.5	24.6

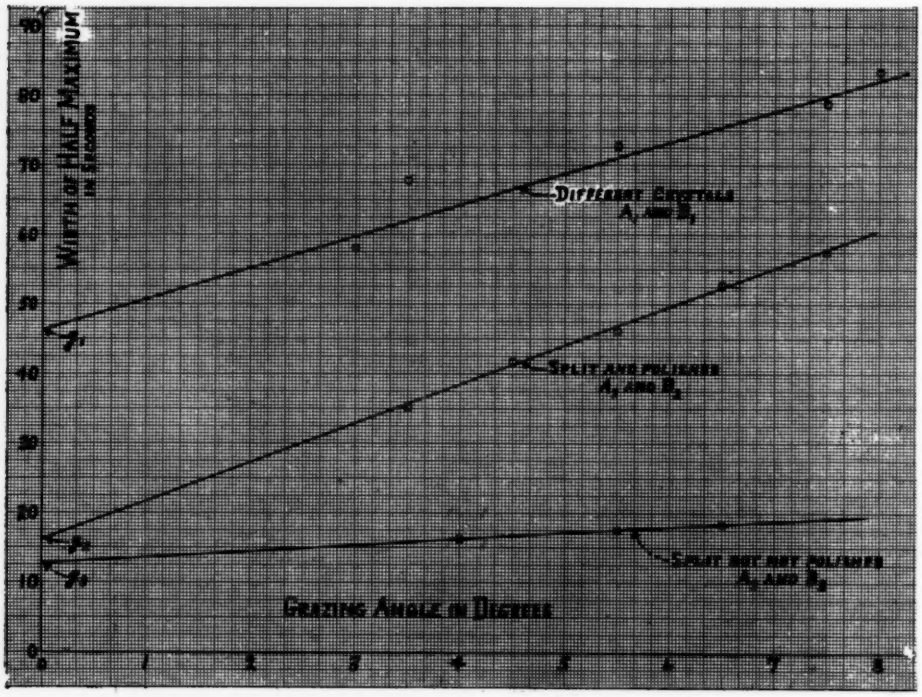

Fig. 8.

case. The reflection obtained from B however depends not only on its perfection but also on the perfection and surface of crystal A. This is indicated by the performance of the combination $A_1 - B_1$ which differed in character from that of the other set of crystals. Crystal B_1 was a perfect specimen of Iceland spar, as perfect in appearance as crystal B_2.

Crystal A_1 on the other hand, a specimen of Montana calcite showed imperfections that were visible in its interior. The irregular results and low value of the reflection obtained with these two crystals can be fairly attributed to the imperfection of A_1. It will be specially noticed by Table I and Fig. 8 that the width at half-maximum in particular is too large at glancing angle $3° + 30'$. The other points in Fig. 8 lie reasonably on a straight line. In addition to the visible evidence, the imperfections of crystal A_1 are indicated by curves of the continuous and line

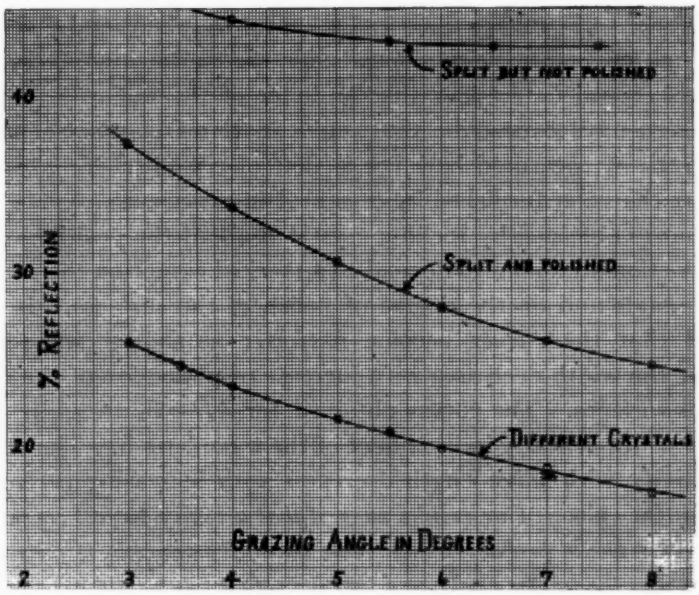

Fig. 9.

spectrum obtained by B. A. Wooten using this crystal (PHYS. REV., Jan., 1918—Fig. 1). The minute false lines there observed are undoubtedly due to imperfections in the crystal. Crystal B_1 on the other hand appears to be fairly perfect as indicated by smooth curves of the continuous and line spectrum obtained by C. T. Ulrey using this crystal (PHYS. REV., May, 1918).

What shall be defined as the coefficient of reflection is a matter for discussion. Using single crystal reflection Professor Bragg has taken the ratio of curve areas obtained by rocking the crystal and moving the slit of the ionization chamber across the beam. This of course can only be done in case of the line spectrum and even then is subject to the error of the general radiation which is present to a considerable extent.

A. H. Compton (*l.c.*) has applied the method of integration of curve

areas in case of reflection from two crystals. The coefficient of reflection is expressed in terms of angular measure (per degree). It is not clear how such a quantity which is really the ratio of intensities before and after reflection can contain angular measure.

We have taken as the coefficient the ratios of the intensities of the beam of X-rays before and after reflection from crystal B at position of maximum reflection. This is the coefficient for crystal B. The reflection from crystal B depends on the degree of homogeneity of the radiation falling on it. It is the function of crystal A to sort out from the general radiation a nearly homogeneous radiation for examination by crystal B. The degree of homogeneity depends on the perfection of crystal A. Since this crystal determines the character of the radiation falling on B it is necessary to describe the results in terms of pairs of crystals. The reflectivity measured however is that of crystal B for rays of the particular character furnished by crystal A in every case.

The curves obtained by rocking crystal B about the position of maximum reflection are found to depend to a marked extent on the perfection of the crystals and on the degree of polish of the surfaces. It will be observed that the curves become narrower at shorter wave-lengths. Also that the width decreases with increase of perfection of the crystals and their surfaces. The curves obtained for $A_3 - B_3$ are quite narrow and their width is nearly independent of the wave-length. The variation of reflectivity with wave-length decreases with increasing perfection of crystal surface also. *Our results suggest that a really perfect crystal (were such possible) would probably reflect more than fifty per cent. of the radiation falling on it at the proper angle, and that the reflectivity would be independent of wave-length.*

The attention of the reader is directed to a short paper on reflection of radiation from an infinite series of equally spaced planes appearing in this number of the PHYSICAL REVIEW. The results obtained are of considerable interest in view of the determination of reflectivity just described.

The width at half-maximum of 16″ obtained for crystals $A_3 - B_3$ is many times too great to be attributed to the Fresnel line width that should be expected with radiation of such short wave-length and a grating of such a large number of elements. The width of 16″ of arc for a reflectivity of about 45 per cent. would indicate that even in the case of a perfect crystal the curve width would still be of the order of a few seconds of arc. This width might be due to very minute differences in spacing in the case of the two crystals, but since contiguous planes were used for reflecting surfaces in case of $A_3 - B_3$ it is doubtful if the crystals

varied sufficiently in grating space in such a small distance as to produce so great an effect.

Another more reasonable explanation of curve width (for perfect crystals) is that it is due in some way to the width of each reflecting plane. That is, it may be due to the distribution of the electrons about the nucleus of the atoms of the crystal. One of us (Stempel) has recently developed a theory of crystal reflection involving the electron distribution that accounts with some success for these curves.

Since the width of the rocking curve would depend directly on a possible difference of crystal spacing in the two crystals one should obtain a great effect by heating one of the crystals slightly. Also by heating both crystals (*A* and *B*), keeping them at the same temperature it should be possible to measure the Debye heat effect with great accuracy by this arrangement of a double spectrometer.

Phoenix Physical Laboratory,
Columbia University,
January, 1921.

REFLECTION OF RADIATION FROM AN INFINITE SERIES OF EQUALLY SPACED PLANES.

By K. W. Lamson.

SYNOPSIS.

Reflection of Radiation from an Infinite Series of Equally Spaced Planes.—If the fractions of the incident radiation upon any plane which are absorbed, reflected and transmitted by that plane are constant and denoted by a, r and t respectively, and if all possible internal reflections are taken account of, the *coefficient of reflection* is shown to equal $(1/2r)\{1 - t^2 - r^2 - \sqrt{[1 - 2t^2 - r^2 + (t^2 - r^2)^2]}\}$. When both a and r are very small, as in the case of the *reflection of X-rays from a crystal surface*, the expression becomes $[1 + a/r - \sqrt{(a^2/r^2 + 2a/r)}]$; thus the proportion reflected depends only on the ratio of absorption to reflection per plane.

THE surprisingly large value of the reflection of X-rays from calcite (about 45 per cent., obtained by Bergen Davis and W. M. Stempel, an account of which appears in this number of the PHYSICAL REVIEW, suggests the problem of investigating the reflection that might be expected from a system of equally spaced reflecting planes.

No special assumptions are made as to the physical nature of the radiation or of the reflecting medium other than that it consists of an indefinite number of equally spaced planes. As the radiation passes through each plane a minute fraction r is reflected and a minute fraction a is absorbed. The amount transmitted is $t = 1 - r - a$. The fraction reflected per plane is quite small being of the order perhaps of 10^{-5} to 10^{-6}.

In the case of a perfect crystal the absorption per plane is probably much less than the reflection[1] for the particular wave-length for which the reflection is a maximum for any given angle. The percentage of transmission, reflection and absorption is assumed to be the same for all planes.

The final emergent (front reflecting face) ray from a system of planes is made up of parts, each of which has been reflected an *odd* number of times and transmitted through an *even* number of planes.

Assume the intensity of the ray incident at the first plane to be unity. Then the intensity of a ray after $2j - 1$ reflections and $2i$ transmissions is

$$I = t^{2i} r^{2j-1}. \qquad (1)$$

Let C_{ij} be the number of ways in which it is possible for a ray to be

[1] C. G. Darwin, Phil. Mag., April, 1914.

transmitted $2i$ times and reflected $2j - 1$ times. Then the total amount reflected is

$$R = \sum_{j=1}^{\infty} C_{ij} t^{2i} r^{2j-1}. \tag{2}$$

The values of C_{ij} were computed directly for all values of i and j up to 5 and were seen to be given by the following formula.

$$C_{ij} = \frac{(i+j-2)!\,(i+j-1)!}{(i-1)!\,i!\,(j-1)!\,j!} = \frac{i(i+1)^2(i+2)^2\cdots(i+j-2)^2(i+j-1)}{(j-1)!\,j!}. \tag{3}$$

This formula has been checked by the independent computation of C_{ij} for $i = 8$ and $j = 7$.

For the case when $j = 1$, $C_{i_1} = 1$, the contribution of a single reflection from all planes is

$$\sum_{i=1}^{\infty} (C_{i1} t^{2i}) r = \frac{r}{1 - t^2} = \frac{1}{2}\left(\frac{1}{1 + a/r}\right). \tag{4}$$

The sum appearing in the formula for R Equation (2) has been found by T. H. Gronwall to be

$$\frac{1}{2r}[1 - t^2 - r^2\sqrt{1 - 2t^2 - 2r^2 + (t^2 - r^2)^2}]. \tag{5}$$

For the values of a, r, t which we are considering, this is equal to

$$R = \frac{a}{r} + 1 - \sqrt{\frac{a^2}{r^2} + \frac{2a}{r}}. \tag{6}$$

Thus the total reflection depends only on the ratio of absorption to reflection at each plane. As r is so small it might be expected that the terms in r^3, r^5, etc., might be neglected, that is, that the contributions of repeated internal reflections might be neglected. This however, is not the case. The number of possible paths increases so rapidly with the number of reflections that for probable values of a/r, the repeated reflections contribute a considerable portion of the total energy reflected.

The following table is computed from formula (6) for various values of the ratio a/r.

Absorption per Plane / Reflection per Plane	0	.02	.05	.1	.2	.3	.4	.5	1	2	3	10
Per cent. reflection.....	100	82	73	64	54	47	42	38	27	17	13	5

COLUMBIA UNIVERSITY,
JANUARY, 1921.

A STUDY OF THE PHOTO-ACTIVE ELECTROLYTIC CELL, PLATINUM—RHODAMINE-B—PLATINUM.

BY CARLETON C. MURDOCK.

SYNOPSIS.

The Range of the Current-time Equations.—Goldmann and Thompson have each suggested equations to represent both the growth and the decay of the current given by a photo-active electrolytic cell having electrodes of platinum and an alcoholic solution of Rhodamine-B as electrolyte. The author points out that in each of these equations it is necessary to use different parameters after the first minute of the growth or decay than before and suggests that this may be due to the failure to correct the data for the inertia and damping of the galvanometer coil. *A method for correcting the galvanometer deflections* for these effects is discussed and correction equations developed. These equations involve constants of the galvonometer, the resistances of the circuit and the polarization capacity of the cell.

The polarization capacity of the cell used is measured by impressing a small potential difference on the cell and observing the instantaneous galvanometer deflections. The capacity as computed from the time constant of the corrected current-time curves gives 26 microfarads per square centimeter of each electrode. This is in good agreement with the results obtained by other observers for the capacity of platinum electrodes in aqueous solutions of inorganic substances.

The Dark Current.—Cells having as electrodes sputtered platinum films are found to give a current when not illuminated if the electrodes are not alike. This current tends to flow (*a*) from the denser to the less dense electrode, (*b*) from the warmer to the cooler electrode. Its value is independent of the external resistance of the circuit within the range 0 to 1 megohm and decreases slowly as fatigue effects the photoelectric sensitiveness of the cell.

Tests of the Current-time Equations.—Data taken by subjecting the cell to exposures of 10 minutes or more (*a*) can not be repeated (*b*) are not when corrected in agreement with either of the above types of equation. Data taken by exposures of 1 minute (*a*) may be repeated very exactly, (*b*) are not, when corrected, in agreement with either type of equation unless the parameters are allowed to change and then only in the case of Goldmann's equation for the growth and Thompson's equation for the decay. In both these cases the change in the parameters occurs at about 8 seconds.

The Hyperbolic Decay Equation.—It is shown that the decay of the current following an exposure of 1 minute or less is well represented throughout the range of experiment by the equation

$$y = y_0 - \frac{t}{Mt + L},$$

an equilateral hyperbola.

The effect of the length of exposure on the decay is investigated for exposures of 15, 30, and 60 seconds making use of this equation. It is found that the initial rate of decay is independent of the length of exposure. This is shown to be not consistent with Goldmann's equation.

THE fact that electrolytic cells containing alcoholic solutions of certain organic dyes have photo-electric properties, was first shown by the work of Nichols and Merritt[1] in 1904. That the effects are electromotive in character rather than resistive, was not understood, however, until the work of Hodge[2] in 1908. He showed that the effects are produced by the action of the light on a very thin layer of the solution at the boundary surface between the illuminated electrode and the electrolyte. The same results were independently obtained by Goldmann[3] who made a systematic study of cells of this type. He found that the current produced in the external part of the circuit is proportional to the light intensity and to the area of the illuminated electrode and that it is practically independent of the external resistance for the range from 3,000 to 100,000 ohms.

When the surface between one of the electrodes and the electrolyte is illuminated, the electrode becomes positively charged and if it is connected to the other, a current will flow from the illuminated to the unilluminated electrode. This current is not constant but increases rapidly at first and then more and more slowly until it reaches a maximum after which it slowly decreases. When the exciting light is cut off the current decreases in a similar manner and very gradually approaches its initial value.

Two types of equations have thus far been proposed to express the law of the variation with time of this photoelectric current. Both apply to the case where the duration of the exposure is so short that the maximum current is not reached. The first of these was proposed by Goldmann. He assumed that the effect is due to an ionization of the solute molecule by the incident light in a manner similar to the Lenard-Hallwachs effect and that there results a charging of the electrolytic capacity of the illuminated electrode. On the basis of this he derived equations (1) and (2) for the growth and decay respectively.

$$i = q(1 - \epsilon^{-mt}), \tag{1}$$

$$i = i_0\epsilon^{-mt}. \tag{2}$$

In these equations, i represents the instantaneous value of the current at time, t; q, the charge liberated per second by the light; i_0, the initial value of the decay current; and m, $1/CR$, where C is the electrolytic capacity and R the external resistance.

In order to represent his experimental data, he found it necessary to modify his equations by the addition of constant terms.

[1] Nichols and Merritt, PHYS. REV., Vol. 19, p. 415.

[2] Hodge, PHYS. REV., Vol. 26, p. 540 and Vol. 28, p. 25.

[3] Goldmann, Ann. d. Phys., Vol. 27, p. 449, 1908.

$$i = A_1 + B_1(1 - \epsilon^{-m_1 t}), \tag{3}$$

$$i = A_2 + B_2\epsilon^{-m_2 t}. \tag{4}$$

Equations (3) and (4) show these modified forms. A_1, A_2, B_1, B_2, m_1, and m_2 are empirical constants and the values of m_1 and m_2 are not equal but differ by about 40 per cent. The values of i computed from equation (3) and (4) are in good agreement with Goldmann's observed values except when t is less than one minute, in which case there is a marked discrepancy.

The other type of equation was proposed by Thompson[1] and was suggested by the fact that most of the dyes exhibiting this property are fluorescent and by the similarity between the curve of the decay of the photoelectric current and that of the decay of phosphorescence. If the reciprocal square root of the intensity of phosphorescent light is plotted against time either a straight line or a series of intersecting straight lines will result. Thompson plotted the reciprocal square root of the photoelectric current against time and obtained with both the growth and decay data, points that lay upon two straight lines. In both cases these lines intersected at a point whose abscissa was approximately one minute.

At present the evidence to show that either of these laws has real physical significance seems inconclusive, the first because of the added terms and the failure for the first part of the curve, the second, because of the absence of any theoretical derivation. These two attempts to express the law of the variation of the current have one striking feature in common. In both the equation which represents the data over most of the range fails to do so during the first minute. This may be due as both Goldmann and Thompson suggest to the fact that there are two effects present of different rates of growth and decay, it may be caused by a systematic error in the method of measurement or it may indicate that the proposed laws are only approximately correct. In the first part of the curves the slope and curvature are large and consequently the damping and inertia of the suspended system of the galvanometer must affect the form of the experimentally determined curves to a considerable extent. Failure to correct the curves for these effects would involve errors that would be of appreciable size during approximately the first minute and this may account for the apparent change in the laws during that interval. It seemed desirable, therefore, to study the current-time curves in this interval making correction for the failure of the glavanometer deflection to follow the rapidly changing current. This

[1] Thompson, PHYS. REV., Ser. 2, Vol. 5, p. 43.

correction can be computed from the differential equation of motion of the galvanometer.

For the case of a circuit consisting of pure resistances this equation is

$$(\alpha\ddot{x} + \beta\dot{x} + x)j = u, \tag{5}$$

in which x represents the scale reading of the deflection and u, the current to be measured at time, t, and j the current constant of the instrument for the scale used. α is also a constant of the instrument but β is a linear function of the reciprocal resistance of the circuit. If we let $\beta = \kappa + \lambda/\rho$ where ρ is this resistance; α, κ and λ are constants whose values are easily determined from observations on the period and logarithmic decrement of the instrument as functions of ρ. Let

$$u = jy, \tag{6}$$

then y is the value of x corrected for the errors introduced by the galvanometer and the desired correction equation is

$$y = x + \alpha\ddot{x} + \beta\dot{x}. \tag{7}$$

Given x as a function of t, $\dot{x}$ and $\ddot{x}$ may be obtained graphically and the correction terms of (7) computed.[1]

In the experiments described below I used a galvanometer having the following constants: $\alpha = 5.3$, $\beta = .46 + (61 \times 10^3)/\rho$ and $j = 3.9 \times 10^{-10}$ (where x is measured in centimeters at 282 centimeters distance; t, in seconds; i, in amperes and ρ in ohms). The condition for critical damping of the galvanometer is that $\beta^2 = 4\alpha = 21.2$ giving $\beta = 4.6$ and $\rho = 14{,}700$ ohms. In practise values of ρ larger than this were used, thus decreasing the value of the correction coefficient, β. The values ranged from 17,000 to 21,000 ohms.

This method of correction was carefully tested and found to be capable of an accuracy considerably greater than demanded by the experiments to be performed. In order to be able to change the effective sensibility of the galvanometer and the resistance of the circuit and at the same time keep the value of ρ within the above range, the galvanometer was shunted as shown in Fig. 1. Because of the inductance of the galvanometer, variable currents will not divide between the galvanometer and the shunt branches strictly in accordance with the law of shunts for steady currents. It will be allowable, however, to assume this law provided $l\dot{u} < pgu$ in which l is the inductance and g the resistance of the galvanom-

[1] This method is in effect the same as that used by Einthoven (Amst. Acad. Proc., 8, p. 210, 1906) in analyzing the curves obtained with his string galvanometer. The details of the measurements are necessarily somewhat different due to the difference in the characteristics of the instruments. The author has failed to find any account of the method as applied to a D'Arsonval galvanometer.

eter and p the fractional error allowed. This may be written

$$\frac{y}{\dot{y}} = \frac{u}{\dot{u}} > \frac{1}{p} \cdot \frac{l}{g}$$

$y/\dot{y}$ may be readily evaluated from the correction curves and the condition is that it shall be greater than the inductive time constant of the galvanometer, l/g, divided by the allowable fractional error. When this condition holds the introduction of a network between the galvanometer

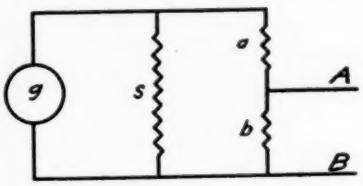

Fig. 1.

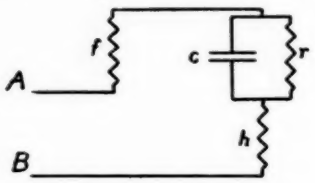

Fig. 2.

and the external part of the circuit does not change the effective values of α, κ and λ but the effective value of j becomes $n \cdot j$ where n is the shunt ratio for the network.

In case there is an electrolytic cell in the external branch, AB, the resistance external to the galvanometer cannot be regarded as a pure resistance as the polarization of the cell by the currents generated in the moving coil reacts to affect the motion of the coil. For the purpose of studying its polarization a cell may be considered as equivalent to a capacity, c, shunted by a resistance, r, and the two in series with a resistance, h, equal to the resistance of the cell as measured on an alternating current bridge. This network is shown in Fig. 2. f is a resistance box which was in series with the cell. The values of r and c which would make such a network strictly equivalent to the cell are not constants but are functions of the polarization. The measurements of r for the cells used in the experiments here described indicate that it is nearly constant within the range of potentials used. No data has been taken with these cells on which conclusive evidence concerning the variation of c with polarization can be based. However it has been shown that the variation of c with polarization in cells containing aqueous solutions is small at small potential differences.[1] It seems safe to assume r and c as constants for the purpose of calculating the correction to the galvanometer deflection due to polarization provided the correction so calculated is small.

Suppose the network shown in Fig. 2 to be connected to a galvanometer

[1] Blondlot, Journ. d. phys., 10, p. 333, 1881.
Sheldon, Leitch and Shaw. PHYS. REV., 2, p. 401, 1895.

through another network for controlling the sensibility and damping of the galvanometer. Let n be the shunt ratio of this network; R, the effective resistance of this network and the galvanometer; and ρ the damping resistance. Let $\zeta = h + f + R$ and $\omega = r\zeta/(r + \zeta)$. Then the equation of motion is

$$\left[\alpha\ddot{x} + \beta\dot{x} + \frac{\lambda\omega}{n^2\zeta^2}\int_{t_0}^{t} \epsilon^{(s-t)/\omega c}[\ddot{x}]_s ds + x\right] nj = u \tag{8}$$

in which α, β, λ and j are the same as in equation (5) and t_0 is the value of t when $\ddot{x} = \dot{x} = 0$. (For the proof of this equation see the appendix.

The correction equation now becomes

$$y = x + \alpha\ddot{x} + \beta\dot{x} + \frac{\lambda\omega}{n^2\zeta^2}\int_{t_0}^{t} \epsilon^{(s-t)/\omega c}[\ddot{x}]_s ds, \tag{9}$$

which differs from equation (7) only in addition of the last term. For the purposes of computation it has been found convenient to modify the form of this new correction term. Let $z = \epsilon^{(s-t)/\omega c}$ and $z_0 = \epsilon^{(s-t_0)/\omega c}$. Using z as the variable of integration instead of s, the term becomes

$$\frac{\lambda\omega^2 c}{n^2\zeta^2}\int_{z_0}^{1} \ddot{x}dz.$$

Now

$$\int_{z_0}^{1} \ddot{x}dz = \int_{0}^{1} \ddot{x}dz - \int_{0}^{z_0} \ddot{x}dz$$

and if we select the time t_0 as some time before the beginning of the experiment when the galvanometer coil was at rest for a finite time, we can write

$$\int_{0}^{z_0} \ddot{x}dz = 0$$

without error as far as the experiment is concerned. Thus we obtain

$$y = x + \alpha\ddot{x} + \beta\dot{x} + \gamma\int_{0}^{1} \ddot{x}dz, \tag{10}$$

where

$$\gamma = \frac{\lambda c}{n^2}\frac{\omega^2}{\zeta^2}.$$

$\int_{0}^{1} \ddot{x}dz$ is the mean value of $\ddot{x}$ weighted with respect to z from $z = 0$ to $z = 1$. When ωc is small the values of $\ddot{x}$ for the time just preceding t weigh heavily and the integral closely approximates the value of $\ddot{x}$ at time t. When this approximation is justified the correction becomes

$$y = x + \alpha'\ddot{x} + \beta\dot{x}, \tag{11}$$

where $\alpha' = \alpha + \gamma$. This form of equation may be used whenever

$\gamma\ddot{\varkappa}\omega c$ is negligible in comparison with y. Otherwise equation (10) must be used and the value of the integral evaluated graphically. In order to make the corrections indicated in equations (10) and (11), it is necessary to know, in addition to the galvanometer constants required for the use of equation (7), the values of r and c for the electrolytic cell.

The cells used by the earlier experimenters had opaque platinum electrodes pressed closely against the front wall of the glass box containing the electrolytic solution. In this type of cell a thin layer of the solution is traversed by the light before it is incident upon the surface of the electrode. This layer absorbs some of the light. There are two serious objections to this type of cell for quantitative work. The thickness of the absorbing layer cannot be measured with sufficient accuracy to enable one to estimate the effective intensity of the light. In such a cell there is always a part of the electrode surface upon which no light falls but which is in contact with the solution. Between this portion of the electrode surface and the illuminated portion there is an electromotive force which the electrode itself short-circuits. Goldmann used as electrodes semitransparent platinum films deposited by Kundt's method on the glass of the front wall of the cell. The light was transmitted through the electrode and was thus incident upon the sensitive layer without previous absorption in the solution. Thompson used, for the most part, cells of the opaque electrode type but he also used cells whose electrodes

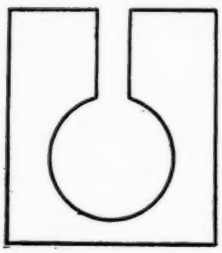

Fig. 3.

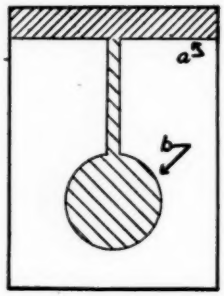

Fig. 4.

were semitransparent silver films. In connection with his results on the current-time curve, he does not state which type of cell was used.

The cell used in the experiments described below consisted of a piece of plate glass, 4 x 5 cm. and 6 mm. thick, cut as shown in Fig. 3 and placed between two plates of optical glass upon which were semitransparent films of platinum as shown in Fig. 4. The part of the film marked, a, in the figure was thick enough to be opaque and was used to make contact between the semitransparent film, b, and the external part of

the circuit. The films were deposited by cathodic sputtering and were then baked at a dull red temperature to make them more permanent. The diameter of the circular part of the film was 2 cm. and the cell was filled so that the meniscus was tangent to the circle at its upper edge. This made the effective electrode area 3.2 sq. cm. The cell as used in the experiments described below was filled with a 6 per cent. solution of rhodamine-*B* in absolute alcohol and had a resistance of about 15,000 ohms. A large part of this resistance was in the narrow strips of platinum film leading from the opaque film above to the circular part in contact with the solution.

The values of the quantities r and c were measured by placing the cell in series with the shunted galvanometer, a megohm box and a small constant electromotive force obtained from the "E. M. F." terminals of a low resistance potentiometer. If we imagine the cell replaced by the equivalent capacity and resistances, the circuit is represented by the network shown in Fig. 2, the shunted galvanometer and the electromotive force in series. The expression for the instantaneous value of the current through h is

$$i = \frac{E}{\zeta + r} + C\epsilon^{-(t/\omega c)}$$

in which C is a constant determined by the initial conditions. If E remains constant, the second term approaches zero and the current, a steady value, $i = E/(\zeta + r.)$ Since i, E, and ζ are known, the value of r can be computed. If the value of E is now changed the current will approach its new value by the exponential curve represented by the above equation and the value of ωc can be determined from the curve. Since both ζ and r are now known ω is known and the value of c may therefore be computed. This method of measuring the polarization capacity of an electrolytic cell, while not yielding results of as high accuracy as other methods, is particularly well adapted to the measurement of cells of high resistance. The large time constants of such cells make most of the methods usually employed, impractical.

Fig. 5 shows results obtained by this method with the cell described above. At time, $t = 0$, E was changed from 0 to .07 volts and at time, $t = 900$ sec., it was again made 0. The variation of the galvanometer deflection with time is shown by the dotted line curve, the small circles representing the actual observations. Equation (7) was used to correct these curves for the errors introduced by the galvanometer as the constants required for the use of the more exact equation were not known. The small crosses indicate the corrected observations wherever the corrections are larger than the radii of the small circles. The two full line

curves are plots of the equations

$$y = 4.6 + 6.7\epsilon^{-.033t} \text{ and } y = 7\epsilon^{-.032t}.$$

The experiment illustrated in Fig. 5 gives as values of ωc, 30 and 31 seconds and, of r, 3.2 megohms. A considerable number of experiments of this type were tried. The resulting values of ωc varied considerably.

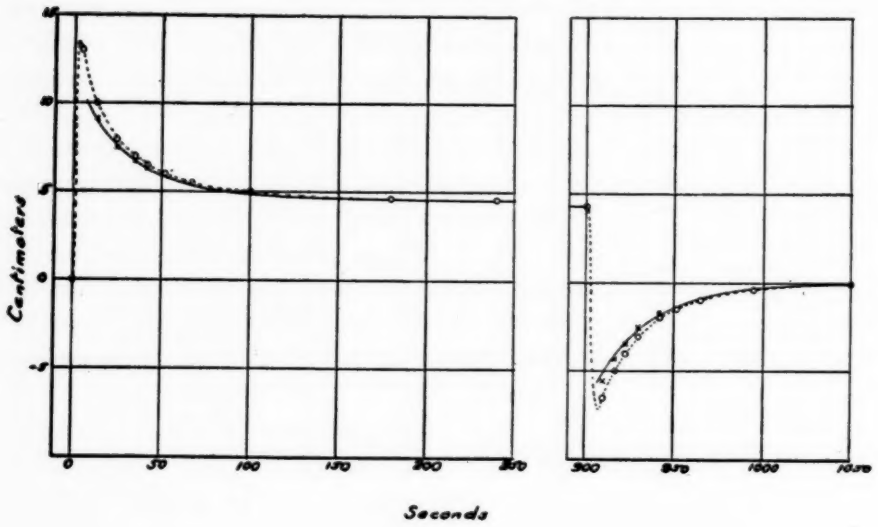

Fig. 5.

The mean vaue was 33 seconds. The values of the steady currents for the whole set of experiments were plotted against the corresponding impressed electromotive forces. The resulting line curved slightly but was practically straight throughout the range covered in the photoelectric experiments. Its slope indicated a value of r of 3.1 megohms. In these experiments $n = 13.4$, $f = 1$ megohm, $h = 15{,}000$ ohms and $R = 4{,}600$ ohms giving $\zeta = 1.02$ megohms, $\omega = .78$ megohms, $\gamma = .01$ sec.^{2} and $c = 42$ microfarads. The value of γ is negligible in comparison with that of α. Thus the additional correction which would have been involved had equation (10) been used instead of equation (7) is zero and no further correction is here needed.

The electrolytic capacity of cells with platinum electrodes has been measured by several observers using a variety of methods. The capacity is proportional to the area of the electrode and varies with the material of the electrode and somewhat with the potential but it is practically independent of the electrolyte. The value here obtained, 42 microfarads, is the capacity of two condensers in series. The capacity of each electrode is therefore 84 microfarads and this gives $84/3.2 = 26$ microfarads per

sq. cm. This compares well with the values that have been obtained by other experimenters who, however, worked with aqueous solutions. Some of the values obtained with platinum electrodes are: Varley,[1] 50; Kohlrausch,[1] 26; Blondlot,[1] 31; Hemholtz,[1] 39; Bouty,[2] 20; Scott,[3] 50. Goldmann obtained the value of 20 microfarads per sq. cm. for his cell which would give 40 microfarads per sq. cm. for each electrode. This was obtained from data taken on open circuit with an electrometer during illumination and the computation was based on his theory of the photoelectric action of the cell, the assumptions at the basis of which are given above.

Many electrodes were made and tested before the two finally used were selected. When a cell was set up and connected in a circuit with a galvanometer there was always a current even with the cell in the dark. This current would vary rapidly at first but when the polarization effects produced by the illumination incident to the operation of setting up the cell had disappeared it would assume a fairly steady value. This dark current was the greater, the more the difference in the density of the two

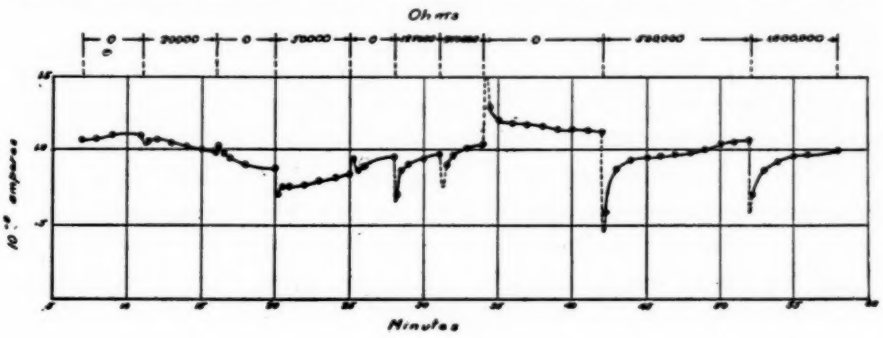

Fig. 6.

films and when the two were at the same temperature, the denser electrode was always positive. Raising the temperature of either electrode made it more positive. The current was so sensitive to temperature variations that unless precautions were taken to keep the temperature of the cell uniform, the dark current varied in an erratic manner.

The dark current was found to be similar to the photoelectric current in that its value is independent of the resistance of the circuit within a large range of variation. This is shown in Fig. 6 in which the value of the dark current is plotted against time. At every change in the value of the resistance there is indicated a throw of the galvanometer such as

[1] Sheldon, Leitch and Shaw, loc. cit.

[2] Bouty, Jour. de phys. (3), Vol. 3, p. 498, 1894.

[3] Scott, Ann. der phys., Vol. 67, p. 402, 1899.

one might expect as the result of the charging or discharging of the electrolytic capacity due to the change in the value of the potential drop in the external resistance. In addition to these throws the diagram shows a slow and apparently erratic drift in the value of the current. There seems to be no relation between this and the resistance changes. This drift is characteristic of that due to temperature variations. In this experiment the resistance of the galvanometer was about 1,000 ohms and the resistance of the cell as measured on an alternating current bridge, 15,000 ohms. We have therefore varied the resistance of the circuit through the range, 16,000 to 1,016,000 ohms without producing an effect upon the current which can be attributed to this variation.

A dark current was also found by Thompson which, however, he was able to partially eliminate by the introduction of resistance into the circuit. This would seem to indicate that there was present in addition to the current of the type described above, one due to a chemico-electromotive force. In all previous work with semitransparent electrodes the films have been deposited simultaneously, side by side on the same piece of glass. Under these conditions the electrodes would ordinarily be so nearly alike in density and temperature that the dark current would be so small as to escape notice. This dark current should be made the subject of a thorough study. Its evident simularity to the photoelectric current makes it probable that the explanation of the latter will also explain the former. Further work on this subject is now under way. In this investigation the effort was rather to reduce the dark current to zero by producing two electrodes of equal densities.

The two films finally selected transmitted respectively 68 per cent. and 72 per cent. of the incident light. The transmission of each was nonselective throughout the visible spectrum. The cell made up with

TABLE I.

Day.	0	1	2	3	10	15
Dark current.....	3.0	2.5	2.0	1.5	1.3	.5
Sensitivity.....	1.	.95	.85		.7	.6

these two electrodes was filled with a 6 per cent. solution of rhodamine-*B* and placed in a glass box which was sealed to prevent the evaporation of the solution. This was then placed in a dark box arranged with a shuttered opening through which one of the electrodes could be illuminated at will. The dark current observed was the smallest that had been obtained with a cell of this type. Its value was observed from time to time for more than two weeks. Table I. gives data on the dark current during

this period. The current varied continually because of temperature changes and the values are the estimated mean values for the day in question measured in 10^{-8} amperes.

During the same period a series of photoelectric experiments was performed under varying conditions as to length of exposure and resistance. Estimated values of the photoelectric sensitivity measured on an arbitrary scale are included in the table for comparison. The data shows a decrease in the value of the dark current with time. It is accompanied by a corresponding decrease in the photoelectric sensitivity. It seems probable that there is a relationship between the two fatigue effects.

Several of the photoelectric current curves of the series just described have been corrected for the errors introduced by the galvanometer and tested for agreement with the Thompson and Goldmann equations. In no case have satisfactory results been obtained. When the Thompson test was applied a curved line always resulted. In most cases, however, it was of such a form that if fewer observations had been plotted it might easily have been interpreted as two straight lines. In taking data for these curves a chronograph was used and a large number of points were recorded. Thompson's diagrams show but few observation points. It seems probable that the difference in the results obtained is due to the fact that his observations were too few and too far apart to indicate the steady character of the curvature.

The cell with which Goldmann obtained the current-time curves whose equations are given above had for its unilluminated electrode a copper plate in an aqueous solution of copper sulphate connected to the alcoholic rhodamine — B solution by a capillary tube. This electrode was designed to avoid the errors due to the polarization of the unilluminated electrode by the photoelectric current. Goldmann found that, when this electrode was used, the current was in general greater than that obtained at corresponding times with the ordinary type of electrode. However during approximately the first minute of an exposure the two results did not differ measurably. I have, as yet, made no attempt to correct for the error due to the polarization of the dark electrode by the photoelectric current. If Goldmann's method of eliminating this error is correct, it is negligible for exposures of less than one minute's duration and in as much as it is the beginning of the growth and decay curves which is the particular object of this study, a series of curves has been made in which the exposure is limited to one minute.

It having been found not feasible to eliminate the dark current with the type of cell in use, its value was made as constant as possible by surrounding the cell by an oil bath in a glass box. This steadied the temperature

variations and no further trouble was experienced from variations of the dark current. The deflection due to the dark current was then taken as the zero from which the photoelectric current was measured.

In exposures of short duration the exact time of the opening and the closing of the shutter becomes important. In order to insure an accurate record of these times the shutter was so arranged that its openings and closings were automatically recorded on the same chronograph used to record the growth and decay curves.

Fig. 7 shows the results of a series of four experiments performed by

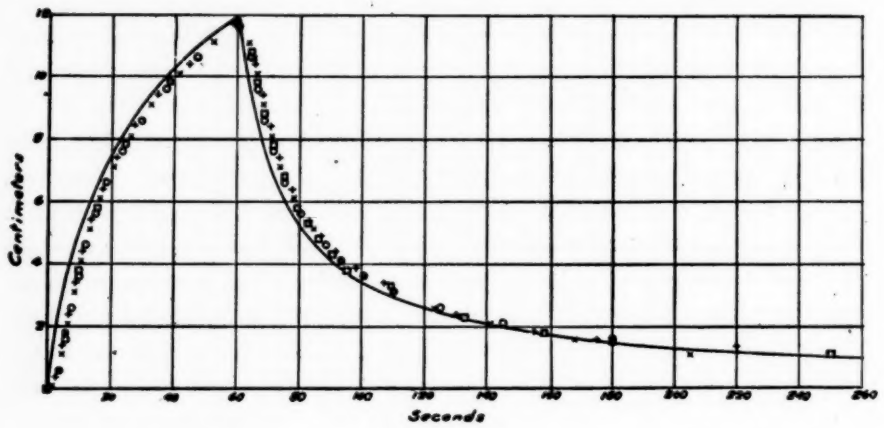

Fig. 7.

this method. The cell was illuminated with an intensity of 5.2 foot candles for one minute. The symbols ○, ×, + and □ represent the data from the first, second, third and fourth experiment respectively. The time is taken as zero at the instant of the opening of the shutter in each experiment and the deflection due to the dark current has been substracted from the ordinates before plotting in each case. The striking feature of these observations is the accuracy with which the results are repeated. In all previous experiments with longer exposures it was found impossible to reproduce results. In every case the current would be less at the second trial.

The curve shown in Fig. 7 is the composite of the four experiments corrected by equation (11). The following are the values of the constants involved.

a, 20,000,	h, 15,000,	n, 2.6,
b, 13,000,	ζ, 22,950,	ωc, .96,
s, 50,000,	r, 3,100,000,	α, 5.3,
g, 480,	ω, 22,750,	β, 3.5,

R,	7,950,	c,	4.2×10^{-6},	γ,	.4,
f,	0,	l,	.015,	α',	5.7,
ρ,	20,400,	l/g,	.00003,	nj,	10^{-9}.

Fig. 8 shows the graphical plots from which the corrections were computed: (a) is $\dot{x}$; (b), $\ddot{x}$ and (c), $\int_0^1 \ddot{x}dz$. Plot (c) was only made for the growth curve as it so closely approximates (b) as to make it possible to

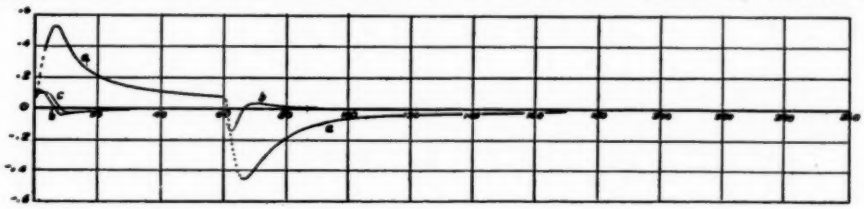

Fig. 8.

use equation (11). The value of the test function, $\gamma\omega c\ddot{x}$ is nowhere greater than .02 which is less than the uncertainty in the value of y. The computation of the values of y for the third experiment of the series is shown in Table II.

In this computation the result is nowhere more accurate than one per cent. In order therefore to justify the assumption of the truth of the law of shunts $y/\dot{y}$ must be greater than $100 \times .00003 = .003$ seconds. An examination of the curves of Fig. 7 shows that this is true except in the range from 0 to .003 seconds. As no data was taken in this range, the assumption is justified.

Fig. 9 shows a test of the data of Table II. for compliance with Thomp-

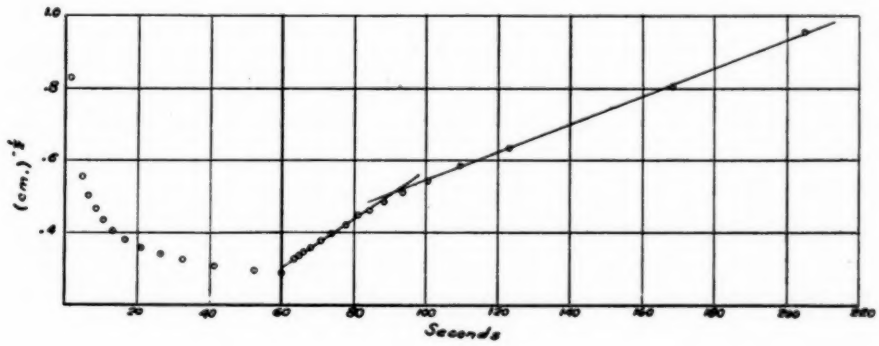

Fig. 9.

son's type of equation. The result here shown is typical of those obtained in all of the experiments performed. In all, the growth data give a smoothly curving line, the point at $t = 60$ lies below the first straight

TABLE II.

t.	x.	$3.5\dot{x}$	$5.7\ddot{x}$	y.
0	0			0
1.4	.1	.6	.75	1.45
4.4	1.1	1.65	.5	3.25
6.3	2.1	1.85	0.	3.95
8.4	3.1	1.7	−.2	4.6
10.5	4.1	1.45	−.2	5.35
13.2	5.1	1.15	−.15	6.1
16.5	6.1	.9	−.1	6.9
20.9	7.1	.7	−.05	7.75
26.2	8.1	.55	−.05	8.6
32.7	9.1	.45		9.55
41.6	10.1	.4		10.5
52.4	11.1	.3		11.4
60.0	11.7	.3		12.0
63.9	11.1	−1.25	−.55	9.3
65.1	10.6	−1.55	−.15	8.9
66.1	10.1	−1.6	−.05	8.45
68.4	9.1	−1.45	.15	7.8
71.1	8.1	−1.2	.2	7.1
74.0	7.1	− .95	.15	6.3
78.1	6.1	− .75	.1	5.45
80.9	5.6	− .65	.05	5.0
84.2	5.1	− .45	.05	4.7
88.5	4.6	− .35	.05	4.3
93.6	4.1	− .25		3.85
100.4	3.6	− .2		3.4
109.9	3.1	− .15		2.95
123	2.6	− .1		2.5
141	2.1	− .1		2.0
168	1.6	− .05		1.55
205	1.1			1.1

line of the decay and the points near the intersection of the two straight lines form a curve tangent to both. It is evident that Thompson's law does not hold for short exposures in the case of the growth data. This result might have been predicted for the case of short exposures from the fact that $y^{-1/2}$ is necessarily infinity when t is zero. In the case of the decay data Fig. 9 probably gives as good verification of the law as that obtained by Thompson. The results, however, show conclusively that the knee in the plot is not to be associated with the errors due to the galvanometer but that it is characteristic of the law of decay. The fact that the point at $t = 60$ in every case falls below the first straight line might be interpreted as indicating the existence of another line through this point and intersecting the first between this point and the next one shown. Similar cases of three intersecting straight lines have been found in phosphorescence decay curves.

It has been found impossible to represent the data by an equation of the type of (1), Goldmann's theoretical equation for the current during illumination. Line "*a*" in Fig. 10 shows the best result that has been obtained in this attempt. Here the values of y from the growth curve have been plotted against $e^{-.048t}$. However an equation of the type of (3) may be found that will represent the data except during the first 10 seconds. This is the same sort of agreement that Goldmann found between his data and the equation. This is shown in Fig. 11 in which y

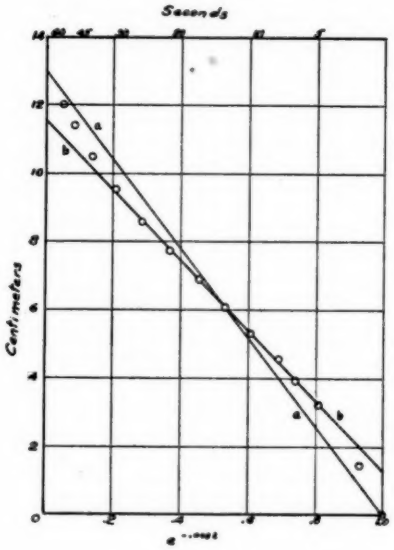

Fig. 10.

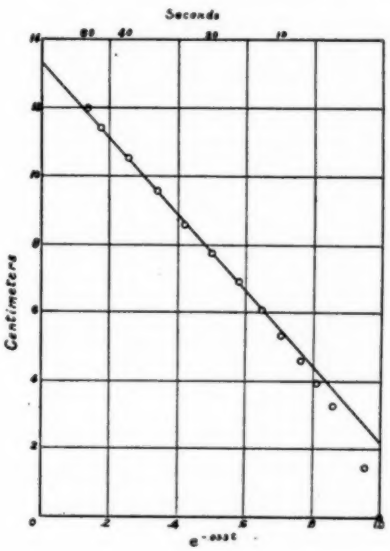

Fig. 11.

is plotted against $e^{-.033t}$. In this case, however, it is doubtful if the agreement is truly significant. If similar plots are made using various larger values of m_1, there is in each case a range within which the points lie upon a straight line. Line "*b*" in Fig. 10 is an example of this and represents the data in the range from 5 to 25 seconds. The deviation of the points from this line for times less than 5 seconds is of the same type as that observed by Goldmann. The deviation for times greater than 25 seconds is in the wrong direction to be explained by the polarization of the dark electrode. As one takes smaller or larger values of m_1, this range of agreement comes later or earlier but the deviation outside of it remains of the same type as shown. In Fig. 11, m_1 has so small a value that the range of agreement extends to the end of the time of exposure. There is every reason to think that, if the exposure had been longer, deviations from the straight line would have been found for times later than 60 seconds. In fact the last point of the plot shows evidence of

the beginning of such a deviation. For values of m_1 less than .033 the agreement is not satisfactory. Fig. 12 shows a test of the data for compliance with (2), Goldmann's theoretical equation for the current during decay. Here $\log_e y$ is plotted against t. The result should be a straight line if the equation holds. This is obviously not the case. Attempts to represent the decay data by an equation of the type of (4) have also been unsuccessful.

It seems fair to conclude that the change in the laws of growth and decay observed by both Goldmann and Thompson at about one minute

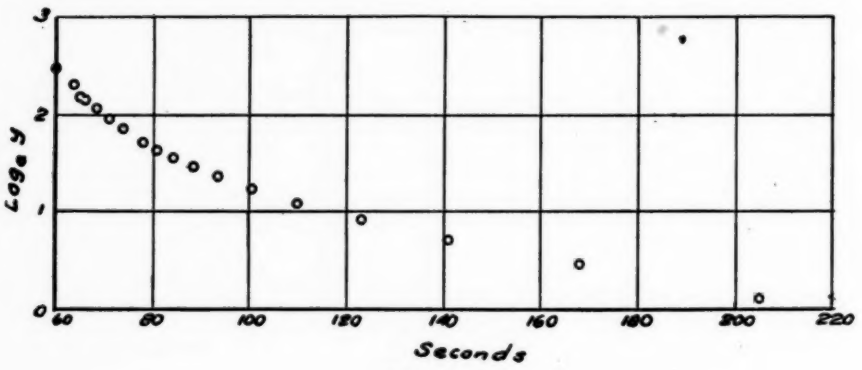

Fig. 12.

are not due to the damping and inertia of the galvanometer coil. None of the laws, with the exception of Thompson's law of decay, accurately represents the data for short exposures. This cannot but cast some doubt upon Goldmann's theory of the mechanism of the photoelectric action as it would seem that if his ideas were correct equations (1) and (2) would more nearly represent the data for short exposures than for long. To make this result conclusive, however, experiments should be carried on over longer periods of exposure under conditions which would allow of correction being made for the polarization of the dark electrode.

In order to study the effect of variations in the composition and concentration of the electrolyte and in the material and density of the electrodes upon the photoelectric properties of cells, it is desirable to have some equation which at least approximately represents the current-time curve. The numerical constants of such an equation, even though it be empirical, are very useful in making comparisons. Thompson's law of decay might be used for this purpose but it has the disadvantage that it involves at least four constants. I have found that an equation of the type,

$$y = y_0 - \frac{t}{Mt + L}, \qquad (12)$$

in which t is measured from the instant of closing the shutter and y_0 is the value of y at that instant, very closely represents the decay curves following exposures of not more than a minute's duration. This equation may be written in the form

$$\left(t - \frac{L}{M}\right)\left(y - y_0 + \frac{1}{M}\right) = \frac{L}{M^2}, \tag{13}$$

the equation of an equilateral hyperbola if y is plotted against t as in Fig. 7. It may be also written,

$$\frac{t}{y_0 - y} = Mt + L, \tag{14}$$

the equation of a straight line if $t/(y_0 - y)$, is plotted against t as in Fig. 13. In making this plot the data from Table II. was used. The values of the constants found to give the best results are $L = 1.28$, and $M = .0844$,

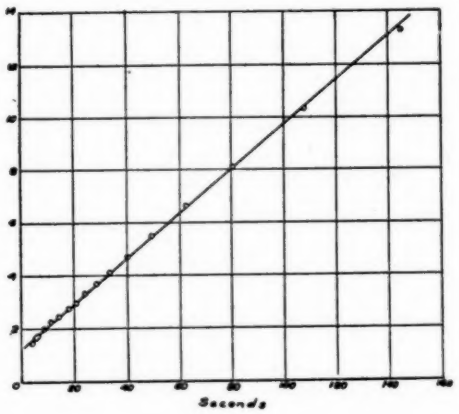

Fig. 13.

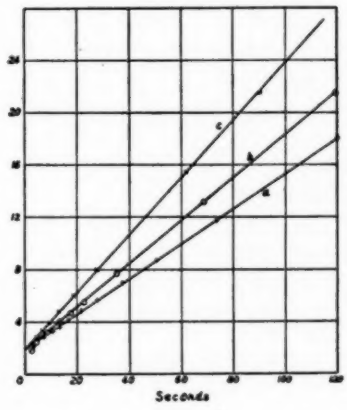

Fig. 14.

giving $1/M = 11.85$, $L/M = 15.2$, $L/M^2 = 180$ and

$$y = \frac{12.2 - t}{.0844t + 1.28}.$$

Table III. gives the observed and computed values of y and their differences.

There seems to be a possible systematic deviation from the hyperbolic law during the early part of the decay. This is indicated in the table by the positive differences in the second, third and fourth items and in Fig. 13 by a downward trend of the points near the left end of the line. Deviations of this type have been found in several experiments and always in the same sense. Frequently, however, there is no such indication.[1] The data in this region is less accurate than the rest and has

[1] See Fig. 14, curve (C).

TABLE III.

y.	y_c.	Diff.	y.	y_c.	Diff.
12.0.....	12.0	0	4.7	4.7	0
9.3.....	9.6	.3	4.3	4.25	−.05
8.9.....	9.0	.1	3.85	3.85	0
8.45.....	8.6	.15	3.4	3.4	0
7.8.....	7.8	0	2.95	2.9	−.05
7.1.....	7.0	−.1	2.5	2.45	−.05
6.3.....	6.3	0	2.0	2.0	0
5.45.....	5.55	.1	1.55	1.6	.05
5.0.....	5.1	.1	1.1	1.25	.15

been given less weight in determining the values of the constants M and L. Moreover the method of plotting used in Fig. 13 is particularly sensitive to errors at the left end of the line.

Use has been made of the hyperbolic relation to study the effect of the length of exposure on the nature of the decay. In another series of experiments, performed with the same cell, decay curves were taken after exposure of 60, 30 and 15 seconds. The cell was only partly filled with the electrolytes as some of the solution had leaked out and the effective area of the electrodes was observed to be about $2/3$ of that in the first series. The values of the constants involved in the correction equation were the same as before except that the change in the effective area of the electrodes modified the values of c and r and of the constants depending on them. Assuming that the new area was $2/3$ of the old, $c = 28$ microfarads, $r = 4.9$ megohms, $\omega c = .64$ seconds and $\gamma = .3$ sec.^{2}. When the cell was illuminated with light of the same intensity as before a growth curve was obtained of which the corrected ordinates were .64 times those obtained in the previous experiments. This verifies the estimated value, $2/3$, as the photoelectric current has been found to be proportional to the effective electrode area.[1]

Fig. 14 shows corrected data for the decay curves plotted in accordance with equation (14). The lines (a), (b), and (c) are the plots for the decays following exposures of 60, 30 and 15 seconds respectively. These lines are seen to have nearly the same value for their y-intercept, L. The significance of this may be shown by differentiating equation (12) obtaining for the rate of decay of the current

$$-\frac{dy}{dt} = \frac{L}{(Mt + L)^2}.$$

Now when $t = 0$, this becomes

$$-\frac{dy}{dt} = \frac{1}{L}.$$

[1] Goldmann, loc. cit., p. 478.

Thus we see that the y-intercept L is the recriprocal of the initial rate of decay of the current and that the intersection of the three lines upon the y-axis signifies that the initial rate of decay of the current is not dependent upon the length of exposure. In order to test this conclusion the equations for all the decay curves of this series have been computed. The results are shown in Table IV. Column 1 gives the duration of the exposure in seconds, 2 and 3 give the values of L and M, and 4, the ordinate of the asymptote of the hyperbola.

TABLE IV.

1, T.	2, L.	3, M.	4, y'.
60.0	2.0	.139	.3
60.3	1.88	.137	.4
60.7	2.0	.134	.15
	Av. 1.96		
31.0	1.77	.166	0
29.5	1.85	.167	0
29.9	1.9	.169	.05
30.0	1.85	.170	.1
	Av. 1.84		
15.7	1.98	.222	0
15.0	1.94	.223	0
15.0	1.91	.230	.05
	Av. 1.94		

An examination of the values in column 2 confirms the conclusion of the constancy of L within its accuracy of measurement which is about 5 per cent. The values of y' in column 4 are either zero or small and positive. It has been frequently observed that the current does not in general decrease to zero but to a small positive value.[1] This value is seen to be practically zero for exposures up to 30 seconds duration but to certainly have a finite value for an exposure of 60 seconds. The possible deviation from the hyperbolic equation during the early part of the decay which was discussed above in connection with Fig. 13 and Table III. does not occur in any of the 15 second exposure data and is not marked in the 30 second exposure data. This suggests the possibility of this deviation being related to y'.

We may in fairness conclude that following a short exposure, the current decreases from an initial value, y_0, to a small value, y', at a variable rate, v, whose initial value, $v_0(=1/L)$, is independent of the duration of

[1] Goldmann, loc. cit., p. 512.

the exposure and that the curve of decay is fairly well represented by an equilateral hyperbola which is completely determined by these three constants y_0, v_0 and y'. Its equation in terms of them is

$$(y - y')\left[t - \frac{1}{v_0}(y_0 - y')\right] = \frac{(y_0 - y')^2}{v_0}.$$

A detailed study of v_0 and y' as functions of the physical and chemical properties of the electrodes and the electrolyte and of y' as a function of the length of exposure promises to give valuable information concerning the nature of the effect.

The invariance of v_0 with the length of exposure in a way explains our failure in the attempt to represent the data for the decay by an exponential equation. It is a well known characteristic of this type of equation that the first derivative of the dependent variably, y, is a linear function of y. Now if v_0 is invariant with respect to the time of exposure it will be invariant with respect to η_0 which is a function of that time. If an exponential equation is to meet this condition it must have exponents which are themselves functions of η_0. This is not the case in Goldmann's theory of the effect.

In a theoretical discussion of this effect there should be taken into account three facts not hitherto considered. The fact that the rate at at which the current starts to decay after a short exposure varies only slightly, if at all, with the length of exposure, is inconsistent with any theory in which the rate of decay depends upon the value of the current. The existence of a dark current, simillar in character to the photoelectric current and varying in value with the photoelectric sensitivity and with the nature and temperature of the electrodes, makes the theory that the current originates solely in the ionization of the rhodamine molecule by the incident light, insufficient. The discovery by Thompson[1] that the material of which the electrode is composed has a marked effect upon the photoelectric sensitivity confirms this view and further points to the probability that the electrodes play an active part which must be considered in explaining the effect.

PHYSICAL LABORATORY,
CORNELL UNIVERSITY.

APPENDIX.

Proof of Equation (8).—Let i, i_r, and i_c represent the currents in h, r, and c respectively, due to the motion of the galvanometer coil. (See Fig. 2.) Then

$$i = i_c + i_r. \tag{15}$$

The potential difference between the ends of the resistance, r, is

$$v_1 - v_2 = ri_r \tag{16}$$

$$= \frac{1}{c}\int i_c dt. \tag{17}$$

[1] Loc. cit.

Eliminating i_r between (15) and (16) and writing

$$e = r\, i_c, \tag{18}$$

$$v_1 - v_2 = ri - e. \tag{19}$$

This equation is of the form of the expression for the difference of potential between the ends of a conductor of resistance, r, carrying a current, i, and containing an electromotive force, e. We may therefore consider the branches c and r replaced by such a conductor for the purpose of studying effects outside of these branches. If we eliminate $v_1 - v_2$ and i_c between equations (17), (18), and (19) we obtain for the condition on the value of e

$$\frac{de}{dt} + \frac{e}{rc} = r\frac{di}{dt}. \tag{20}$$

Let E be the electromotive force induced in g by the motion of the coil. The current in r due to E equals the current which E would produce in g if it were situated in r which is $E/[n(r + \zeta)]$.[1] This current is superimposed upon the current in r due to e. Therefore

$$i = \frac{E}{n(r + \zeta)} + \frac{e}{r + \zeta}. \tag{21}$$

Eliminating i between (20) and (21) and writing ω for $r\zeta/(r + \zeta)$,

$$\frac{de}{dt} + \frac{e}{c\omega} = \frac{r}{n\zeta}\frac{dE}{dt} \tag{22}$$

or

$$e = \frac{r}{n\zeta}\int_{t_0}^{t} \epsilon^{(s-t)/\omega c}\left[\frac{dE}{dt}\right]_s ds, \tag{23}$$

where s is the variable of integration and t_0 is the value of t when $e = o$.

Now the total current in the galvanometer coil will be that resulting from the superposition of the current due to E, that due to e and that portion of the current to be measured which flows through the galvanometer.

$$i_g = \frac{E}{\rho} + \frac{e}{n(r + \zeta)} + \frac{u}{n}. \tag{24}$$

The electromotive force E equals $-Nd\theta/dt$, where N is product of the area and number of turns of the coil and the magnetic induction of the field in which it is suspended. Substituting this value of E in (23) and (24) and eliminating e between the two equations,

$$i_g = \frac{u}{n} - \frac{N}{\rho}\dot{\theta} - \frac{N\omega}{n^2\zeta^2}\int_{t_0}^{t} \epsilon^{(s-t)/\omega c}\,\ddot{\theta}_s\, ds. \tag{25}$$

There act upon the galvanometer coil the following torques:—that due to the current, $-Ni_g$; that due to the elastic suspension, $-\tau\theta$; that due to friction, $-\mu(d\theta/dt)$. Equating the sum of these to the rate of change of the angular momentum, $I\ddot{\theta}$, and eliminating i_g by equation (25), we obtain

$$I\ddot{\theta} + \left(\mu + \frac{N^2}{\rho}\right)\dot{\theta} + \frac{N^2\omega}{n^2\zeta^2}\int_{t_0}^{t} \epsilon^{(s-t)/\omega c}\,\ddot{\theta}_s\, ds + \tau\theta = \frac{N}{n}u \tag{26}$$

Suppose θ to be measured on a scale at distance, m, from the mirror. Then $\theta = x/2m$. Substituting this value for θ and multiplying through by $2m/\tau$, we obtain

$$\alpha\ddot{x} + \left(\kappa + \frac{\lambda}{\rho}\right)\dot{x} + \frac{n^2\zeta^2}{\lambda\omega}\int_{t_0}^{t} \epsilon^{(s-t)/\omega c}\,[\ddot{x}]_s\, ds + x = \frac{u}{nj}, \tag{27}$$

in which α is written for I/τ; κ, for μ/τ; λ for N^2/τ and j, for $\tau/2mN$. Writing β for $\kappa + \lambda/\rho$ and multiplying by nj gives equation (8).

Now t_0 has been defined by the condition, $t = t_0$ when $e = 0$. This condition holds when $\ddot{x}$ and $\dot{x}$ are both zero for then $u = njx$, a constant, and the current in each resistance of the network of Fig. 2 is constant. But

$$e = ri_c = cr\frac{d}{dt}(v_1 - v_2) = c\frac{di}{dt}$$

and thus must be zero when i is constant.

[1] Maxwell, "Electricity and Magnetism," Sec. 281.

NEW BOOKS.

The Concept of Nature. By A. N. WHITEHEAD. Cambridge, England: The University Press, 1920. Pp. ix + 202.

A sequel to the author's Principles of Natural Knowledge in which his method of extensive abstraction is further elaborated.

The dependence of the character of space on the character of time is used as a basis for the systematic explanation of both.

Memoria de la Facultad de Ciencias Fisicas, Matematicas Y Astronomicas. Correspondiente A 1918. No. 8. La Plata: Facultad de Ciencias Fisicas, Matematicas Y Astronomicas, 1920. Pp. 1 + 136.

The annual Record of the Scientific Activities of the University of La Plata for 1918 containing:

1. A list of titles of scientific work published by the faculty with rather full abstracts.

2. A statement of courses offered and various statistics concerning the university.

Tables Logarithmiques et Trigonometriques A Quatre Décimales et Tables a Trois Décimales A L'Usage des Physiciens et des Navigateurs. By H. ROCQUES DESVALLEES. Paris: Gauthier-Villars et Cie, 1920. Pp. xxiv + 72.

This set of tables contains the usual directions for use; logarithms and anti-logarithms; addition logarithms and subtraction logarithms; and values of the trigonometrical functions conveniently arranged.

Organizacao do Estudo da Fisica. By ALVARO R. MACHADO. Porto: Tipografia Sequeira, 1920. Pp. 1 + 146.

Notes and Observations upon the facilities for the study of physics in Spain, France, Switzerland, Belgium and England.

Course de Cinematique Theorique. By H. LACAZE. Paris: Gauthier-Villars et Cie, 1920. Pp. 1 + 138.

The five chapters of this brief treatise deal respectively with:

Vectors; Kinematics of a point; Movement of a Solid; The Composition of Accelerations; The Displacement of a Vector in a Plane.